

**Transcriptional Control Mechanisms of the  
Uncoupling Protein 3  
Gene and their Functional Implications**



**DISSERTATION**

zur

Erlangung des Doktorgrades  
der Naturwissenschaften

(Dr. rer. nat.)

dem Fachbereich Biologie der Philipps-Universität Marburg vorgelegt von

**Tobias Fromme**

aus Geseke

Marburg / Lahn 2007

Vom Fachbereich Biologie der Philipps-Universität Marburg als Dissertation am

\_\_\_\_\_ angenommen.

Erstgutachter

\_\_\_\_\_

Zweitgutachter

\_\_\_\_\_

Tag der mündlichen Prüfung am \_\_\_\_\_

# CONTENTS

## GLOSSARY OF TERMS

## REPRESENTATION OF PROTEIN AND GENE NAMES

## SUMMARY

INTRODUCTION	1
AIMS & SCOPE	4
RESULTS & DISCUSSION	5
CONCLUSION	10
REFERENCE LIST	12

## PUBLICATIONS & MANUSCRIPTS

CHAPTER 1.....	17
“Chicken ovalbumin upstream promoter transcription factor II regulates uncoupling protein 3 gene transcription in <i>Phodopus sungorus</i> ” Fromme T., Reichwald K., Platzer M., Li XS. and Klingenspor M. <i>BMC Molecular Biology 2007, 8:1</i>	
“Chicken ovalbumin upstream promoter transcription factor II regulates the uncoupling protein 3 gene” Fromme T., Reichwald K., Platzer M., Li XS. and Klingenspor M. <i>Poster presented at Keystone Symposium „Nuclear Receptors: Orphan Brothers“, 2006.</i>	
CHAPTER 2 .....	33
“An intronic single base exchange leads to brown adipose tissue specific lack of Ucp3 and an altered body weight trajectory” Fromme T., Nau K., Rozman J., Hoffmann C., Reichwald K., Utting M., Platzer M., Klingenspor M. <i>(submitted to Biochemical Journal)</i>	
“A single base exchange leads to tissue specific ablation of Ucp3 expression” Fromme T., von Praun C., Liebig M., Reichwald K., Platzer M., Klingenspor M. <i>Poster presented at the 14th European Bioenergetics Conference, 2006.</i>	
CHAPTER 3 .....	62
“Brown adipose tissue specific lack of uncoupling protein 3 is associated with impaired cold tolerance and reduced transcript levels of metabolic genes” Nau K., Fromme T., Meyer C.W., von Praun C., Heldmaier G., Klingenspor M. <i>(submitted to Journal of Comparative Physiology B)</i>	
“Tissue specific lack of UCP3 leads to transcriptional down-regulation of glycolytic, lipogenic and lipolytic pathways in <i>Phodopus sungorus</i> ” Weber K., Fromme T., von Praun C., Yang LX., Klingenspor M. <i>Poster presented at the 99. Jahrestagung der Deutschen Zoologischen Gesellschaft, 2006.</i>	

CHAPTER 4 .....	83
“Marsupial uncoupling protein 1 sheds light on the evolution of mammalian nonshivering thermogenesis”	
Jastroch M., Withers K.W., Taudien S., Frappell P.B., Helwig M., Fromme T., Hirschberg V., Heldmaier G., McAllan B.M., Firth B.T., Burmester T., Platzer M., Klingenspor M.	
<i>(accepted for publication in Physiological Genomics)</i>	
CHAPTER 5 .....	120
“Rapid single step subcloning procedure by combined action of type II and type IIs endonucleases with ligase”	
Fromme T., Klingenspor M.	
<i>(in preparation for Biotechnology and Bioengineering)</i>	
Patent “Klonierungssystem”, Nr. DE 103 37 407 A1	
Fromme T., Klingenspor M.	
<i>Deutsches Patent- und Markenamt</i>	
ZUSAMMENFASSUNG	137
CURRICULUM VITAE	138
DANKSAGUNG	140
ERKLÄRUNG	141

## Glossary of terms

ATP	adonosine triphosphate
BAT	brown adipose tissue
BMI	body mass index
CO <sub>2</sub>	carbon dioxide
Coup-TFII	chicken ovalbumin upstream promotor transcription factor II
DR-1	direct repeat element with one base between repeats
EMSA	electrophoretic mobility shift assay
GDP	guanosine diphosphate
Myod	myogenic differentiation 1
p300	p300/CBP-associated factor
PCR	polymerase chain reaction
Ppar	peroxisome proliferator activated receptor
PPRE	Ppar response element
ROS	reactive oxygen species
Rxr	retinoid X receptor
TR	thyroid hormone receptor
Ucp	uncoupling protein

## Representation of protein and gene names

Gene or mRNA (non-human):	first letter capitalised, <i>italic</i>	e.g. <i>Ucp3</i>
Protein (non-human):	first letter capitalised	e.g. Ucp3
Gene or mRNA (human):	all letters capitalised, <i>italic</i>	e.g. <i>UCP3</i>
Protein (human):	all letters capitalised	e.g. UCP3

Exception: Consistent with existing literature the thyroid hormone receptor (TR) is written 'all letters capitalised' regardless of origin.

## Summary

### Introduction

The first member of the family of uncoupling proteins to be discovered was uncoupling protein 1 (Ucp1) or thermogenin, as it was initially called (Nicholls *et al.*, 1978). Ucp1 is specifically located in the inner membrane of mitochondria in brown adipose tissue (BAT), the central heating organ of small endotherm vertebrates (Cannon *et al.*, 1982). Moreover, until today Ucp1 is regarded the one central component that in fact defines a fat tissue to be genuine BAT (Sell *et al.*, 2004). The molecular function of Ucp1 is to facilitate a proton flux from the mitochondrial intermembrane space into the matrix circumventing ATP synthesis (Nicholls & Locke, 1984). In other words ATP synthesis becomes “uncoupled” from the proton pumps of the respiratory chain. Since a portion of the energy amount stored in the proton motive force of the gradient across the mitochondrial inner membrane is not chemically conserved during uncoupled respiration, it is released as heat. In BAT this process is complemented by high molar amounts of Ucp1 located in an enormous number of mitochondria that are fueled by lipid droplets specifically altered in size and composition to allow fast substrate provision. Hence BAT is an organ highly specialized to allow efficient nonshivering thermogenesis (Klingenspor, 2003).

Ucp1 function can be activated by fatty acids and inhibited by purine nucleotides such as GDP (Cunningham *et al.*, 1986; Nicholls & Locke, 1984). It is not yet fully understood, how the proton flux across the mitochondrial inner membrane itself is accomplished by Ucp1 and several hypotheses have been put forward (Figure 1). The principal mechanisms suggested include a simple proton channel concept (Klingenberg & Winkler, 1985) as well as models in which fatty acids act as steric or catalytic cofactors (Shabalina *et al.*, 2004 ;Rial *et al.*, 2004). Ucp1 might in fact not even be a proton importer, but rather an anion exporter. If unprotonated fatty acid anions would be transported from the mitochondrial matrix into the intermembrane space they would be able to return in their protonated form by a so-called flip-flop mechanism and thereby indirectly facilitate a proton flux into the matrix (Garlid *et al.*, 1996).

In 1997 two paralogues of Ucp1 were discovered and named Ucp2 and Ucp3 (Vidal-Puig *et al.*, 1997; Boss *et al.*, 1997; Fleury *et al.*, 1997). These two novel uncoupling proteins share the same genomic locus being directly neighbouring genes. They are about 75% identical to each other on the amino acid level, while both share about 55% identity with Ucp1. It was soon established that these novel Ucps serve a different purpose than thermogenesis (Nedergaard *et al.*, 1999).

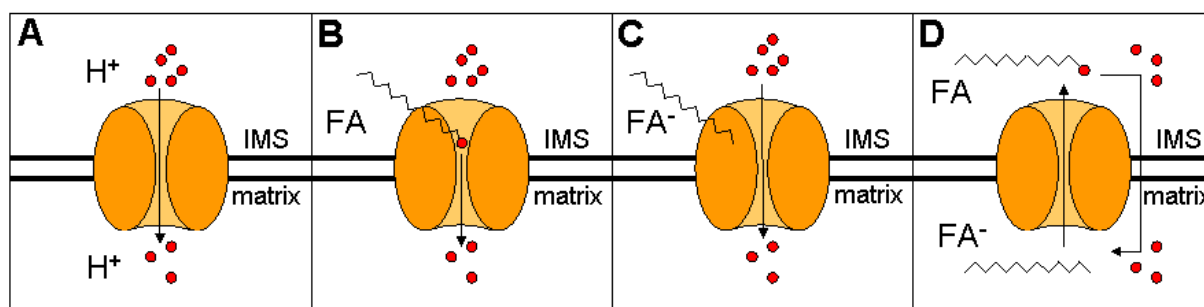


**Figure 1 – Models of uncoupling protein function. (A)** The uncoupling protein acts as a proton channel. **(B)** A fatty acid anion acts as catalytic component, passing on protons via its carboxyl group. **(C)** A fatty acid anion acts as steric activator of uncoupling protein function. **(D)** Fatty acid anions are exported from the mitochondrial matrix, protonated in the intermembrane space and re-enter the matrix by a flip-flop mechanism. IMS = intermembrane space, FA(¯) = fatty acid (anion), H<sup>+</sup> = proton.

The *Ucp3* gene is predominantly expressed in skeletal muscle and BAT (Vidal-Puig *et al.*, 1997). One of the first observations doubting a role in thermogenesis - an energy wasting mechanism - was the transcriptional upregulation of the *Ucp3* gene upon starvation (Boss *et al.*, 1998). Further studies reported additional physiological situations of increased *Ucp3* expression, among them acute exercise (Tsuboyamakasaoka *et al.*, 1998), streptozotocin-induced diabetes (Stavinoha *et al.*, 2004) and cold exposure (Larkin *et al.*, 1997; von Praun *et al.*, 2001). Weigle and coworkers noticed that a common physiological parameter of these situations is an elevation of circulating fatty acid levels and proposed this to be the responsible cue (Weigle *et al.*, 1998). This model was fortified by lipid infusion experiments that did indeed lead to *Ucp3* upregulation. Based on these observations further experiments led to the hypothesis that it is the function of *Ucp3* to export fatty acid anions from the mitochondrial matrix (Himms-Hagen & Harper, 2001).

The biochemical properties of *Ucp3* as measured in mitochondrial proton leak assays, however, are quite similar to those of the thermogenic protein *Ucp1*. Consequently another hypothesis regards *Ucp3* to be a mediator of ‘mild uncoupling’ thereby mitigating the generation of reactive oxygen species (ROS) (Echtay *et al.*, 2002; Echtay *et al.*, 2003). A controversial third model takes into account both physiological and biochemical data. In analogy to one of the models of *Ucp1* function it has been proposed that *Ucp3* exports fatty acid anions which are then protonated and can re-enter the mitochondrial matrix uncatalyzed by a so called flip-flop-mechanism (Figure 1D). This process would lead to a net proton flux across the inner mitochondrial membrane and thus mildly uncouple respiration from ATP production (Jaburek *et al.*, 2004; Jezek *et al.*, 1998).

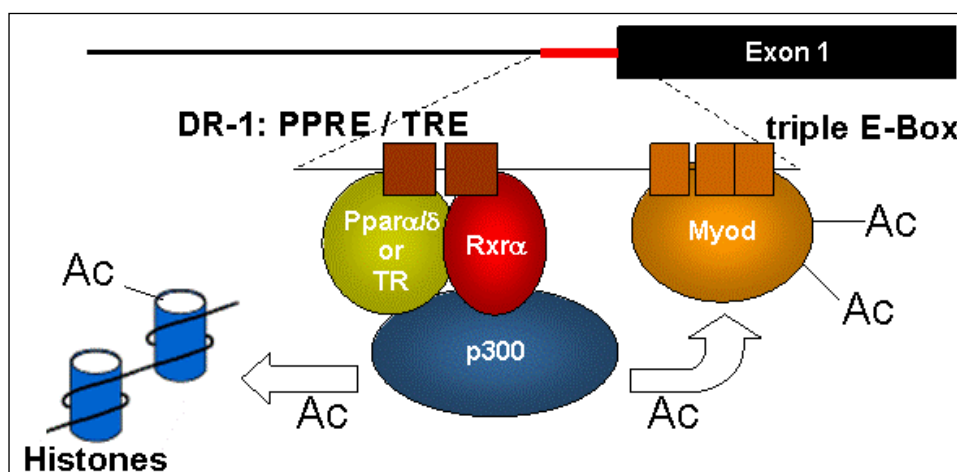


**Figure 2 – Published regulatory mechanisms of *Ucp3* gene expression.** The proximal promoter region comprises a triple E-Box binding Myod and a DR-1 site, that functions as response element for heterodimers of either Ppars or TR with Rxra. Upon binding the heterodimer recruits p300, which acetylates surrounding histones and Myod, thereby initiating transcription. Ac – Acetyl-group, PPRE – Ppar response element, TRE – TR response element. (modified from Solanes *et al.*, 2003)

On the molecular level transcription of the *Ucp3* gene is regulated by a complex machinery of transcription factors and has been thoroughly investigated in skeletal muscle tissue (Figure 2). The proximal *Ucp3* promoter region exhibits a triple E-Box that binds myogenic differentiation factor 1 (Myod) (Solanes *et al.*, 2000). A direct repeat DR-1 element in close proximity can serve as binding site for various heterodimers with one partner always being the retinoid X receptor (Rxra) while the second partner can be a peroxisome proliferator activated receptor (Ppara $\alpha$  or Ppara $\delta$ ) (Pedraza *et al.*, 2006; Solanes *et al.*, 2003) or a thyroid hormone receptor (TR) (Solanes *et al.*, 2005). Upon binding the heterodimer recruits a cofactor with acetylase activity (probably p300/CBP-associated factor (p300)) which acetylates Myod as well as surrounding histones. While histone acetylation leads to increased promoter accessibility, activation of Myod by acetylation is thought to trigger the transcription process itself (Solanes *et al.*, 2003).

This arrangement seems to comprehensively account for the physiological cues that have been observed to increase *Ucp3* transcription in skeletal muscle. The effect of free fatty acid levels is mediated by PPARs, nuclear receptor that are activated and imported into the nucleus upon binding of fatty acids as ligand. An alternative thyroid hormone signal is integrated via TR while tissue specificity is established by the necessity for Myod. Despite this substantial knowledge on *Ucp3* gene regulation many questions have not been addressed yet. In BAT for instance these implicated mechanisms have never been confirmed and at least the presence of Myod can be doubted.



Serendipitously our group got hold of an animal model perfectly suited to address these remaining questions. Shortly after the discovery of *Ucp3* in 1997 individual Djungarian hamsters with a BAT specific lack of *Ucp3* were identified in our *Phodopus sungorus* breeding colony. By breeding littermates of these individuals an inbred line was established. All hamsters of this line were devoid of *Ucp3* expression in BAT proving heritability of this trait (Liebig *et al.*, 2004).

## Aims & scope

All proposed hypotheses regarding the physiological function of *Ucp3* are at least in part based on the transcriptional regulation of this gene. This fact illustrates how important knowledge of the regulation of a gene is to be able to infer its role. Our mutant hamster model, however, could not be fully explained by the existing model of transcriptional control and thereby challenged its integrity.

During my PhD study period I addressed open questions on *Ucp3* regulation employing two parallel approaches. On the one hand our mutant hamster model served as a tool to identify the unknown regulatory pathway affected by this mutation. On the other hand an unbiased analysis of the hamster *Ucp3* promoter aimed at the identification and verification of so far unknown transcription factor binding sites.

## Results & Discussion

### *Chapter 1 - Chicken ovalbumin upstream promoter transcription factor II regulates uncoupling protein 3 gene transcription in *Phodopus sungorus**

In chapter 1 I report on the results of an unbiased sequence analysis of the *P. sungorus Ucp3* promoter. An alignment with the syntenic genomic regions of other vertebrates revealed a high conservation of the known binding sites for Myod and Ppar heterodimers confirming their importance. In the same region we identified a further well conserved sequence element resembling a putative Coup-TFII binding site. Coup-TFII has been reported to be able to interact with Ppar factors, Myod and p300 and is involved in skeletal muscle development (Bailey *et al.*, 1998). Furthermore it coregulates a number of key metabolic genes, which led us to investigate this candidate in detail (Robinson *et al.*, 1999; Eubank *et al.*, 2001; Cabrero *et al.*, 2003; Lou *et al.*, 1999).

We found *Coup-TFII* to be coexpressed with *Ucp3* in skeletal muscle and in BAT. In skeletal muscle of starved and in BAT of cold-exposed hamsters the mRNA levels of these two genes were highly correlated with each other in individual samples. This interdependence was absent in control animals implying that the effect of Coup-TFII is dependent on other transcriptional activators already present on the promoter. Consistently, in reporter gene assays we observed a strong induction of *Ucp3* promoter activity by Coup-TFII on the background of other known transcriptional regulators of *Ucp3* expression but not alone.

In electrophoretic mobility shift assays (EMSA) we proved physical binding of the Coup-TFII protein to an inverted repeat response element about 800bp upstream of the proximal promoter. We mutated this element to investigate the contribution of both repeat half-sites on Coup-TFII interaction in both EMSA and reporter gene studies. Mutation of the 5' half-site led to loss of Coup-TFII binding, while disruption of the 3' half-site only mildly affected binding. Concordantly, reporter gene assays with a mutation 3' half-site did not affect expression of the reporter, while a lack of the 5' half-site led to complete loss of expression. Surprisingly, the latter mutation did not only affect Coup-TFII dependent transcription but did also completely prevent activation of the promoter by Myod, Rxr $\alpha$  and p300 cotransfection. This observation is not consistent with Coup-TFII simply being a direct transcriptional activator and led us to postulate a so far unknown repressor protein, that has to be deactivated or displaced by Coup-TFII.

In this study the complex machinery of transcription factors controlling *Ucp3* expression has been expanded by a further player. Notably, Coup-TFII appears to be the factor, that determines the final appropriate rate of gene transcription. Unfortunately, this factor is a

so-called orphan nuclear receptor, i.e. a nuclear receptor with unknown activating ligand or even without such a ligand at all. Thus, Coup-TFII cannot easily be interpreted as a sensor for a certain physiological signal (such as Ppar $\alpha$  linking fatty acid levels to *Ucp3* transcription). Our study implicates that activation of *Ucp3* by Coup-TFII is rather dependent on *Coup-TFII* expression levels itself, a process about which little is known so far. On the functional level, however, Coup-TFII has been hypothesized to be a negative regulator of glucose-induced gene expression (Lou *et al.*, 1999). The activation of genes implicated in lipid metabolism like lipoprotein lipase (Robinson *et al.*, 1999) and *Ucp3* appears to be a complementing aspect, broadening the role of Coup-TFII to regulate the shift in substrate usage from carbohydrates to fatty acids. Therefore, positive regulation of *Ucp3* by Coup-TFII strengthens its proposed role in lipid metabolism.

### *Chapter 2 – An intronic single base exchange leads to brown adipose tissue specific lack of Ucp3 and an altered body weight trajectory*

Chapter 2 covers our analysis of Djungarian hamsters with a tissue specific lack of *Ucp3* mRNA and protein. We initially sequenced the entire *Ucp3* gene and compared sequences derived from mutant and wildtype animals. Two positions within the first intron proved to be the only difference in this gene. By performing reporter gene assays with constructs harbouring the first intron in all four possible haplotypes we determined the base position, that leads to BAT specific *Ucp3* deficiency. The responsible allele could be identified in breeding colonies across the world including three, that were established from animals caught in Siberia independently from each other. We concluded, that this allele naturally occurs within the wild population.

We analyzed this binding site *in silico* and were able to identify corresponding elements in the first intron of seven other vertebrate species including humans. The pattern of conserved bases in this comparison reveals a putative forkhead factor binding site with the wildtype version of the polymorphic position being conserved in all species.

On the phenotypic level we observed a differential body weight trajectory between genotypes. Interestingly, heterozygous hamsters tended to resemble homozygous mutants in this respect, although *Ucp3* expression in these animals is only mildly affected. It seems that small changes in *Ucp3* expression can already lead to a full scale impact on body weight. This observation may be useful to re-evaluate human association studies, in which a certain *UCP3* promoter polymorphism (rs1800849; -55(C/T)) is associated with an altered BMI or waist-to-hip ratio (Otabe *et al.*, 2000; Cassell *et al.*, 2000). The close proximity of the *UCP2*

gene has always raised the question whether this effect can be clearly attributed to *UCP3* or to possible other polymorphisms within linkage disequilibrium (Walder *et al.*, 1998). Our study proves that an effect on the *Ucp3* promoter and hence its transcriptional regulation can very well be the causal link to an altered body weight. We so far cannot, however, decide between an effect attributable to lack of *Ucp3* in BAT and to a mildly reduced expression in skeletal muscle. While on the one hand the drastic difference in BAT *Ucp3* expression seems tempting to be held responsible, on the other hand skeletal muscle tissue accounts for a huge proportion of energy expenditure.

Regarding the mechanistic regulation of *Ucp3* we identified an essential component of tissue specific gene regulation, probably a forkhead domain containing protein.

### *Chapter 3 – Brown adipose tissue specific lack of Ucp3 is associated with impaired cold tolerance and reduced transcript levels of metabolic genes*

We further extended the phenotypical analysis of hamsters lacking BAT *Ucp3* as I report in Chapter 3. In Chapter 2 I already described an impact of this mutation on body weight development, here we investigated whether this may be a consequence of defective BAT function.

Hamsters of both homozygous genotypes were subjected to decreasing ambient temperatures while we measured oxygen consumption and CO<sub>2</sub> production. From this data set we derived and compared basal metabolic rate, maximal oxygen consumption, thermal conductance, respiratory quotient and cold tolerance limit (Heldmaier, 1974; Heldmaier & Ruf, 1992; Heldmaier *et al.*, 1982). All of these metabolic parameters seemed to be comparable between genotypes except cold tolerance, which was significantly impaired in mutant animals. This pattern implies defective thermogenic mechanisms on the background of an overall unchanged metabolism.

To explore whether BAT specific nonshivering thermogenesis or rather skeletal muscle mediated shivering thermogenesis is affected by altered *Ucp3* levels we injected hamsters with norepinephrine. This treatment induces maximal nonshivering thermogenesis without shivering, while in our cold exposure experiments the animals employed both shivering and nonshivering thermogenic mechanisms. Therefore, the provoked rise in metabolic rate can be used to dissect the contribution of both shivering and nonshivering thermogenic mechanisms (Böckler *et al.*, 1982). We analyzed individual values plotted against the respective body mass due to the high dependency between these parameters. The individual data points of

nonshivering thermogenic capacity of mutant hamsters were lower than expected from the wildtype regression, suggesting a brown fat specific thermogenic abnormality.

By analysis of gene expression we were able to demonstrate, that this defect is likely to be the physiological manifestation of a global decrease in metabolic gene expression in BAT. We measured mRNA levels of genes implicated in all major metabolic pathways including fatty acid mobilization, oxidation and synthesis, glucose import, glycolysis and citric acid cycle as well as ketone body utilization. Strikingly, 15 out of 16 genes analyzed displayed at least a trend towards lower mRNA levels in mutant hamsters.

Taken together these findings strongly suggest that Ucp3 is not itself an *a priori* thermogenic protein, but rather a component of the machinery delivering energy to thermogenic mechanisms in BAT. Furthermore this study demonstrates that the body weight phenotype we describe in chapter 2 might well be a consequence of impaired thermogenesis in BAT.

#### *Chapter 4 – Marsupial Ucp1 sheds light on the evolution of mammalian nonshivering thermogenesis*

In chapter 4 I present a publication that for the first time unequivocally proves the presence of Ucp1 in marsupial species and suggests the presence of an archetypical BAT in these early mammals.

My contribution to this study included the initial *in silico* analysis of genomic sequences and deduction of primers amplifying Ucp-like sequence fragments from *Monodelphis domestica* DNA. I cloned and sequenced these amplicons to infer nested oligonucleotides used to screen genomic *M. domestica* BAC libraries. This screening finally led to the definitive identification of all three marsupial uncoupling protein genes by phylogenetic inference and genomic localization between syntenic, neighbouring genes as compared to the human genome.

Furthermore, I brought in my expertise in the comparative analysis of promoter sequences. The eutherian *Ucp1* gene is regulated by a condensed enhancer sequence packed with transcription factor response elements (Silva & Rabelo, 1997). This enhancer box is located about 1kb upstream of the transcriptional start site and is essential for BAT specific and cold induced gene expression. I was able to pinpoint this enhancer box in a conserved formation in all eutherian mammals under investigation including the ancient afrotherian species *Echinops telfairi* but not in the marsupial *M. domestica*. Thus the condensed enhancer box first evolved in eutherian mammals, although the response elements located within this box may already be present dispersed across the marsupial promoter. The alignment of all six identified enhancer boxes and analysis of conservation did not only support the existence of several published

response elements but also highlighted a well conserved region encompassing a novel Ppar response element (PPRE).

### *Chapter 5 – Rapid single step subcloning procedure by combined action of type II and type IIs endonucleases with ligase*

Several of the methods I employed during my studies demand the subcloning of a DNA fragment from a given entry vector into one or more destination vector(s). A typical example would be the cloning of a PCR amplified promoter fragment followed by subcloning into destination vectors with different reporter genes. Another representative scenario is cloning of a coding sequence and subsequent subcloning into multiple expression vectors harbouring different promoters and/or tags. A standard laboratory practise is to excise the desired fragment, open the destination vector with the same restriction enzyme(s) and to purify and re-ligate the respective restriction products. This principal procedure is performed on a daily basis in innumerable variations in molecular biology labs around the world. In our hands it routinely includes an overnight ligation step decelerating progress. Alternative single step procedures based on recombinases (e.g. the Gateway® technique, Invitrogen) permit successful subcloning much faster but require recombinase recognition sites in all employed vectors, thus effectively limiting options to vectors sold by the same company.

In chapter 5 I describe a single step subcloning procedure independent of specialized sequence elements on the destination vector. The sole requirement is a certain restriction enzyme recognition site as it is found in the cloning site of virtually all plasmid vectors. All required steps can be performed within one hour, in a single tube and at room temperature.

Subcloning is facilitated by combination of a so-called ‘outside cutter’ restriction enzyme (type IIs) with a regular type II endonuclease and ligase. Specifically designed sequence elements of the entry vector and a regular restriction enzyme recognition site of the destination vector are randomly cut and ligated. The desired combination of insert and destination vector is the sole stable product, while all other intermediates are constantly re-digested. After one hour the complete mixture can be applied to transform competent bacterial cells without further purification.

In our experiments we provide proof of principle by the repeated, successful subcloning of a promoter fragment from a modified pGEM-T easy (Promega) entry vector into a pEGFP-N1 (Clontech) destination vector. We protected this novel cloning procedure by filing a patent.

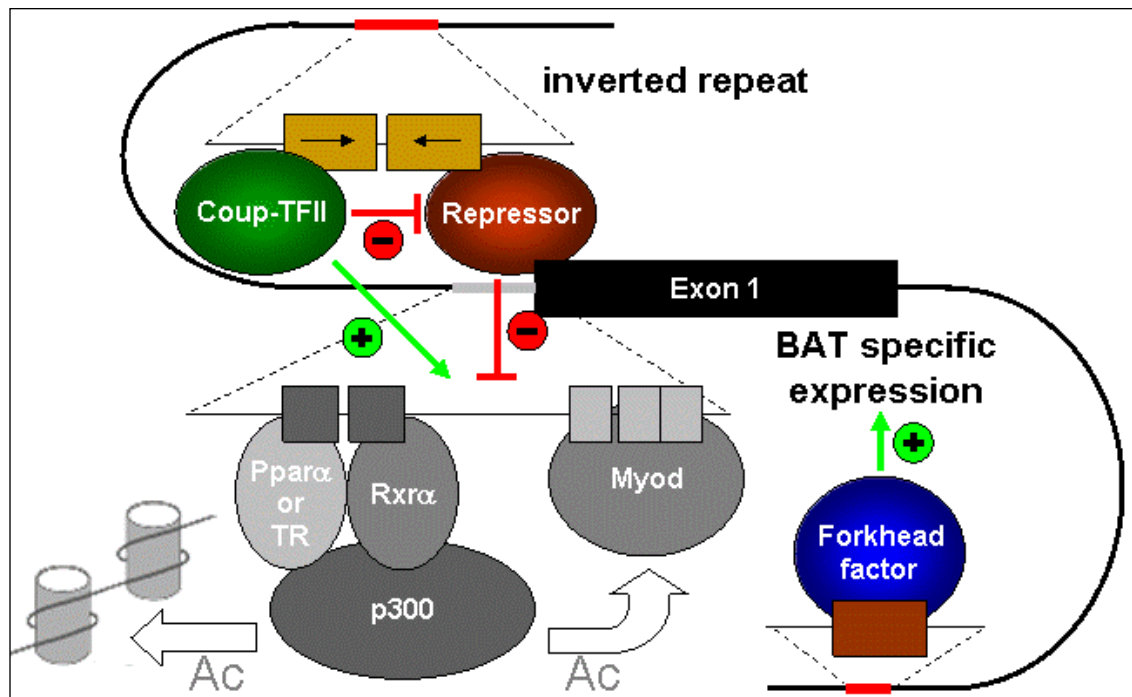


**Figure 3 – Regulation of *Ucp3* gene expression extended by novel findings.** An upstream inverted repeat binds Coup-TFII, which deactivates or displaces a repressor of *Ucp3* gene transcription. Downstream of the transcriptional start site an intronic forkhead factor response element governs brown adipose tissue (BAT) specific gene expression. Mechanisms depicted in gray shades are explained in Figure 2.

## Conclusion

The basal machinery underlying *Ucp3* transcription in skeletal muscle had been described previously and comprises Myod, Ppar $\alpha/\delta$ , TR and p300. I employed an unbiased promoter analysis and investigated a mutant hamster model devoid of *Ucp3* in brown adipose tissue to elucidate further mechanisms of transcriptional control.

Identification of a phylogenitically conserved promoter element led to the discovery of Coup-TFII being the factor, that may determine the final appropriate transcript levels in both skeletal muscle and BAT. Coup-TFII function is facilitated by deactivation or displacement of a so far unknown repressor protein (Figure 3). Coup-TFII is implicated in the regulation of a shift in energetic substrate usage from carbohydrates to fat and thereby substantiates a role of *Ucp3* in lipid metabolism.

By thorough investigation of Djungarian hamsters with a defect in *Ucp3* transcription we were able to identify a putative forkhead factor binding site essential for BAT specific *Ucp3* mRNA expression (Figure 3). This is the first and only tissue specific mechanism of *Ucp3* regulation known so far. Furthermore the far distal, intronic location of this regulatory element seems exceptional in itself.

On the phenotypic level lack of *Ucp3* in BAT led to a global decrease in metabolic gene expression that in turn seemed to be responsible for a defective BAT nonshivering thermogenesis. Mutant hamsters also displayed an increased body weight, that might be attributed to this disrupted mechanism of ‘wasting’ energy. These data implicate that *Ucp3* is necessary to sustain high metabolic rates in BAT.

Taken together, our analysis of the transcriptional regulation of *Ucp3* yielded two novel regulatory mechanisms with unique and remarkable characteristics, offers valuable clues about the physiological role of *Ucp3* and demonstrates the power of promoter analysis to elucidate regulation, function and origin of a gene.



## Reference List

- Bailey, P., Sartorelli, V., Hamamori, Y., & Muscat, G. E. (1998). The orphan nuclear receptor, COUP-TF II, inhibits myogenesis by post-transcriptional regulation of MyoD function: COUP-TF II directly interacts with p300 and myoD. *Nucleic Acids Res* **26**, 5501-5510.
- Böckler, H., Steinlechner, S., & Heldmaier, G. (1982). Complete cold substitution of noradrenaline-induced thermogenesis in the Djungarian hamster, *Phodopus sungorus*. *Experientia* **38**, 261-262.
- Boss, O., Samec, S., Kuhne, F., Bijlenga, P., Assimacopoulosjeannet, F., Seydoux, J., Giacobino, J. P., & Muzzin, P. (1998). Uncoupling protein-3 expression in rodent skeletal muscle is modulated by food intake but not by changes in environmental temperature. *J Biol Chem* **273**, 5-8.
- Boss, O., Samec, S., Paolonigiacobino, A., Rossier, C., Dulloo, A. G., Seydoux, J., Muzzin, P., & Giacobino, J. P. (1997). Uncoupling protein-3: A new member of the mitochondrial carrier family with tissue-specific expression. *FEBS Lett* **408**, 39-42.
- Cabrero, A., Jove, M., Planavila, A., Merlos, M., Laguna, J. C., & Vazquez-Carrera, M. (2003). Down-regulation of acyl-CoA oxidase gene expression in heart of troglitazone-treated mice through a mechanism involving chicken ovalbumin upstream promoter transcription factor II. *Mol.Pharmacol.* **64**, 764-772.
- Cannon, B., Hedin, A., & Nedergaard, J. (1982). Exclusive occurrence of thermogenin antigen in brown adipose tissue. *Elsevier Biomedical Press* **150**, 129-132.
- Cassell, P. G., Saker, P. J., Huxtable, S. J., Kousta, E., Jackson, A. E., Hattersley, A. T., Frayling, T. M., Walker, M., Kopelman, P. G., Ramachandran, A., Snehalatha, C., Hitman, G. A., & McCarthy, M. I. (2000). Evidence that single nucleotide polymorphism in the uncoupling protein 3 (UCP3) gene influences fat distribution in women of European and Asian origin. *Diabetologia* **43**, 1558-1564.
- Cunningham, S. A., Wiesinger, H., & Nicholls, D. G. (1986). Quantification of fatty acid activation of the uncoupling protein in brown adipocytes and mitochondria from the guinea-pig. *Eur J Biochem* **157**, 415-420.
- Echtay, K. S., Esteves, T. C., Pakay, J. L., Jekabsons, M. B., Lambert, A. J., Portero-Otin, M., Pamplona, R., Vidal-Puig, A. J., Wang, S., Roebuck, S. J., & Brand, M. D. (2003). A signalling role for 4-hydroxy-2-nonenal in regulation of mitochondrial uncoupling. *EMBO J* **22**, 4103-4110.

Echtay, K. S., Roussel, D., St Pierre, J., Jekabsons, M. B., Cadenas, S., Stuart, J. A., Harper, J. A., Roebuck, S. J., Morrison, A., Pickering, S., Clapham, J. C., & Brand, M. D. (2002). Superoxide activates mitochondrial uncoupling proteins. *Nature* **415**, 96-99.

Eubank, D. W., Duplus, E., Williams, S. C., Forest, C., & Beale, E. G. (2001). Peroxisome proliferator-activated receptor gamma and chicken ovalbumin upstream promoter transcription factor II negatively regulate the phosphoenolpyruvate carboxykinase promoter via a common element. *J Biol Chem* **276**, 30561-30569.

Fleury, C., Neverova, M., Collins, S., Raimbault, S., Champigny, O., Levi-Meyrueis, C., Bouillaud, F., Seldin, M. F., Surwit, R. S., Ricquier, D., & Warden, C. H. (1997). Uncoupling protein-2: a novel gene linked to obesity and hyperinsulinemia. *Nat. Genet.* **15**, 269-272.

Garlid, K. D., Orosz, D. E., Modriansky, M., Vassanelli, S., & Jezek, P. (1996). On the mechanism of fatty acid-induced proton transport by mitochondrial uncoupling protein. *J Biol Chem* **271**, 2615-2620.

Heldmaier, G. (1974). Temperature adaptation and brown adipose tissue in hairless and albino mice. *J Comp Physiol* **98**, 161-168.

Heldmaier, G. & Ruf, T. P. (1992). Body temperature and metabolic rate during natural hypothermia in endotherms. *Journal of comparative physiology.B, Biochemical, systemic, and environmental physiology.* **162**, 696-706.

Heldmaier, G., Steinlechner, S., & Rafael, J. (1982). Nonshivering thermogenesis and cold resistance during seasonal acclimatization in the Djungarian hamster. *J Comp Physiol* **149**, 1-9.

Himms-Hagen, J. & Harper, M. E. (2001). Physiological role of UCP3 may be export of fatty acids from mitochondria when fatty acid oxidation predominates: an hypothesis. *Exp Biol Med* **226**, 78-84.

Jaburek, M., Miyamoto, S., Di Mascio, P., Garlid, K. D., & Jezek, P. (2004). Hydroperoxy fatty acid cycling mediated by mitochondrial uncoupling protein UCP2. *J Biol Chem* **279**, 53097-53102.

Jezek, P., Engstova, H., Zackova, M., Vercesi, A. E., Costa, A. D. T., Arruda, P., & Garlid, K. D. (1998). Fatty acid cycling mechanism and mitochondrial uncoupling proteins. *Biochim Biophys Acta* **1365**, 319-327.

Klingenberg, M. & Winkler, E. (1985). The reconstituted isolated uncoupling protein is a membrane potential driven H<sup>+</sup> translocator. *EMBO J* **4**, 3087-3092.

Klingenspor, M. (2003). Cold-induced recruitment of brown adipose tissue thermogenesis. *Exp Physiol* **88**, 141-148.

Larkin, S., Mull, E., Miao, W., Pittner, R., Albrandt, K., Moore, C., Young, A., Denaro, M., & Beaumont, K. (1997). Regulation of the third member of the uncoupling protein family, UCP3, by cold and thyroid hormone. *Biochem Biophys Res Commun* **240**, 222-227.

Liebig, M., von Praun, C., Heldmaier, G., & Klingenspor, M. (2004). Absence of UCP3 in brown adipose tissue does not impair nonshivering thermogenesis. *Physiological and biochemical zoology : PBZ.* **77**, 116-126.

Lou, D. Q., Tannour, M., Selig, L., Thomas, D., Kahn, A., & Vasseur-Cognet, M. (1999). Chicken ovalbumin upstream promoter-transcription factor II, a new partner of the glucose response element of the L-type pyruvate kinase gene, acts as an inhibitor of the glucose response. *Journal of Biological Chemistry* **274**, 28385-28394.

Nedergaard, J., Matthias, A., Golozoubova, V., Jacobsson, A., & Cannon, B. (1999). UCP1: the original uncoupling protein--and perhaps the only one? New perspectives on UCP1, UCP2, and UCP3 in the light of the bioenergetics of the UCP1-ablated mice [In Process Citation]. *J.Bioenerg.Biomembr.* **31**, 475-491.

Nicholls, D. G., Bernson, V. S., & Heaton, G. M. (1978). The identification of the component in the inner membrane of brown adipose tissue mitochondria responsible for regulating energy dissipation. *Experientia Suppl.* **32**, 89-93.

Nicholls, D. G. & Locke, R. M. (1984). Thermogenic mechanisms in brown fat. *Physiol Rev* **64**, 1-64.

Otabe, S., Clement, K., Dina, C., Pelloux, V., Guy-Grand, B., Froguel, P., & Vasseur, F. (2000). A genetic variation in the 5' flanking region of the UCP3 gene is associated with body mass index in humans in interaction with physical activity. *Diabetologia* **43**, 245-249.

Pedraza, N., Rosell, M., Villarroya, J., Iglesias, R., Gonzalez, F. J., Solanes, G., & Villarroya, F. (2006). Developmental and tissue-specific involvement of peroxisome proliferator-activated receptor-alpha in the control of mouse uncoupling protein-3 gene expression. *Endocrinology* **147**, 4695-4704.

Rial, E., Aguirregoitia, E., Jimenez-Jimenez, J., & Ledesma, A. (2004). Alkylsulfonates activate the uncoupling protein UCP1: implications for the transport mechanism. *Biochim.Biophys.Acta* **1608**, 122-130.

Robinson, C. E., Wu, X., Nawaz, Z., Onate, S. A., & Gimble, J. M. (1999). A corepressor and chicken ovalbumin upstream promoter transcriptional factor proteins modulate peroxisome

proliferator-activated receptor-gamma<sup>2</sup>/retinoid X receptor alpha-activated transcription from the murine lipoprotein lipase promoter. *Endocrinology* **140**, 1586-1593.

Sell, H., Deshaies, Y., & Richard, D. (2004). The brown adipocyte: update on its metabolic role. *International Journal of Biochemistry & Cell Biology* **36**, 2098-2104.

Shabalina, I. G., Jacobsson, A., Cannon, B., & Nedergaard, J. (2004). Native UCP1 displays simple competitive kinetics between the regulators purine nucleotides and fatty acids. *J Biol Chem* **279**, 38236-38248.

Silva, J. E. & Rabelo, R. (1997). Regulation of the uncoupling protein gene expression. *Eur J Endocrinol* **136**, 251-264.

Solanes, G., Pedraza, N., Calvo, V., Vidal-Puig, A. J., Lowell, B. B., & Villarroya, F. (2005). Thyroid hormones directly activate the expression of the human and mouse uncoupling protein-3 genes through a thyroid response element in the proximal promoter region. *Biochem J* **386**, 505-513.

Solanes, G., Pedraza, N., Iglesias, R., Giralt, M., & Villarroya, F. (2000). The human uncoupling protein-3 gene promoter requires MyoD and is induced by retinoic acid in muscle cells. *FASEB J* **14**, 2141-2143.

Solanes, G., Pedraza, N., Iglesias, R., Giralt, M., & Villarroya, F. (2003). Functional relationship between MyoD and peroxisome proliferator-activated receptor-dependent regulatory pathways in the control of the human uncoupling protein-3 gene transcription. *Mol Endocrinol* **17**, 1944-1958.

Stavinoha, M. A., RaySpellicy, J. W., Essop, M. F., Graveleau, C., Abel, E. D., Hart-Sailors, M. L., Mersmann, H. J., Bray, M. S., & Young, M. E. (2004). Evidence for mitochondrial thioesterase 1 as a peroxisome proliferator-activated receptor-alpha-regulated gene in cardiac and skeletal muscle. *American Journal of Physiology* **287**, E888-E895.

Tsuboyamakasaoka, N., Tsunoda, N., Maruyama, K., Takahashi, M., Kim, H., Ikemoto, S., & Ezaki, O. (1998). Up-regulation of uncoupling protein 3 (UCP3) mRNA by exercise training and down-regulation of UCP3 by denervation in skeletal muscles. *Biochem Biophys Res Commun* **247**, 498-503.

Vidal-Puig, A. J., Solanes, G., Grujic, D., Flier, J. S., & Lowell, B. B. (1997). UCP3: an uncoupling protein homologue expressed preferentially and abundantly in skeletal muscle and brown adipose tissue. *Biochem Biophys Res Commun* **235**, 79-82.

von Praun, C., Burkert, M., Gessner, M., & Klingenspor, M. (2001). Tissue-specific expression and cold-induced mRNA levels of uncoupling proteins in the Djungarian hamster. *Physiological and biochemical zoology : PBZ.* **74**, 203-211.

Walder, K., Norman, R. A., Hanson, R. L., Schrauwen, P., Neverova, M., Jenkinson, C. P., Easlick, J., Warden, C. H., Pecqueur, C., Raimbault, S., Ricquier, D., Silver, M. H., Shuldiner, A. R., Solanes, G., Lowell, B. B., Chung, W. K., Leibel, R. L., Pratley, R., & Ravussin, E. (1998). Association between uncoupling protein polymorphisms (UCP2-UCP3) and energy metabolism/obesity in Pima indians. *Hum.Mol.Genet.* **7**, 1431-1435.

Weigle, D. S., Selfridge, L. E., Schwartz, M. W., Seeley, R. J., Cummings, D. E., Havel, P. J., Kuijper, J. L., & Beltrandelrio, H. (1998). Elevated free fatty acids induce uncoupling protein 3 expression in muscle: A potential explanation for the effect of fasting. *Diabetes* **47**, 298-302.

Research article

**Chicken ovalbumin upstream promoter transcription factor II regulates uncoupling protein 3 gene transcription in *Phodopus sungorus***Tobias Fromme\*<sup>1</sup>, Kathrin Reichwald<sup>2</sup>, Matthias Platzer<sup>2</sup>, Xing-Sheng Li<sup>1</sup> and Martin Klingenspor<sup>1</sup>Address: <sup>1</sup>Department of Animal Physiology, Faculty of Biology, Philipps-University, D-35043 Marburg, Germany and <sup>2</sup>Genome Analysis, Leibniz-Institute for Age Research – Fritz Lipmann Institute, D-07745 Jena, GermanyEmail: Tobias Fromme\* - [fromme@staff.uni-marburg.de](mailto:fromme@staff.uni-marburg.de); Kathrin Reichwald - [kathrinr@fli-leibniz.de](mailto:kathrinr@fli-leibniz.de); Matthias Platzer - [mplatzer@fli-leibniz.de](mailto:mplatzer@fli-leibniz.de); Xing-Sheng Li - [lixs@ioz.ac.cn](mailto:lixs@ioz.ac.cn); Martin Klingenspor - [klingens@staff.uni-marburg.de](mailto:klingens@staff.uni-marburg.de)

\* Corresponding author

Published: 04 January 2007

Received: 07 July 2006

BMC Molecular Biology 2007, 8:1 doi:10.1186/1471-2199-8-1

Accepted: 04 January 2007

This article is available from: <http://www.biomedcentral.com/1471-2199/8/1>

© 2007 Fromme et al; licensee BioMed Central Ltd.

This is an Open Access article distributed under the terms of the Creative Commons Attribution License (<http://creativecommons.org/licenses/by/2.0>), which permits unrestricted use, distribution, and reproduction in any medium, provided the original work is properly cited.**Abstract**

**Background:** Ucp3 is an integral protein of the inner mitochondrial membrane with a role in lipid metabolism preventing deleterious effects of fatty acids in states of high lipid oxidation. Ucp3 is expressed in brown adipose tissue and skeletal muscle and controlled by a transcription factor complex including PPARalpha, MyoD and the histone acetyltransferase p300. Several studies have demonstrated interaction of these factors with chicken ovalbumin upstream promoter transcription factor II (Coup-TFII). This nuclear receptor is involved in organogenesis and other developmental processes including skeletal muscle development, but also co-regulates a number of metabolic genes. In this study we *in silico* analyzed the upstream region of Ucp3 of the Djungarian hamster *Phodopus sungorus* and identified several putative response elements for Coup-TFII. We therefore investigated whether Coup-TFII is a further player in the transcriptional control of the Ucp3 gene in rodents.

**Results:** By quantitative PCR we demonstrated a positive correlation of Coup-TFII and Ucp3 mRNA expression in skeletal muscle and brown adipose tissue in response to food deprivation and cold exposure, respectively. In reporter gene assays Coup-TFII enhanced transactivation of the Ucp3 promoter conveyed by MyoD, PPARalpha, RXRalpha and/or p300. Using deletions and mutated constructs, we identified a Coup-TFII enhancer element 816–840 bp upstream of the transcriptional start site. Binding of Coup-TFII to this upstream enhancer was confirmed in electrophoretic mobility shift and supershift assays.

**Conclusion:** Transcriptional regulation of the Coup-TFII gene in response to starvation and cold exposure seems to be the regulatory mechanism of Ucp3 mRNA expression in brown adipose and skeletal muscle tissue determining the final appropriate rate of transcript synthesis. These findings add a crucial component to the complex transcriptional machinery controlling expression of Ucp3. Given the substantial evidence for a function of Ucp3 in lipid metabolism, Coup-TFII may not only be a negative regulator of glucose responsive genes but also transactivate genes involved in lipid metabolism.

## Background

Uncoupling protein 3 (Ucp3) is a member of the family of uncoupling proteins, which are located in the inner mitochondrial membrane and uncouple the respiratory chain from ATP synthesis by dissipating the proton motive force [1,2]. The physiological function of Ucp3 is subject to an ongoing debate [3]. Regulation of *Ucp3* expression suggests a role in lipid metabolism. Skeletal muscle *Ucp3* transcription is increased in response to food deprivation, a robust mechanism consistently observable in man, rodents and even fish [4]. Further physiological conditions positively regulating *Ucp3* include cold exposure [5,6], acute exercise [7] and streptozotocin-induced diabetes [8]. Increased levels of circulating free fatty acids (FFA) are common to all these physiological states; infusion experiments imply that these are the primary cause for *Ucp3* upregulation [9]. Therefore it has been suggested, though not proven experimentally, that Ucp3 is a fatty acid anion carrier [10].

The biochemical properties of the protein as measured in mitochondrial proton leak assays by parallel recording of membrane potential and oxygen consumption infer a role for Ucp3 in the defense against radical oxygen species (ROS), mitigating their generation by mild uncoupling [11]. This possible function is corroborated by the finding that a product of ROS induced lipid peroxidation, 4-hydroxy-2-nonenal, specifically induces uncoupling by Ucp3 and that even a small reduction of membrane potential markedly decreases ROS production [12]. A controversial hypothesis which takes into account both physiological and biochemical data emphasizes that the export of fatty acids or hydroperoxy fatty acids and subsequent protonated re-influx of a certain fraction into the matrix would result in a net proton import detectable as mild uncoupling [13,14]. This mechanism would reduce ROS production and at the same time reduce the level of non-esterified fatty acids in the matrix susceptible to peroxidation, thereby preventing deleterious effects in states of high lipid oxidation.

*Ucp3* is predominantly expressed in skeletal muscle (SKM) and brown adipose tissue (BAT), both tissues with exceptionally high lipid oxidation capacities. The principal molecular constituents of *Ucp3* gene regulation have recently been identified by several copious studies. Heterodimers of peroxisome proliferator activated receptor  $\alpha$  (PPAR $\alpha$ ) and the retinoic X receptor  $\alpha$  (RXR $\alpha$ ) bind to a response element (PPRE) within the proximal promoter region and activate transcription depending on the presence of myogenic differentiation antigen 1 (MyoD). MyoD binds to a series of non-canonical E-boxes directly adjacent to the transcriptional start site (TSS). Induction is enhanced by the coactivator p300 protein (p300), which acetylates MyoD and possibly surrounding histones [15].

Furthermore, the PPRE in the *Ucp3* promoter is multifunctional, i.e. can alternatively be targeted by heterodimers of the thyroid hormone receptor (TR) and RXR $\alpha$  stimulating expression in the presence of MyoD [16]. The ligands of PPAR $\alpha$  (fatty acids) and TRs (T3) along with the requirement of MyoD indicate that this mechanism is involved in the acute response of *Ucp3* expression in SKM to physiological stimuli. However, to our knowledge neither BAT-specific nor differentiation specific regulation has been characterized in detail to date.

Notably several studies have demonstrated interaction of PPARs, MyoD and/or p300 with chicken ovalbumin upstream promoter transcription factor II (Coup-TFII, official gene name: *Nr2f2*) [17-20]. This nuclear receptor is involved in organogenesis and other developmental processes [21] including SKM development [22], but also co-regulates a number of metabolic genes [18,23-25].

In this study we analyzed the upstream region of *Ucp3* of the Djungarian hamster *Phodopus sungorus in silico* and identified several putative response elements for Coup-TFII. We therefore investigated whether Coup-TFII is a further player in the transcriptional control of the *Ucp3* gene in rodents.

## Results

### Structure of the hamster *Ucp3* gene

We successfully cloned the genomic *Ucp3* locus of the hamster. Primers to amplify fragments of the upstream region (approx. -3500 to +50) were deduced from conserved segments of corresponding rodent genomic sequences. Resulting PCR products were sequenced and served as a framework to select primers for gap closure. We extended this contig to the putative 5' adjacent gene. *Ucp3* introns were amplified with exonic primers based on the known hamster cDNA [GenBank: [AF271265](#)] and on the exon 1 sequence obtained as described above. The resulting genomic contig of 12,720bp included 3632 bp of *Ucp3* 5' gene flanking region as well as all *Ucp3* exons and introns; the sequence of the terminal exon extends 210 bp 3' of the stop codon [GenBank: [AY523564](#)].

We identified two novel splice variants of the *Ucp3* transcript in BAT [GenBank: [DQ244043](#), [DQ244044](#); not shown]. One transcript is characterized by partial mobilization of the second intron, presumably resulting in a premature stop [GenBank: [DQ244044](#)], the other lacks the second exon, possibly leading to alternative usage of the next in frame start codon which is located in exon3 [GenBank: [DQ244043](#)].

In our 5' RACE analysis, the TSS was variable within a range of 72 bp (Fig. 1). To determine a reference point for relative sequence positions we arbitrarily chose position





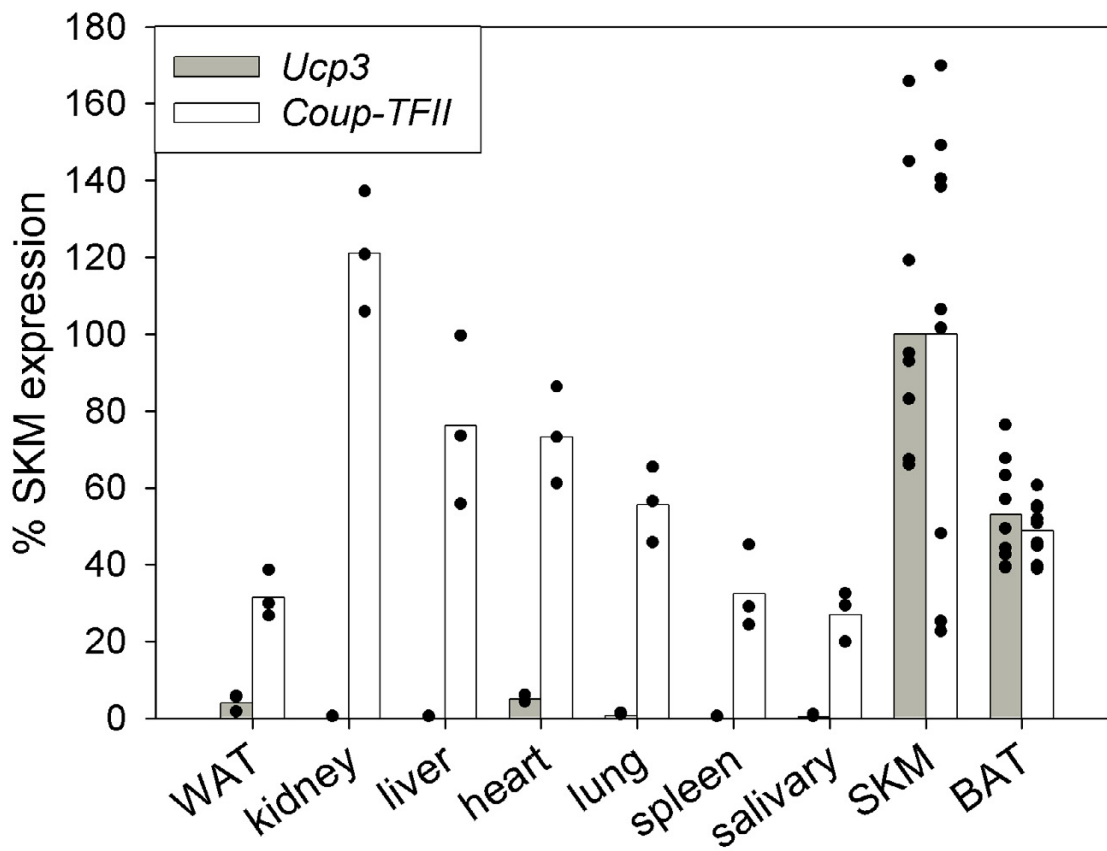


**Figure 2**

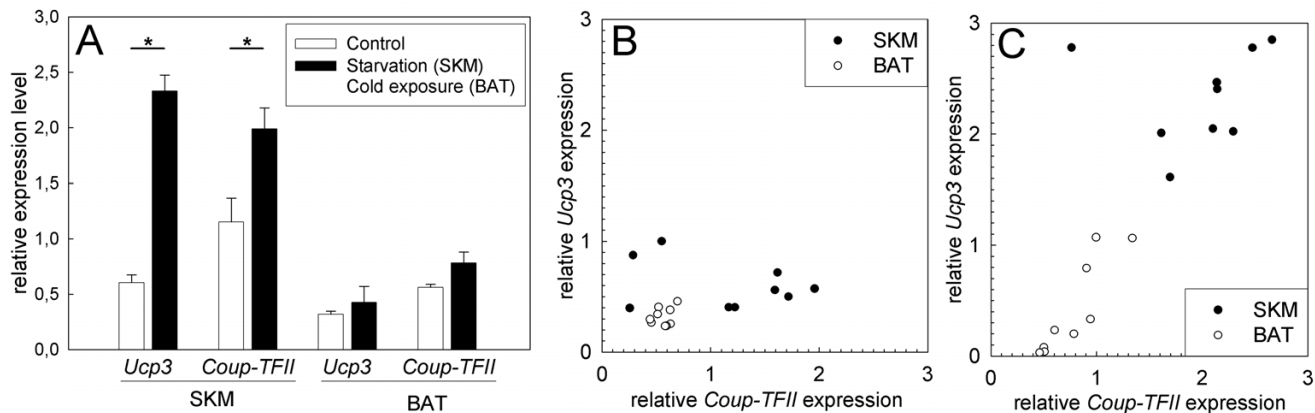
**Expression level of *Coup-TFII* and *Ucp3* mRNA in tissues of *P. sungorus*.** *Coup-TFII* mRNA is expressed in all examined tissue types as measured by qPCR. *Ucp3* mRNA is found together with *Coup-TFII* mRNA in BAT and SKM. Both display highest variability in SKM (SKM/BAT n = 9, other tissues n = 3). Black dots represent individual results, bars are mean values. WAT = white adipose tissue, SKM = skeletal muscle, BAT = brown adipose tissue.

cant induction of *Ucp3* and *Coup-TFII*. In BAT of cold exposed hamsters *Ucp3* was not systematically upregulated but displayed an increased individual variation. A similar degree of variation without significant cold-induced regulation was observed for *Coup-TFII*. To test for a possible coregulation we measured *Ucp3* and *Coup-TFII* transcript abundancies and compared respective levels of control and challenged animals (Fig. 3B and 3C). Under control conditions no correlation was observed. However, we detected a highly significant correlation ( $r^2 = 0.834$ ,  $p < 0.001$ ) between *Ucp3* and *Coup-TFII* levels in challenged animals.

#### **Luciferase reporter gene assays with cotransfected transcription factors**

We tested *Coup-TFII* in cotransfection reporter gene assays with regard to its potential in coactivating a *Ucp3* promoter fragment of 2244 bp cloned into the luciferase reporter gene vector pGL3basic (-2244*Ucp3*luc). To evaluate the influence of *Coup-TFII* we compared cotransfections with or without expression vectors for PPAR $\alpha$ , MyoD, RXR $\alpha$  and/or the histone acetyltransferase p300, factors known to regulate *Ucp3* expression [15] (Fig. 4A).

Without *Coup-TFII* none of the tested factors upregulated -2244*Ucp3*luc more than 5-fold. Cotransfection of several factors exhibited a synergistic effect, which was augmented by p300, e.g. adding RXR $\alpha$  to MyoD hardly increased reporter gene activity, but in the presence of

**Figure 3****Response of *Coup-TFII* and *Ucp3* mRNA expression to physiological challenges inducing lipid utilization. (A)**

Expression of *Coup-TFII* and *Ucp3* mRNA in BAT of cold exposed and SKM of food deprived hamsters as compared to control conditions. Shown are mean values with standard error, \* =  $p < 0.05$ . (B) Relationship of *Ucp3* and *Coup-TFII* mRNA levels in SKM and BAT of hamsters housed under standard conditions with *ad libitum* access to food;  $r^2 = 0.211$ ,  $p =$  not significant (SKM  $n = 9$ , BAT  $n = 9$ ). (C) Correlation of *Ucp3* and *Coup-TFII* mRNA abundancies in SKM of food deprived and BAT of cold exposed animals;  $r^2 = 0.834$ ,  $p < 0.001$  (SKM  $n = 9$ , BAT  $n = 9$ ).

p300 notably induced expression. The strongest induction (47-fold) was achieved by a cotransfection of PPAR $\alpha$ , MyoD and p300 in the presence of the synthetic PPAR $\alpha$  agonist Wy14,643.

Cotransfection of Coup-TFII systematically increased reporter gene expression in all combinations tested. Together with a single other factor it was particularly effective with MyoD or p300, attaining an additional 3–5 fold induction. In combination with multiple factors Coup-TFII cotransfection consistently led to an approximate doubling of induction. The maximal induction in comparison to the basal construct activity was achieved in combination with RXR $\alpha$ , MyoD and p300 (95-fold), which is two fold higher than the maximal level observed in any experiment without Coup-TFII (ligand-activated PPAR $\alpha$  + MyoD + p300, 47-fold). The dimension of induction by Coup-TFII is illustrated by comparison with the PPAR $\alpha$  activation through the ligand Wy14,643 on a background of PPAR $\alpha$ , MyoD and p300. Here transactivation by Coup-TFII and the ligand Wy14,643, respectively, is in the same order of magnitude.

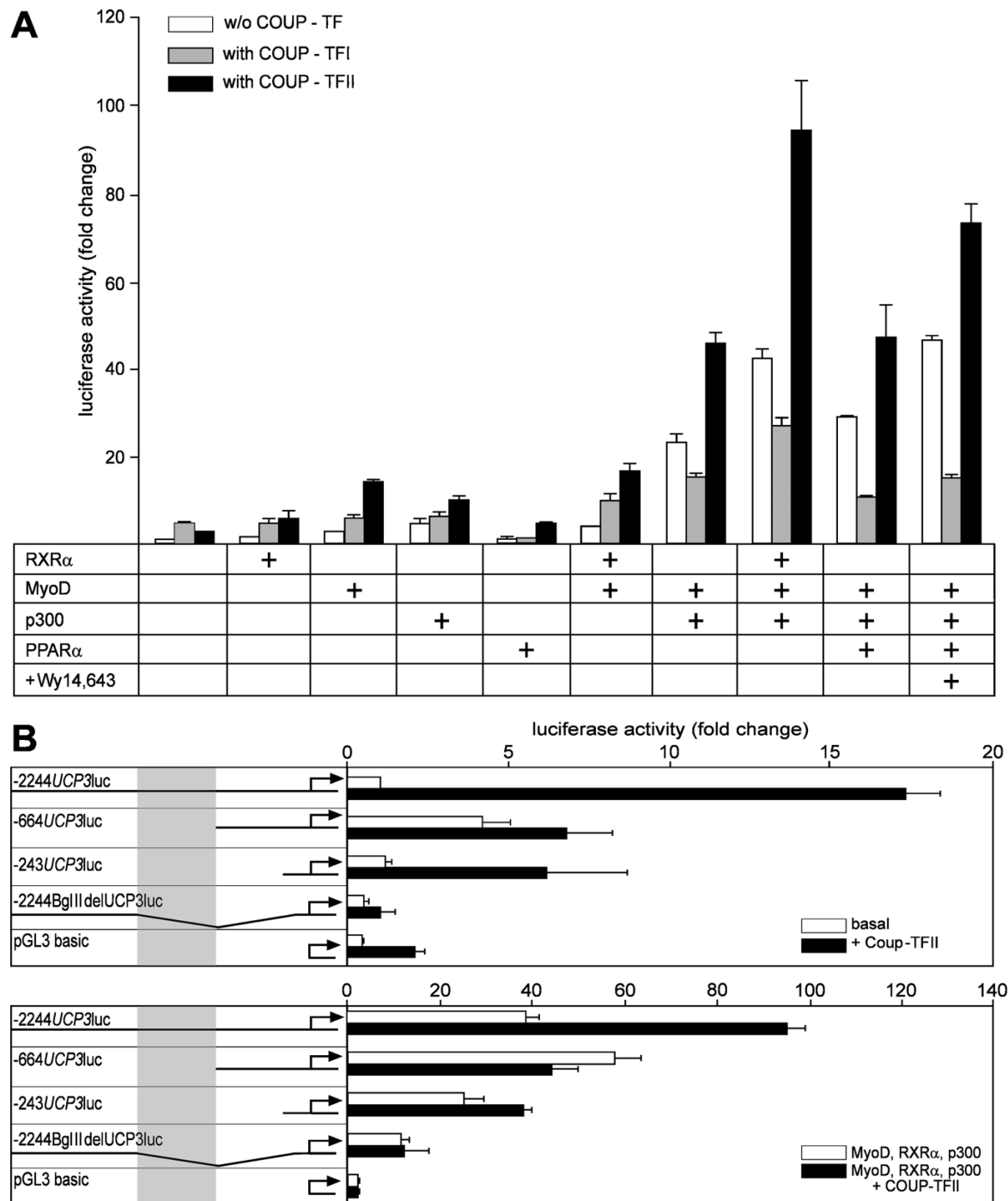
To exclude that overexpression of any nuclear receptor or Coup-TF family member unspecifically leads to an induction of the *Ucp3* promoter we utilized an expression vector for Coup-TFI, which is a close Coup-TFII relative sharing 85.5% of identical amino acid sequence, as a control. Replacing Coup-TFII by Coup-TFI in cotransfections with transcription factor combinations did not lead to activa-

tion of the *Ucp3* promoter, but conversely downregulated reporter gene activity (Fig. 4A), possibly due to competition for RXR $\alpha$ . We therefore conclude that Coup-TFII specifically transactivated the *Ucp3* promoter in synergy with other known transcription factors and coactivators.

To locate the responsible *cis* element, we studied the potential of Coup-TFII to activate several reporter gene deletion constructs (Fig. 4B). Coup-TFII transfection alone in this assay increased luciferase activity on -2244*Ucp3*luc 16-fold while all other constructs are much less sensitive. There is, however, a certain unspecific effect on the empty pGL3 basic vector, that can also be seen for all constructs used. This handicap was absent when we cotransfected the deletion constructs with MyoD, RXR $\alpha$  and p300, the combination exhibiting the strongest effect on -2244*Ucp3*luc. The Coup-TFII effect is limited to -2244*Ucp3*luc, locating the crucial region between nucleotides -1307 to -664, which are exclusively found on this construct. We identified several possible binding sites for Coup-TFII in this fragment: -1269 (A), -901 (B), -837 and -827 (C), -807 (D) and -779 (E).

**Electrophoretic mobility shifts assays**

We tested five oligonucleotide probes corresponding to the putative response elements A-E (see above) for binding of Coup-TFII in electrophoretic mobility shift assays. Elements A, B, D and E did not display any specific interaction (Fig. 5A). For element C we were able to show a strong complex formation in the presence of Coup-TFII,

**Figure 4**

**Coup-TFII transactivates the *Ucp3* promoter in cotransfection reporter gene assays. (A)** Activity of reporter gene construct -2244UCP3luc in cotransfection experiments with various transcription factors (fold change relative to basal -2244UCP3luc level). Coup-TFII coactivates the *Ucp3* promoter in all combinations. It is especially effective together with MyoD, RXRα and p300. Coup-TFI does not activate reporter gene expression demonstrating a specific effect of Coup-TFII. **(B)** Identification of the region mediating Coup-TFII transactivation by analysis of deletion reporter gene constructs. Shown in the upper panel is the basal activity and induction by Coup-TFII of all constructs, in the lower panel the experiment was repeated on a background of MyoD, RXRα and p300 (note the different axis scaling). The shaded area highlights the region that is exclusively found on -2244UCP3luc and is responsible for the Coup-TFII effect in both setups.

that was specifically supershifted by the respective antibody. Binding of proteins to this probe was effectively blocked by competition with the unlabelled oligonucleotide.

The antibody was specific for Coup-TFII and did not bind the close relative Coup-TFI. Virtually all Coup-TFII was detected in the nuclear fraction (Fig. 5B).

Nuclear extracts from skeletal muscle tissue of food deprived (n = 3) and control (n = 3) hamsters were able to form a bandshift on element C of comparable size. In two

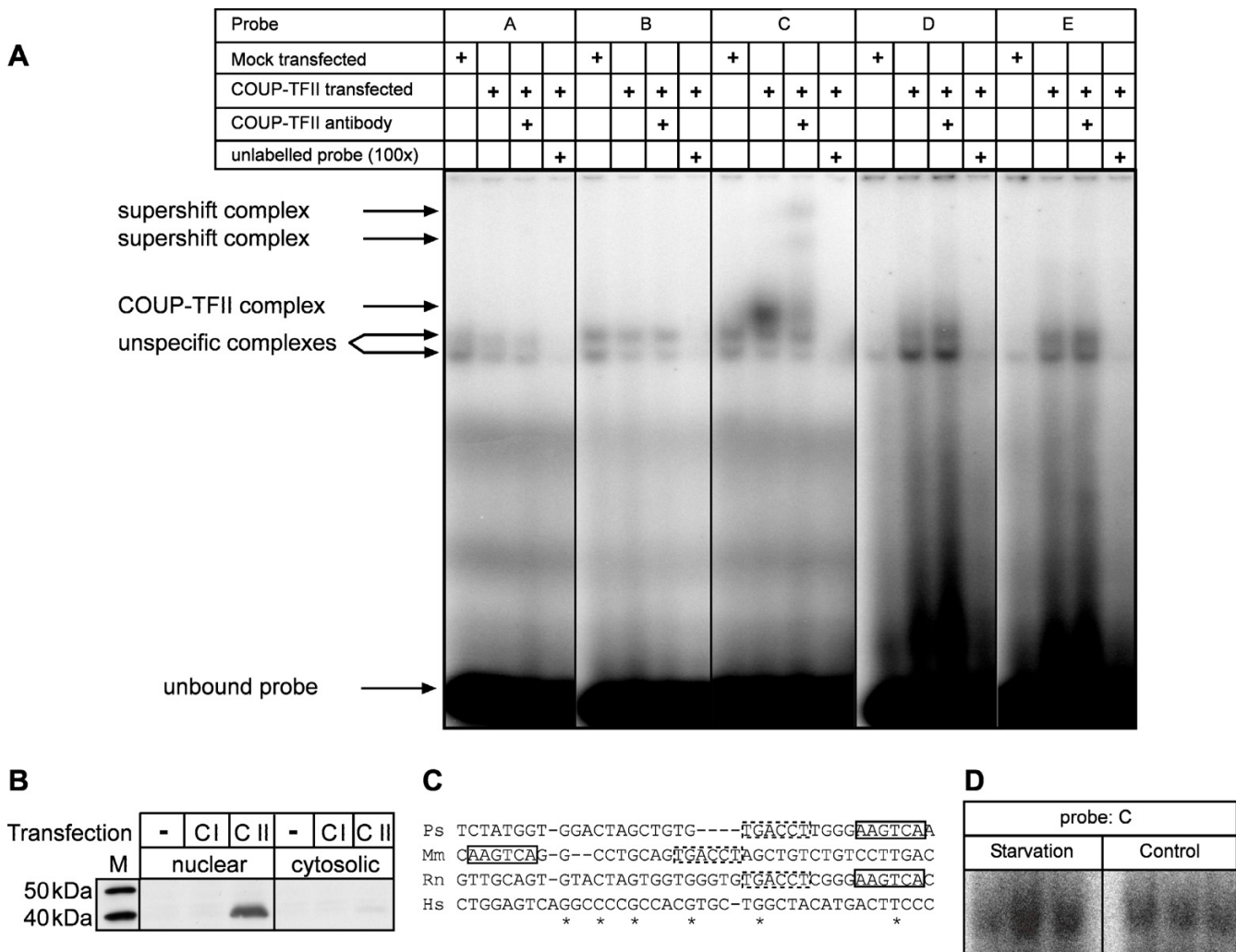


**Figure 5**

**Coup-TFII binds to a conserved element of the Ucp3 promoter.** (A) Electrophoretic mobility shift assay with candidate probes A-E and nuclear extracts of HEK293 cells. Overexpression of Coup-TFII leads to formation of a specific complex on probeC only, that can be supershifted with a Coup-TFII antibody. All complexes are subject to competition with 100 fold molar excess of unlabelled probe C. (B) Western Blot of protein fractions of HEK293 cells with a Coup-TFII-antibody. Coup-TFII is specifically detected in the nuclear fraction and absent in untransfected cells. M = Marker, - = mock transfected, CI = Coup-TFI transfected, CII = Coup-TFII transfected. (C) Alignment of the human and rodent promoter regions of the *Ucp3* gene (Ps: -821 to -857). The positions of identical bases are marked (\*). The putatively Coup-TFII binding elements (box, dashed box) located on probe C are conserved in all rodent species. In the murine promoter they are found in reverse order slightly more upstream. The human promoter does not feature comparable sequences in the compared region. Rn = *R. norvegicus*, Mm = *M. musculus*, Ps = *P. sungorus*, Hs = *H. sapiens* (D) Electrophoretic mobility shift assay with skeletal muscle nuclear extracts from control and food deprived hamsters. The complex shown is of a size comparable to the Coup-TFII complex above. Starvation induces complex formation in comparison to control conditions.

out of three starvation samples the complex was stronger than in control conditions (Fig. 5D).

The two elements present in oligonucleotide C form a functional repeat as is typical for binding sites of nuclear receptor dimers. This inverse repeat is conserved in the rat *Ucp3* promoter, and also found slightly more upstream in the murine promoter albeit in reverse order (Fig. 5C).

#### Mutational analyses of the Coup-TFII binding element

We further analysed the two repeat elements on oligonucleotide C (Cwt) by disrupting the 5' half (Cmut5'), the 3' half (Cmut3') or both (Cmut5'3') on bandshift assay probes (Fig. 6D). We chose to change two bases of the 3' half-site into adenine and two bases of the inverse 5' half-site into thymine correspondingly. These probes were employed either labelled with nuclear extracts of mock or Coup-TFII transfected cells or unlabelled as competitors for the interaction of Coup-TFII with element C (Fig. 6A).

All mutated probes displayed a reduced complex formation with Coup-TFII (Fig. 6B). While probes Cmut5' and Cmut5'3' did not show any significant complex formation, probe Cmut3' still formed a complex that was weaker in intensity and slightly smaller than the wt probe. In competition assays the mutated competitor oligonucleotides were less efficient in competing Coup-TFII complex formation on the Cwt probe than the unlabelled Cwt oligonucleotide itself (Fig. 6C). Again Cmut5' and Cmut5'3' generated a similar pattern of no binding of Coup-TFII to these mutated elements. Mutation Cmut3' did not entirely lose its ability to compete complex formation, which is in line with its demonstrated retained capability of interaction with Coup-TFII.

We introduced the same mutations Cmut5' and Cmut3' into our reporter gene vector -2244UCP3luc generating -2244Cmut5'luc and -2244Cmut3'luc (Fig. 7). Disruption of the 3' half-site on -2244Cmut3'luc did not lower respon-

## A

probe	Cwt	Cmut3'	Cmut5'	Cmut5'3'		Cwt											
comp.	none					Cwt 2x	Cwt 10x	Cwt 100x	Cmut3' 2x	Cmut3' 10x	Cmut3' 100x	Cmut5' 2x	Cmut5' 10x	Cmut5' 100x	Cmut5'3' 2x	Cmut5'3' 10x	Cmut5'3' 100x
CII	+	+	+	+	+	+	+	+	+	+	+	+	+	+	+	+	+
mock	+	+	+	+	+												

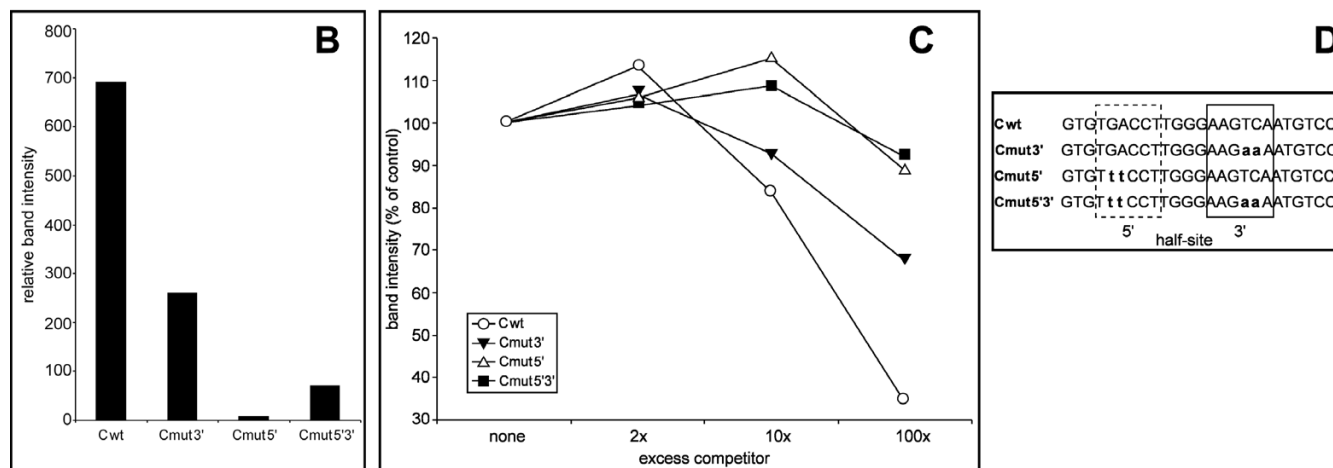


**Figure 6**

**Disruption of the 5' half-site leads to loss of Coup-TFII binding.** (A) Electrophoretic mobility shift assay with element C and mutated derivatives (compare (D)). Bands were quantified, background corrected and analyzed. Probe = labelled oligonucleotide used; comp. = unlabelled competitor oligonucleotide used; CII = nuclear extract of Coup-TFII transfected HEK293 cells; mock = nuclear extract of mock transfected HEK293 cells. (B) Quantification of complex intensity on labelled probes Cwt, Cmut5', Cmut3' and Cmut5'3'. Probe Cmut3' retained a lowered ability to bind Coup-TFII while Cmut5' and Cmut5'3' were unable to do so. (C) Accordingly unlabelled competitor probe Cmut3' was still able to partially compete for Coup-TFII binding to the labelled wt probe, while Cmut5' and Cmut5'3' were not. (D) Overview of the probes used in electrophoretic mobility shift assays. Probe Cwt represents element C, the mutated derivatives are depicted below.

siveness to Coup-TFII alone or on a background of MyoD, RXR $\alpha$  and p300, but did even proportionally increase luciferase activity by a small amount. Conversely, -2244*Cmut5*'luc was devoid of any luciferase activity in all conditions tested and displayed a pattern resembling our empty control vector pGL3 basic.

## Discussion

A prominent hypothesis considers uncoupling protein 3 (Ucp3) to be a crucial component of lipid metabolism with implications for the regulation of body weight and composition [3]. This role is further substantiated by the identification of polymorphisms/alleles in the human *Ucp3* gene that are associated with an elevated body mass index [28]. A more detailed analysis of the machinery regulating *Ucp3* transcription is therefore of importance for identifying regulatory networks controlling energy partitioning.

Our comparison of previously characterized *Ucp3* promoter elements in rat, mouse and human with the hamster sequence, shows full conservation of the binding sites for MyoD, PPAR $\alpha$ /RXR $\alpha$  and TR/RXR $\alpha$  heterodimers. The sequence alignment furthermore demonstrates that two TATA-like boxes present in the human promoter [26] are

absent in rodent sequences including the hamster. This might prove to be crucial considering, that in the study of Riquet and coworkers (2003) the activities of human constructs were investigated in murine tissue.

The TSS of the human *Ucp3* gene is quite variable and displays a distinct tissue specificity, whereas in mouse the TSS is located at a single site [29]. Our result of variable TSS in *P. sungorus* demonstrates that the constancy in mouse does not reflect a common trait of rodent species. However, in the hamster the TSS did not show a distinct tissue specificity as found in humans.

By *in silico* analysis we identified Coup-TFII as a candidate transcription factor for the regulation of *Ucp3* expression. Coup-TFII is a 45 kD nuclear orphan receptor and member of the COUP-TF family. The amino acid sequence of the ligand binding and the DNA binding domain is conserved across species to a very high extent (human vs. *Drosophila* ~90%) indicating an important role for these domains. Coup-TFII has mainly been described as a crucial factor in developmental processes [21,22].

By qPCR we measured *Ucp3* and *Coup-TFII* transcript levels in a panel of nine different tissues. We confirmed that

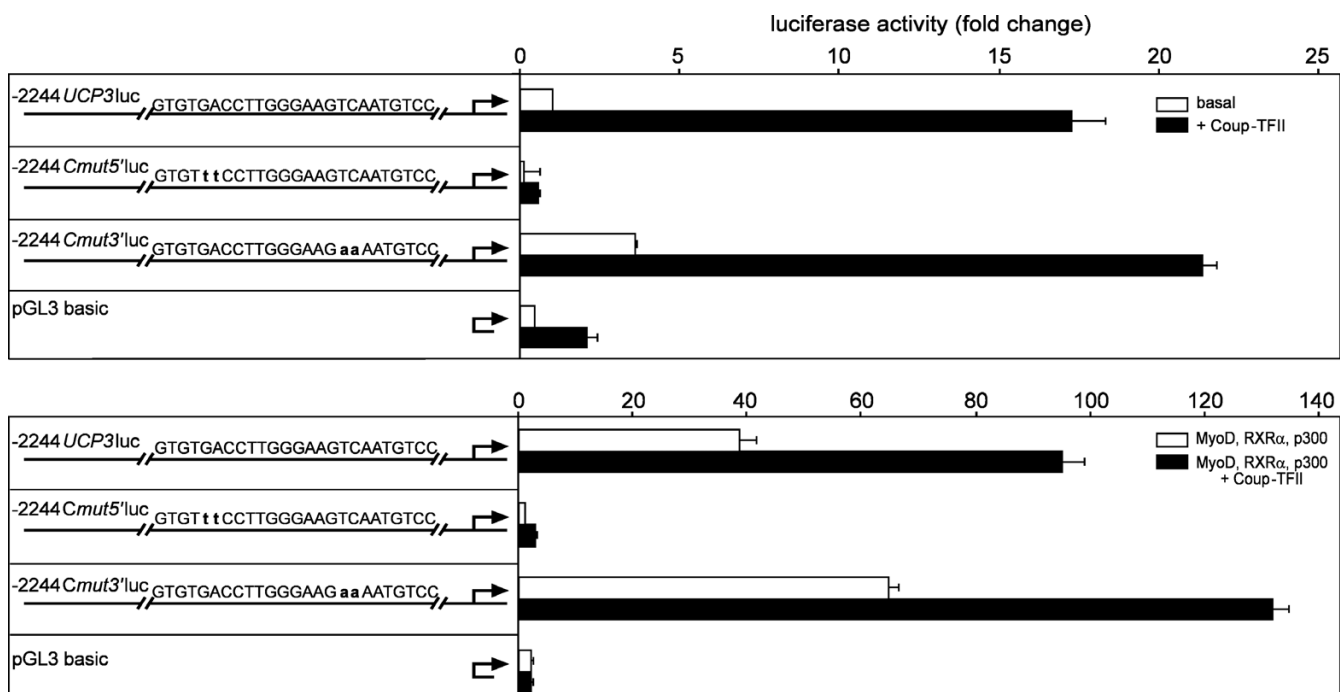


**Figure 7**

**Disruption of the 5' half-site leads to complete loss of activity.** Reporter gene assays with mutated luciferase constructs. In the upper panel basal luciferase activity and induction by Coup-TFII is shown, in the lower panel the experiment was repeated on a background of MyoD, RXR $\alpha$  and p300. Disruption of the 3' half site on -2244*Cmut3*'luc did not lower activity in any condition tested. Disrupting the 5' half-site on -2244*Cmut5*'luc led to a complete loss of basal activity and responsiveness to Coup-TFII and MyoD, RXR $\alpha$  and p300.

BAT and SKM are the major sites of *Ucp3* mRNA expression. *Coup-TFII* was detected in both tissues, but in line with previous data on human adult tissue distribution [30] is rather ubiquitously expressed with highest levels in kidney, liver and heart. Contrary to reports that *Coup-TFII* is expressed in preadipocytes and myoblasts and down-regulated during differentiation [23,31], we were able to detect considerable amounts of *Coup-TFII* transcript in BAT and SKM tissue. Apparently cell culture systems are devoid of the appropriate physiological stimuli promoting *Coup-TFII* mRNA expression in tissues. This is supported by the absence of *Coup-TFII* in human embryonal kidney cells as shown in our Western blot experiment (Fig. 5B) despite its presence in human kidney tissue *in vivo* [30]. It has been demonstrated that *Coup-TFII* plays an important role in the regulation of several genes encoding key metabolic enzymes [18,23-25], which are certainly regulated in terminally differentiated cells.

*Ucp3* gene expression was upregulated in SKM of food deprived hamsters. In line with the function of *Coup-TFII* in metabolic regulation we also observed a significant increase of mRNA expression in response to this challenge. Probably owing to the short duration of cold exposure in our study we did not observe a significant cold induced increase in *Ucp3* mRNA expression in BAT as published previously [5,6]. However, *Coup-TFII* and *Ucp3* mRNA expression in BAT displayed a similar cold-induced increase in variation. The resemblance of expression levels in SKM and BAT and the response to physiological stimuli culminates in a highly significant correlation of *Coup-TFII* and *Ucp3* mRNA abundance under challenged conditions (food deprivation and cold). The absence of such a correlation in the control group suggests that *Coup-TFII* requires additional factors in order to enhance *Ucp3* mRNA expression which must be recruited and/or activated beforehand.

We could support this model in reporter gene assays, in which *Coup-TFII* strongly coactivated *Ucp3* promoter activity in synergy with PPAR $\alpha$ , MyoD, RXR $\alpha$  and/or p300, while the effect of *Coup-TFII* was much lower alone. These constituents of the well described basal transcription factor complex in our experiments affected *Ucp3* expression as described previously [15], i.e. strong activation by PPAR $\alpha$ /RXR $\alpha$  and p300, dependent on agonist stimulation and presence of MyoD. *Coup-TFII* specifically enhanced expression in synergy with these factors.

In contrast to our data, *Coup-TFII* has been shown to negatively interact with MyoD and p300 in SKM, reducing their potential to activate E-box driven reporter gene constructs [17]. This discrepancy may be explained by a differential recruitment of the multiple COUP-TF family cofactors in different physiological environments [e.g. N-

Cor, SMRT, RIP140, SRC-1; for a review see [32]]. The specific complex of transcription factors, to which *Coup-TFII* is recruited, may determine the final function as described for interaction with the glucocorticoid receptor [33]. In general, COUP-TF proteins display a conflicting pattern of positive or negative interaction with nuclear receptors like PPARs or the estrogen receptor depending on the target gene [discussed in [18]]. There are genes where transcription is increased by PPARs and decreased by COUP-TFs [e.g. malic enzyme [19]] as well as genes for which the situation is opposite [e.g. transferrin [20]] or at which both PPARs and COUP-TFs act synergistically [e.g. lipoprotein lipase [18]]. Even a complete reversal of the effect of *Coup-TFII* on a single target has been reported [23]; transcription of the phosphoenolpyruvate carboxykinase gene is induced or repressed by *Coup-TFII* in a tissue specific manner.

Interestingly, specific PPAR $\gamma$  agonists upregulate *Coup-TFII* in the heart [24] and also *Ucp3* gene expression in BAT and SKM [34,35], although to our knowledge no direct interaction of PPAR $\gamma$  with the *Ucp3* promoter has been verified so far. This effect might therefore be due to PPAR $\gamma$  mediated transactivation of *Coup-TFII*, which in turn enhances *Ucp3* expression.

We were able to confine the sequence element mediating the *Coup-TFII* effect to -1307 to -664 by utilizing reporter gene deletion constructs. -2244UCP3luc was the only construct being induced by *Coup-TFII* on a background of MyoD, RXR $\alpha$  and p300 and was exclusively activated high above an unspecific effect by *Coup-TFII* alone.

Of five candidate elements A-E within this region tested by electrophoretic mobility shift assays we confirmed specific binding of *Coup-TFII* to element C. Notably, element C did not only show complex formation with overexpressed *Coup-TFII* but also with nuclear extracts of hamster SKM (Fig. 5D). Extracts of all six animals tested were able to form a complex of comparable size and food deprivation of hamsters led to an increase in band intensity. The element is located at -816 to -840 and constitutes a functional repeat structure. By mutational analyses we were able to confine *Coup-TFII* binding to the 5' half-site of this element. In reporter gene assays disruption of this site surprisingly led to a complete loss of activity and responsiveness to any treatment tested. While this fact certainly underlines the importance of this element, its indifference to MyoD, RXR $\alpha$  and p300 treatment is in conflict with the retained effect of this treatment on -664UCP3luc and -243UCP3luc, that are also devoid of this element. It seems that the element exhibits a function beyond direct transactivation by *Coup-TFII*, that depends on the presence of the surrounding region. These characteristics point towards a model of *Coup-TFII* deactivating or displacing a

so far unknown repressor of *Ucp3* transcription. This repressor could be expected to bind in proximity to the 5' half-site of elementC, possibly even to the 3' half-site of this same element. In the light of this hypothetical model several formerly negligible seeming facts gain relevancy: Mutated construct -2244*Cmut3'*luc displayed an overall increase of luciferase activity as compared to -2244*UCP3*luc (Fig. 7). Deletion construct -664*UCP3*luc had a higher basal activity and could be activated by MyoD, RXR $\alpha$  and p300 to a higher extent than -2244*UCP3*luc (Fig. 4B). The complex size of bandshift probe *Cmut5'* was slightly changed (Fig. 6A).

This model alone, however, does not account for the activation of -2244*UCP3*luc by MyoD, RXR $\alpha$ , p300 and PPAR $\alpha$  in the absence of cotransfected Coup-TFII. Therefore there would have to be an endogenous Coup-TFII expression in HEK293 cells that we can either not detect with our Western blots or is induced by transfection of factors like MyoD and p300. At present we cannot decide whether repressor displacement/deactivation itself or subsequent direct coactivation is the dominant means of Coup-TFII mediated transcriptional induction.

The conservation of the inverse repeat structure and its Coup-TFII binding site across rodent species suggests an important role for this element; its preservation in the murine promoter despite an obvious event of rearrangement during evolution supports this role. The upstream location of the binding element and its synergy with PPAR $\alpha$  resembles a comparable situation, where Coup-TFII directly coactivates the lipoprotein lipase gene in cooperation with PPAR/RXR heterodimers as described previously [18]. Notably lipoprotein lipase is a crucial determinant of fatty acid uptake from circulating triglycerides.

An explanation of the link between increased lipid utilization and the recruitment of Coup-TFII in BAT and SKM is hampered by the lack of knowledge about a specific ligand and the posttranslational mechanism of activation. It is beyond the scope of this study to clarify whether Coup-TFII is directly regulated in response to FFA levels and thus possibly conveys FFA-dependent *Ucp3* transcription. Our qPCR data indicate that *de novo* synthesis of Coup-TFII is the dominant means of target gene upregulation rather than ligand binding or posttranslational modification. So far, transcription of *Coup-TFII* has been linked to MAP kinase pathway activity [36] and the presence of ETS family transcription factors [37]. Further research is required to clarify whether these mechanisms represent a link between lipid utilization and *Coup-TFII* upregulation.

On the functional level beyond its role in organismic development Coup-TFII has been assumed to be an inte-

gral part of the glucose response complex, where it functions as an inhibitor of glucose dependent activators [25]. This hypothesis is based on the ability of Coup-TFII to inhibit upstream stimulatory factor (USF)-dependent transactivation of a glucose response element in the L-type pyruvate kinase gene (*PKLR*) and a similar finding regarding the *ATPA* gene encoding the alpha subunit of the F1F0 ATP synthase complex [38]. Recently, Bardoux and coworkers (2005), after discovering a role for Coup-TFII in insulin secretion and sensitivity, assigned Coup-TFII as an important regulator of glucose homeostasis [39]. Our finding of *Coup-TFII* upregulation in states of augmented lipid oxidation confirms these models and extends them to a new aspect. The inhibition of glucose induced gene transcription may occur in conjunction with a positive regulation of lipid metabolism genes like *Ucp3* and lipoprotein lipase.

## Conclusion

Coup-TFII is a strong activator of *Ucp3* gene transcription by binding to an upstream element in the *Ucp3* promoter as shown by luciferase assays and electrophoretic mobility shift assays. *Coup-TFII* mRNA expression correlates with *Ucp3* mRNA levels in tissues of hamsters subjected to physiological challenges inducing lipid oxidation. Transcriptional upregulation of the *Coup-TFII* gene in response to these challenges seems to regulate the *Ucp3* gene in brown adipose and skeletal muscle tissue determining the final appropriate rate of *Ucp3* mRNA synthesis. The mechanism of Coup-TFII inducing *Ucp3* transcription seems to involve displacement/deactivation of an unknown repressor. These findings add a crucial component to the complex transcriptional machinery controlling expression of *Ucp3*. At the same time they further manifest a function of Coup-TFII in the regulation of lipid metabolism genes.

## Methods

### Animal experimentation and nucleic acid preparations

Djungarian hamsters (*Phodopus sungorus*) were housed under standard laboratory conditions with *ad libitum* access to food (Hamsterzucht diät 7014, Altromin) and water unless stated otherwise. All experiments involving animals were conducted in accordance with the German animal welfare law. For tissue dissections hamsters were sacrificed by CO<sub>2</sub> exposure. Genomic DNA was prepared from spleen with the DNeasy Tissue Kit (Qiagen). We either cold exposed hamsters to 4°C ambient temperature for 24 hours (n = 9) or food deprived hamsters for 48 hours at room temperature (n = 12). A third group of hamsters was kept at room temperature and fed *ad libitum* to serve as control group (n = 12). All hamsters were of an age of 10 to 15 months. We obtained samples of suprasternal BAT and hindlimb SKM (*Musculus quadriceps*) from 9 animals of each group. From three control group hamsters we also dissected samples of inguinal



WAT, kidney, liver, heart, lung, spleen and salivary gland. Samples were frozen in liquid nitrogen, total RNA prepared with Trizol (Invitrogen) and quantified photometrically. We dissected the entire leg musculature of three control and starved animals for tissue nuclear protein extracts.

#### Primer design, sequencing and sequence analysis

All sequencing reactions were carried out by a commercial service provider (MWG Biotech). Primer sequences were selected using the program Primer3 (Code available at [40]). Primers to amplify fragments of the *Ucp3* genomic locus were deduced from conserved regions of corresponding genomic sequences from the ENSEMBL mouse and rat genomic databases (ENSMUSG00000032942, ENSRNOG00000017716), from cDNA sequences of the putative 5' adjacent gene [GenBank: [AU020772](#), [AI170065](#)] and from *P. sungorus Ucp3* cDNA [Genbank: [AF271265](#)]. PCR products were cloned and sequenced. Assembled contigs were resequenced with homologous primers and a minimum 5-fold coverage. To analyse the *P. sungorus Ucp3* transcript 2 µg of RNA were reverse transcribed into cDNA with oligo-dT-primers and Superscript II reagents (Invitrogen). We deduced PCR primers from the assembled genomic contig to amplify, clone and sequence two overlapping fragments representing exon1 to exon6 and exon2 to exon7 of the *Ucp3* transcript, respectively. Sequencing results were visualized, edited and assembled in the GAP4 module of the Staden Sequence Analysis Package [41]. All sequence alignments were conducted with ClustalW [42]. Promoter sequences were analyzed for putative transcription factor binding sites by considering results obtained with the programs AliBaba2.1, MATCH™ and PATCH™ [43] all based upon the TRANSFAC® database [44].

#### Mapping the transcriptional start site (TSS)

To determine TSS by 5' rapid amplification of cDNA ends (5' RACE), 1 µg of SKM and BAT total RNA was reverse transcribed into RACE-ready first-strand cDNA using an amplification kit (BD SMART RACE, Clontech). We PCR-amplified the 5'-end with the *Ucp3* specific reverse primer ATGGCTTGAAATCGGACCTTCACCAC combined with the kit primer mix according to the manual. Products were cloned into pCR2.1-TOPO (Invitrogen) and independent clones were picked and sequenced.

#### Real time qPCR

We cloned a fragment of *P. sungorus Coup-TFII* [GenBank: [DQ244042](#)] representing parts of exon2 and 3 by deducing heterologous primers from conserved regions of the respective mouse and rat transcripts. Nested, homologous primers were inferred for qPCR analysis. SuperScript® III Platinum® SYBR® Green Two-Step qRT-PCR Kit (Invitrogen) was used to reverse transcribe total RNA prepared as

described above and to measure mRNA expression levels on an iCycler IQ (Biorad). The PCR Mix was supplemented with 20 nM Fluorescein (Biorad). Amplification efficiency was calculated based on dilution series standard curves by the Biorad iCycler IQ 3.0 software and used to determine starting quantity levels (PCR base line subtracted) normalized to  $\beta$ -actin levels. Primers:  *$\beta$ -actin* AGAGGGAAATCGTGCGTGAC, CAATAGTGATGACCTGGCCGT; *Coup-TFII* ATATCCCGGATGAGGGTTTC, AAAGTCCCAGTGTGCTTTGG; *Ucp3* AGGAAGGAATCAGGGCTTA, TCCAGCAGCTTCTCCTTGAT. Group differences were tested for significance with the Mann-Whitney rank sum test, correlations were calculated by the Spearman rank order method (SigmaStat 3.1, Systat Software).

#### Vector origins and construction

Expression vectors pCMV-SPORT6 harbouring the complete coding sequence of human *Coup-TFII* (IMAGE:5177487), *COUP-TFI* (IMAGE:2824138) and murine *MyoD* in pME18S-FL (IMAGE:1499265) were obtained from the "Deutsches Ressourcenzentrum für Genomforschung" (RZPD, Berlin) and verified by sequencing. Human full length *RXR $\alpha$*  in pSG5 was kindly provided by A. Baniahmad (Gießen, Germany), human *p300* in pCMV $\beta$  by C. Platzer (Jena, Germany) and human *PPAR $\alpha$*  in pCMV7 by H. Shimano (Tokyo, Japan).

A region comprising a BamHI fragment from -2244 to +38 of the *Ucp3* gene was amplified by Pfu polymerase (Fermentas). It was cloned into a BglII site of pGL3 basic (Promega) exploiting the endogenous, compatible BamHI sites to generate -2244*Ucp3*luc. Subsequently, three different deletion constructs were cloned (outlined in Fig. 4B). By restriction with BglII and religation we created -2244BglII~~Ucp3~~luc, bearing a 1161 bp deletion from -1307 to -146. The construct -664*Ucp3*luc was generated by restriction of -2244*Ucp3*luc with the compatible enzymes XbaI and NheI, but owing to a XbaI site in the vector backbone we applied a partial restriction followed by gel purification and religation of the appropriate fragment. We constructed -243*Ucp3*luc by restriction of -664*Ucp3*luc with BfrBI and SmaI and religation of the agarose gel purified larger fragment.

For mutational analyses of element C we constructed two further reporter gene constructs -2244*Cmut5'*luc and -2244*Cmut3'*luc by PCR overlap extension site directed mutagenesis as described previously [45]. To mutate the first half-site (*Cmut5'*) we used the overlapping mutated primers TCAAGGACATTTTCTTCCCA and CCTTGGGAA-GAAAATGTCCT, to mutate the second half-site (*Cmut3'*) ACTTCCCAAGGAAACACAGC and GCTGTGTTTCCTT-GGGAAGT. For both primer pairs we designed the outer primers TCACTGTTGTCTCTGCTGCC and GCAG-CAGCCATCCTTAGAAC to produce an amplicon includ-

ing the two endogenous BglII sites described above. The two resulting mutated fragments were cloned into pGEM-Teasy (Promega) and sequenced to verify the introduced mutation. BglII-fragments derived from these vectors were subcloned into -2244BglII~~del~~ Ucp3luc and again sequenced to guarantee successful subcloning of the respective mutated site.

#### Cell culture and luciferase assays

We utilized the human embryonal kidney cell line HEK293 as a heterologous system for our reporter gene studies. Cells were grown in DMEM supplemented with 10% FCS and split every second day. For luciferase assays cells were detached by trypsin and passaged onto 12 well-plates. Cells were transfected by the calcium-phosphate method using the ProFection Kit (Promega). We used 25 ng reporter gene construct, 1.25 ng phRL-tk (Promega), 500 ng for each expression vector and added empty pcDNA3 (Invitrogen) to a final mass of 2 µg and added 100 µl of precipitate solution per well to the medium. For every vector combination we prepared three replicate wells. Cells were incubated with the transfection mixture for 16 hours, medium was changed and cells harvested 24 hours later. When 10 µM of the PPAR $\alpha$  ligand Wy14,643 was applied as a stimulant, it was added in DMSO during the medium change. In all measurements without stimulant, medium was supplied with the same volume of DMSO only. Luciferase activity was measured with the Dual Luciferase Reporter Assay System (Promega). Initial experiments revealed that cotransfection of cells with vectors driving expression of nuclear receptors systematically affected phRL-tk activity, a known handicap of this system [46]. We therefore used primary, unnormalized data for activity calculations. To validate these data we measured protein content by the Bradford method and confirmed that this normalization did not result in values significantly different from unnormalized data. All results are shown as fold changes relative to the basal activity of the respective construct used.

#### Electrophoretic mobility shift assay

HEK293 cells were harvested in 200 µl homogenisation buffer (10 mM HEPES, 1.5 mM MgCl<sub>2</sub>, 10 mM KCl, 0.5 mM DTT, 20 mM NaF), homogenized in a glass potter and centrifuged (3300 g, 15 min, 4°C). The pellet was resuspended in 100 µl low salt buffer (20 mM HEPES, 1.5 mM MgCl<sub>2</sub>, 0.2 mM EDTA, 0.5 mM DTT, 20 mM NaF, 25% (v/v) glycerol) and subsequently mixed with 100 µl high salt buffer (= low salt buffer with 1.2 M KCl). The mixture was agitated vigorously for 30 min at 4°C and centrifuged (25,000 g, 30 min, 4°C). The supernatant containing nuclear proteins was purified with a Microcon YM-50 column (Millipore), aliquoted and stored at -80°C. All above mentioned buffers were supplied with protease inhibitors (Complete Mini Protease Inhibitor

Cocktail Tablet, Roche) and phosphatase inhibitors (Phosphatase Inhibitor Cocktail II, Sigma). Protein concentrations were measured by the Bradford method with BSA as a standard.

For tissue nuclear extracts we excised the complete leg musculature of a hamster and grinded it in liquid nitrogen to yield a fine powder. The powder was treated as described above with the following modifications. We used 1 ml homogenisation buffer, washed the pellet in 1 ml homogenisation buffer and subsequently used 200 µl of high and low salt buffer. We did not employ the concentrator column for tissue extracts.

Complementary oligonucleotides were annealed by heating to 80°C in TE (10 mM Tris/HCl, 1 mM EDTA) and slow cooling to room temperature. Double strands were further purified by elution from a 12% polyacrylamide gel. Three pmol of the resulting doublestrand were endlabelled with T4 polynucleotide kinase and [ $\gamma$ -<sup>32</sup>P]ATP and purified with a ChromaSpin+10-TE column (Clontech). Sequence of oligonucleotide probes (sense strand): (A) GCCCTCCAGTCTGACTCCTCGTAGC, (B) AGCCTC-CAATGACTTGTTCATGGAG, (C) GTGTGACCTT-GGGAAGTCAATGTCC, (D) TGTCTTGAAGTTCAGTTTCTGT, (E) AGTAAGCATT-GACACATGAGGGTT. Sequence of mutated element C oligonucleotide probes (sense strand): GTGTTTCCTT-GGGAAGTCAATGTCC (Cmut5'), GTGTGACCTT-GGGAAGAAAATGTCC (Cmut3'), GTGTTTCCTTGGGAAGAAAATGTCC (Cmut5'3').

For gel retardation assays we incubated 3 µg (HEK293) or 20 µg (tissue) nuclear extract with ~7.5 fmol probe for 20 min on ice in a final volume of 2 µl containing 4% (v/v) glycerol, 1 mM MgCl<sub>2</sub>, 0.5 mM EDTA, 0.5 mM DTT, 50 mM NaCl, 10 mM Tris/HCl (pH 7.5) and 50 µg/ml poly(dIdC) · poly(dIdC). Samples were analyzed by electrophoresis in a 5.2% nondenaturing polyacrylamide gel at 4°C and 200 V for 3 hours in 0.5 × TBE. The gel was exposed to a phosphoscreen for 18 hours. For competition assays we included a 2–100 fold molar excess of unlabelled oligonucleotide in the reaction. For supershift assays we added 1 µl of Coup-TFII antibody (Santa Cruz, sc6576-X). The specificity of this antibody and the presence of Coup-TFII protein in the nuclear fraction of transfected cells was confirmed by Western blot.

Densitometrical quantification of band intensities was performed with the software ImageJ 1.34s [47]. All values were background corrected.

#### Authors' contributions

TF performed all experiments and computational analyses and drafted the manuscript. KR collaborated in computa-

tional analyses and provided knowledge on database handling and bioinformatics. MP supplied technical expertise and participated in experimental design. XL helped in performing experiments shown in Fig. 2 and 3. MK coordinated this study, provided its conceptual basis, participated in experimental design and helped to draft the manuscript. All authors read and approved the final manuscript.

## Acknowledgements

This work was supported by the Deutsche Forschungsgemeinschaft (DFG), grant KL973/7-3 and NGFN2 [01GR0504, 01GS0483(TP23)]. T. Fromme was recipient of a fellowship of the Friedrich-Naumann-Foundation and associated member of GRK767. K. Reichwald was supported by DHGP2 grant 01KW0007. We thank A. Banihmad, C. Platzer and H. Shimano for kindly supplying vectors, D. Kruhl for technical assistance and J. Kämper for the generous provision of access to an iCycler.

## References

- Vidalpuig A, Solanes G, Grujic D, Flier JS, Lowell BB: **UCP3: An uncoupling protein homologue expressed preferentially and abundantly in skeletal muscle and brown adipose tissue.** *Biochem Biophys Res Commun* 1997, **235**:79-82.
- Boss O, Samec S, Paoloni Jacobino A, Rossier C, Dulloo AG, Seydoux J, Muzzin P, Giacobino JP: **Uncoupling protein-3: A new member of the mitochondrial carrier family with tissue-specific expression.** *FEBS Lett* 1997, **408**:39-42.
- Nedergaard J, Cannon B: **The 'novel' 'uncoupling' proteins UCP2 and UCP3: what do they really do? Pros and cons for suggested functions.** *Exp Physiol* 2003, **88**:65-84.
- Jastroch M, Wuertz S, Kloas W, Klingenspor M: **Uncoupling protein 1 in fish uncovers an ancient evolutionary history of mammalian nonshivering thermogenesis.** *Physiol Genomics* 2005, **22**:150-156.
- Liebig M, von Praun C, Heldmaier G, Klingenspor M: **Absence of UCP3 in brown adipose tissue does not impair nonshivering thermogenesis.** *Physiol Biochem Zool* 2004, **77**:116-126.
- von Praun C, Burkert M, Gessner M, Klingenspor M: **Tissue-specific expression and cold-induced mRNA levels of uncoupling proteins in the Djungarian hamster.** *Physiol Biochem Zool* 2001, **74**:203-211.
- Giacobino JP: **Effects of dietary deprivation, obesity and exercise on UCP3 mRNA levels.** *Int J Obes Relat Metab Disord* 1999, **23 Suppl 6**:S60-S63.
- Stavinoha MA, RaySpellicy JW, Essop MF, Graveleau C, Abel ED, Hart-Sailors ML, Mersmann HJ, Bray MS, Young ME: **Evidence for mitochondrial thioesterase I as a peroxisome proliferator-activated receptor-alpha-regulated gene in cardiac and skeletal muscle.** *Am J Physiol* 2004, **287**:E888-E895.
- Weigle DS, Selfridge LE, Schwartz MW, Seeley RJ, Cummings DE, Havel PJ, Kuijper JL, Beltrandelrio H: **Elevated free fatty acids induce uncoupling protein 3 expression in muscle: A potential explanation for the effect of fasting.** *Diabetes* 1998, **47**:298-302.
- Schrauwen P, Hoeks J, Schaart G, Kornips E, Binas B, Van De Vusse GJ, Van Bilsen M, Luiken JJ, Coort SL, Glatz JF, Saris WH, Hesselink MK: **Uncoupling protein 3 as a mitochondrial fatty acid anion exporter.** *FASEB J* 2003, **17**:2272-2274.
- Echtay KS, Roussel D, St Pierre J, Jekabsons MB, Cadenas S, Stuart JA, Harper JA, Roebuck SJ, Morrison A, Pickering S, Clapham JC, Brand MD: **Superoxide activates mitochondrial uncoupling proteins.** *Nature* 2002, **415**:96-99.
- Echtay KS, Esteves TC, Pakay JL, Jekabsons MB, Lambert AJ, Portero-Otin M, Pamplona R, Vidal-Puig AJ, Wang S, Roebuck SJ, Brand MD: **A signalling role for 4-hydroxy-2-nonenal in regulation of mitochondrial uncoupling.** *EMBO J* 2003, **22**:4103-4110.
- Jaburek M, Miyamoto S, Di Mascio P, Garlid KD, Jezek P: **Hydroperoxy fatty acid cycling mediated by mitochondrial uncoupling protein UCP2.** *J Biol Chem* 2004, **279**:53097-53102.
- Jezek P, Engstova H, Zackova M, Vercesi AE, Costa ADT, Arruda P, Garlid KD: **Fatty acid cycling mechanism and mitochondrial uncoupling proteins.** *Biochim Biophys Acta* 1998, **1365**:319-327.
- Solanes G, Pedraza N, Iglesias R, Giralt M, Villarroya F: **Functional relationship between MyoD and peroxisome proliferator-activated receptor-dependent regulatory pathways in the control of the human uncoupling protein-3 gene transcription.** *Mol Endocrinol* 2003, **17**:1944-1958.
- Solanes G, Pedraza N, Calvo V, Vidal-Puig A, Lowell BB, Villarroya F: **Thyroid hormones directly activate the expression of the human and mouse uncoupling protein-3 genes through a thyroid response element in the proximal promoter region.** *Biochem J* 2004.
- Bailey P, Sartorelli V, Hamamori Y, Muscat GE: **The orphan nuclear receptor, COUP-TF II, inhibits myogenesis by post-transcriptional regulation of MyoD function: COUP-TF II directly interacts with p300 and myoD.** *Nucleic Acids Res* 1998, **26**:5501-5510.
- Robinson CE, Wu X, Nawaz Z, Onate SA, Gimble JM: **A corepressor and chicken ovalbumin upstream promoter transcriptional factor proteins modulate peroxisome proliferator-activated receptor-gamma/retinoid X receptor alpha-activated transcription from the murine lipoprotein lipase promoter.** *Endocrinology* 1999, **140**:1586-1593.
- Baes M, Castelein H, Desmet L, Declercq PE: **Antagonism of COUP-TF and PPAR alpha/RXR alpha on the activation of the malic enzyme gene promoter: modulation by 9-cis RA.** *Biochem Biophys Res Commun* 1995, **215**:338-345.
- Hertz R, Seckbach M, Zakin MM, Bar-Tana J: **Transcriptional suppression of the transferrin gene by hypolipidemic peroxisome proliferators.** *J Biol Chem* 1996, **271**:218-224.
- Qiu Y, Krishnan V, Pereira FA, Tsai SY, Tsai MJ: **Chicken ovalbumin upstream promoter-transcription factors and their regulation.** *J Steroid Biochem Mol Biol* 1996, **56**:81-85.
- Lee CT, Li L, Takamoto N, Martin JF, Demayo FJ, Tsai MJ, Tsai SY: **The nuclear orphan receptor COUP-TFII is required for limb and skeletal muscle development.** *Mol Cell Biol* 2004, **24**:10835-10843.
- Eubank DW, Duplus E, Williams SC, Forest C, Beale EG: **Peroxisome proliferator-activated receptor gamma and chicken ovalbumin upstream promoter transcription factor II negatively regulate the phosphoenolpyruvate carboxykinase promoter via a common element.** *J Biol Chem* 2001, **276**:30561-30569.
- Cabrero A, Jove M, Planavila A, Merlos M, Laguna JC, Vazquez-Carrera M: **Down-regulation of acyl-CoA oxidase gene expression in heart of troglitazone-treated mice through a mechanism involving chicken ovalbumin upstream promoter transcription factor II.** *Mol Pharmacol* 2003, **64**:764-772.
- Lou DQ, Tannour M, Selig L, Thomas D, Kahn A, Vasseur-Cognet M: **Chicken ovalbumin upstream promoter-transcription factor II, a new partner of the glucose response element of the L-type pyruvate kinase gene, acts as an inhibitor of the glucose response.** *J Biol Chem* 1999, **274**:28385-28394.
- Riquet FB, Rodriguez M, Guigal N, Dromaint S, Naime I, Boutin JA, Galizzi JP: **In vivo characterisation of the human UCP3 gene minimal promoter in mice tibialis anterior muscles.** *Biochem Biophys Res Commun* 2003, **311**:583-591.
- Cadenas S, Buckingham JA, Samec S, Seydoux J, Din N, Dulloo AG, Brand MD: **UCP2 and UCP3 rise in starved rat skeletal muscle but mitochondrial proton conductance is unchanged.** *FEBS Lett* 1999, **462**:257-260.
- Schonfeld-Warden NA, Warden CH: **Physiological effects of variants in human uncoupling proteins: UCP2 influences body-mass index.** *Biochem Soc Trans* 2001, **29**:777-784.
- Esterbauer H, Oberkofler H, Krempler F, Strosberg AD, Patsch W: **The uncoupling protein-3 gene is transcribed from tissue-specific promoters in humans but not in rodents.** *J Biol Chem* 2000, **275**:36394-36399.
- Suzuki T, Moriya T, Darnel AD, Takeyama J, Sasano H: **Immunohistochemical distribution of chicken ovalbumin upstream promoter transcription factor II in human tissues.** *Mol Cell Endocrinol* 2000, **164**:69-75.
- Muscat GE, Rea S, Downes M: **Identification of a regulatory function for an orphan receptor in muscle: COUP-TF II affects**

- the expression of the myoD gene family during myogenesis. *Nucleic Acids Res* 1995, **23**:1311-1318.
32. Park JI, Tsai SY, Tsai MJ: **Molecular mechanism of chicken ovalbumin upstream promoter-transcription factor (COUP-TF) actions.** *Keio J Med* 2003, **52**:174-181.
  33. De Martino MU, Bhattacharya N, Alesci S, Ichijo T, Chrousos GP, Kino T: **The glucocorticoid receptor and the orphan nuclear receptor chicken ovalbumin upstream promoter-transcription factor II interact with and mutually affect each other's transcriptional activities: implications for intermediary metabolism.** *Mol Endocrinol* 2004, **18**:820-833.
  34. Hwang CS, Lane MD: **Up-regulation of uncoupling protein-3 by fatty acid in C2C12 myotubes.** *Biochem Biophys Res Commun* 1999, **258**:464-469.
  35. Kelly LJ, Vicario PP, Thompson GM, Candelore MR, Doebber TW, Ventre J, Wu MS, Meurer R, Forrest MJ, Conner MW, Cascieri MA, Moller DE: **Peroxisome proliferator-activated receptors gamma and alpha mediate in vivo regulation of uncoupling protein (UCP-1, UCP-2, UCP-3) gene expression.** *Endocrinology* 1998, **139**:4920-4927.
  36. More E, Fellner T, Doppelmayr H, Hauser-Kronberger C, Dandachi N, Obrist P, Sandhofer F, Paulweber B: **Activation of the MAP kinase pathway induces chicken ovalbumin upstream promoter-transcription factor II (COUP-TFII) expression in human breast cancer cell lines.** *J Endocrinol* 2003, **176**:83-94.
  37. Petit FG, Salas R, Tsai MJ, Tsai SY: **The regulation of COUP-TFII gene expression by Ets-1 is enhanced by the steroid receptor co-activators.** *Mech Ageing Dev* 2004, **125**:719-732.
  38. Jordan EM, Worley T, Breen GA: **Transcriptional regulation of the nuclear gene encoding the alpha-subunit of the mammalian mitochondrial F1F0 ATP synthase complex: role for the orphan nuclear receptor, COUP-TFII/ARP-1.** *Biochemistry* 2003, **42**:2656-2663.
  39. Bardoux P, Zhang P, Flamez D, Perilhou A, Lavin TA, Tanti JF, Hellemans K, Gomas E, Godard C, Andreelli F, Buccheri MA, Kahn A, Marchand-Brustel Y, Burcelin R, Schuit F, Vasseur-Cognet M: **Essential role of chicken ovalbumin upstream promoter-transcription factor II in insulin secretion and insulin sensitivity revealed by conditional gene knockout.** *Diabetes* 2005, **54**:1357-1363.
  40. **Primer 3 Source Code** 2006 [[http://www-genome.wi.mit.edu/genome\\_software/other/primer3.html](http://www-genome.wi.mit.edu/genome_software/other/primer3.html)].
  41. Staden R: **The Staden sequence analysis package.** *Mol Biotechnol* 1996, **5**:233-241.
  42. Thompson JD, Higgins DG, Gibson TJ: **CLUSTAL W: improving the sensitivity of progressive multiple sequence alignment through sequence weighting, position-specific gap penalties and weight matrix choice.** *Nucleic Acids Res* 1994, **22**:4673-4680.
  43. **Biobase Biological Databases** 2006 [<http://www.gene-regulation.com>].
  44. Matys V, Fricke E, Geffers R, Gossling E, Haubrock M, Hehl R, Hornischer K, Karas D, Kel AE, Kel-Margoulis OV, Kloos DU, Land S, Lewicki-Potapov B, Michael H, Munch R, Reuter I, Rotert S, Saxel H, Scheer M, Thiele S, Wingender E: **TRANSFAC: transcriptional regulation, from patterns to profiles.** *Nucleic Acids Res* 2003, **31**:374-378.
  45. Ho SN, Hunt HD, Horton RM, Pullen JK, Pease LR: **Site-directed mutagenesis by overlap extension using the polymerase chain reaction.** *Gene* 1989, **77**:51-59.
  46. Everett LM, Crabb DW: **Sensitivity of virally-driven luciferase reporter plasmids to members of the steroid/thyroid/retinoid family of nuclear receptors.** *J Steroid Biochem Mol Biol* 1999, **70**:197-201.
  47. **ImageJ - Image Processing and Analysis in Java** 2006 [<http://rsb.info.nih.gov/ij/>].

Publish with **BioMed Central** and every scientist can read your work free of charge

"BioMed Central will be the most significant development for disseminating the results of biomedical research in our lifetime."

Sir Paul Nurse, Cancer Research UK

Your research papers will be:

- available free of charge to the entire biomedical community
- peer reviewed and published immediately upon acceptance
- cited in PubMed and archived on PubMed Central
- yours — you keep the copyright

Submit your manuscript here:  
[http://www.biomedcentral.com/info/publishing\\_adv.asp](http://www.biomedcentral.com/info/publishing_adv.asp)





# Chicken ovalbumin upstream promotor transcription factor II (Coup-TFII) regulates the uncoupling protein 3 (Ucp3) gene

T. Fromme<sup>1#</sup>, K. Reichwald<sup>2</sup>, M. Platzer<sup>2</sup>, X.S. Li<sup>3</sup>, M. Klingenspor<sup>1</sup>

<sup>1</sup> Philipps-Universität Marburg, Faculty of Biology, Dept. of Animal Physiology, Marburg, Germany

<sup>2</sup> Leibniz Institute for Age Research, Fritz Lipmann Institute (FLI), Jena, Germany

<sup>3</sup> Institute of Zoology, Chinese Academy of Sciences, Beijing, China

#fromme@staff.uni-marburg.de

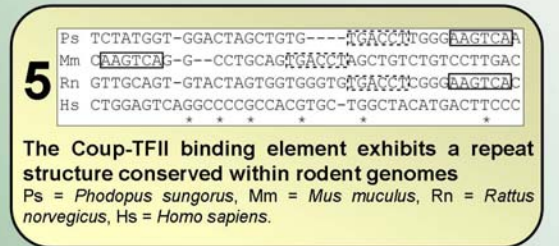
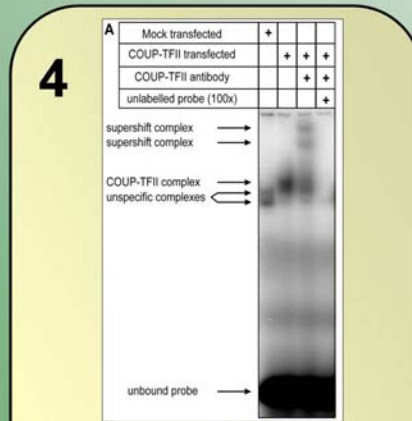
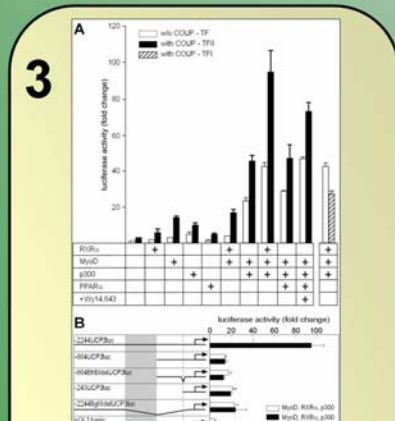
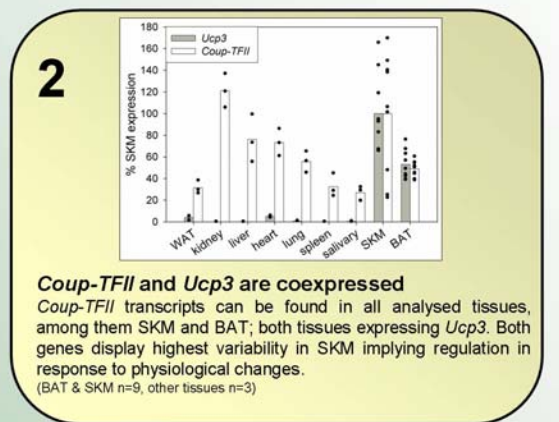
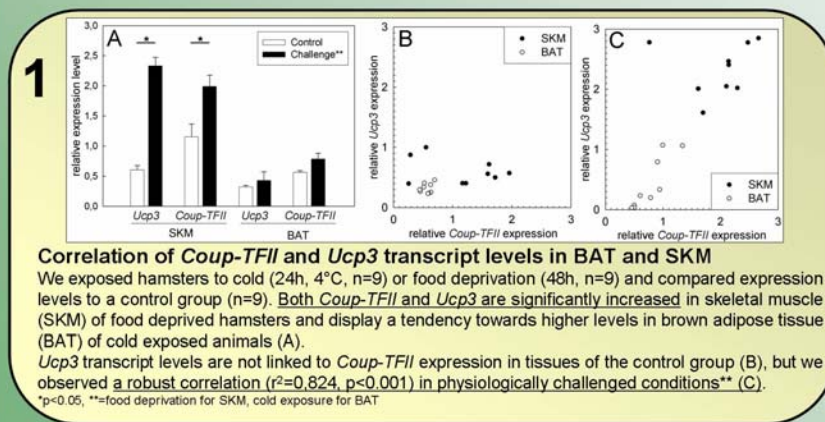


## Introduction

**Uncoupling protein 3 (Ucp3)** is an integral protein of the inner mitochondrial membrane with a role in lipid metabolism preventing deleterious effects of fatty acids in states of high lipid oxidation.

We analyzed 3.6 kb of upstream region of the *Ucp3* gene in the Djungarian hamster (*Phodopus sungorus*) for transcription factor binding sites and identified a response element for chicken ovalbumin upstream promotor transcription factor II (Coup-TFII, official gene name *Nr2f2*) *in silico*.

Coup-TFII is an orphan transcription factor involved in myogenesis and other developmental processes, but also negatively regulates glucose induced gene expression and modulates insulin sensitivity and secretion. Furthermore, Coup-TFII upregulates several metabolic genes, e.g. the lipoprotein lipase gene.



## Conclusion

### *Coup-TFII*...

- enhances *Ucp3* expression by physical binding to an upstream element.
- acts in synergy with the basal transcription factor complex.
- expression levels seem to determine the final rate of *Ucp3* transcription.

*Coup-TFII* mediated inhibition of glucose induced gene transcription may occur in conjunction with a positive regulation of lipid metabolism genes like *Ucp3*.

### Acknowledgements.

This work was supported by the Deutsche Forschungsgemeinschaft (DFG), grant KL973/7-3 and NGFN2 (01GR0504; 01GS04831TF231). T. Fromme was recipient of a fellowship of the Friedrich-Naumann-Foundation and is associated member of GRK767. K. Reichwald was supported by DHP2 grant 01KW0007. We thank A. Banihmad, C. Platzer and H. Shimano for kindly supplying vectors, D. Kruhl for technical assistance and J. Kämper for the generous provision of access to an iCycler.

## **An intronic single base exchange leads to a brown adipose tissue specific loss of Ucp3 expression and an altered body mass trajectory**

**Tobias FROMME<sup>\*1</sup>, Kerstin NAU<sup>\*</sup>, Jan ROZMAN<sup>\*</sup>, Christoph HOFFMANN<sup>\*</sup>, Kathrin REICHWALD<sup>†</sup>, Michael UTTING<sup>†</sup>, Matthias PLATZER<sup>†</sup> and Martin KLINGENSPOR<sup>\*</sup>**

<sup>\*</sup> Department of Animal Physiology, Faculty of Biology, Philipps-University, D-35043 Marburg, Germany

<sup>†</sup> Genome Analysis, Leibniz-Institute for Age Research - Fritz Lipmann Institute, D-07745 Jena, Germany

<sup>1</sup> To whom correspondence should be addressed: Tel. +49(0)6421-2825372, Fax. +49(0)6421-2828937, E-Mail: [fromme@staff.uni-marburg.de](mailto:fromme@staff.uni-marburg.de)

Abbreviations used: BAT, brown adipose tissue; BMI, body mass index; Coup-TFII, chicken ovalbumin upstream promoter transcription factor II; DEXA, Dual Energy X-Ray Absorptionmetry; IVS, intervening sequence; MyoD, myogenic differentiation factor 1; PPAR $\alpha$ , peroxisome proliferator activated receptor  $\alpha$ ; RFLP, restriction fragment length polymorphism; RXR $\alpha$ , retinoic X receptor  $\alpha$ ; SKM, skeletal muscle; Ucp, uncoupling protein; WAT, white adipose tissue

Page heading title:  
Brown adipose tissue specific Ucp3 expression

## Synopsis

Uncoupling protein 3 (Ucp3) is a transport protein of the inner mitochondrial membrane and presumably implicated in the maintenance or tolerance of high lipid oxidation rates. Ucp3 is predominantly expressed in skeletal muscle and brown adipose tissue and regulated by a transcription factor complex involving PPAR $\alpha$ , MyoD and Coup-TFII. By analysis of a mutant Djungarian hamster model lacking *Ucp3* transcription specifically in brown adipose tissue we were able to identify a putative forkhead transcription factor binding site conferring tissue specificity. A naturally occurring, intronic point mutation disrupting this site leads to brown adipose tissue specific loss of *Ucp3* expression and an altered body weight trajectory. Our findings provide insight into tissue specific *Ucp3* regulation and for the first time unambiguously demonstrate that changes in *Ucp3* expression can interfere with body weight regulation.

Key words: uncoupling protein 3, brown adipose tissue, body mass, forkhead domain, intronic binding site, tissue specificity

## Introduction

Uncoupling protein 3 (Ucp3) belongs to the group of anion carrier proteins and is located within the inner mitochondrial membrane. It is predominantly expressed in skeletal muscle and brown adipose tissue [1;2]. Initially described as a homologue of the classical brown fat thermogenic Ucp1 it was soon established that Ucp3 has a function other than thermogenesis. One major argument against a thermogenic role was the positive transcriptional regulation of the *Ucp3* gene in response to starvation in which activation of an energy wasting mechanism seems unlikely [3]. Many studies describe *Ucp3* upregulation in response to physiological situations associated with increased plasma fatty acid levels and lipid utilization including cold exposure [4], acute exercise [5] and streptozocin-induced diabetes [6] as well as direct lipid infusion [7]. The inferred relevance of this anion carrier protein in lipid metabolism is a cornerstone of the hypothesis of Ucp3 being a fatty acid anion exporter, a biochemical function necessary to eliminate free fatty acid from the mitochondrial matrix and not assigned to a specific protein previously [8]. This molecular function of Ucp3 however is subject to an ongoing debate [9]. Despite its obviously different role *in vivo*, certain biochemical properties of the protein as measured in mitochondrial proton leak assays resemble those of Ucp1, i.e. causing a GDP-sensitive inducible proton leak [10]. Therefore other major hypotheses consider Ucp3 to primarily be a proton translocator, pyruvate transporter, superoxide transporter, constituent of a radical defense system and constituent of the mitochondrial  $\text{Ca}^{2+}$  uniporter (reviewed in [9] and [11]).

Apart from the controversy about the actual molecular function there is general consent that Ucp3 is implicated in the maintenance or tolerance of high lipid oxidation rates by either being an integral part of fatty acid metabolism or an accompanying phenomenon. In addition to its localisation in tissues with highest  $\beta$ -oxidative capacities and its regulation by serum free fatty acid levels there is complementary evidence for a role in lipid metabolism from a different perspective. In a number of association and linkage studies, polymorphisms in the human *UCP3* locus have been reported to influence markers of obesity like BMI and waist-to-hip ratio [12;13]. Since *Ucp3* and *Ucp2* share the same genomic locus and are well within linkage disequilibrium it has been problematic to assign association of the respective phenotype to a polymorphism in either of the paralogues [14].

In our breeding colony of the Djungarian hamster *Phodopus sungorus* we identified animals lacking *Ucp3* mRNA expression exclusively in brown adipose tissue (BAT) without phenotypic consequences for resting metabolic rate [15]. We further analyzed this mutation



on a broad genetic background to elucidate the affected regulatory mechanism and the phenotypic consequences.

The expression of *Ucp3* is controlled by an interacting network of multiple factors including PPAR $\alpha$ /RXR $\alpha$  heterodimers, MyoD, Coup-TFII and several more [16;17]. The function of all these known components of the machinery controlling *Ucp3* transcription is mediated by a genomic region upstream of *Ucp3* exon 1. We here report on a novel intronic regulatory element which is essential for brown fat *Ucp3* transcription and thereby confers tissue specificity of *Ucp3* expression. We show that disruption of this element leads to BAT specific loss of *Ucp3* expression and an altered body mass trajectory.

## Experimental procedures

### **DNA sequence analysis**

We chose primers for comparative sequencing of the hamster *Ucp3* locus with the software Primer3 (code available at [18]) based on Genbank entry AY523564 to yield overlapping PCR fragments of about 500 bp in length. Amplicons were Sanger sequenced from both ends. Sequences were aligned and analysed with the GAP module of the Staden Package [19]. Sequence positions and variations are named following nomenclature recommendations and based on Genbank entry AY523564 [20]. Accordingly positions in intron 1 are called “intervening sequence 1” IVS1+x, counting from the first base +1 of this intron. Positions outside introns are given relative to the A (+1) of start codon ATG in AY523564. Analyses of transcription factor binding sites were conducted with Match™ [21].

For two sequence variations located in *Ucp3* intron 1 we developed restriction fragment length polymorphism (RFLP) assays. The region surrounding IVS1+1505A constitutes a recognition site for AarI which is absent when the IVS1+1505G-allele is present. At IVS1+2668A there is an Eco57I site that is lacking if the IVS1+2668G-allele is present. We amplified a genomic fragment including both polymorphic sites with primers TGTCCTGATGGCTCCTCTCTA / CCCAGGAACTTCACAACCTG and digested with either AarI (Fermentas) or Eco57I (Fermentas).

To genotype a larger number of animals we utilized the Pyrosequencing® technique employing the PSQ 96MA system (Biotage AB). We first amplified a long intronic DNA fragment with primers CAAGTCACCCAGCAGCCTA / GGCGGCATCTATCTGGAATA. In a second, nested PCR we used primers CAGTACCTCCTGCTGGGAAG and 5'-biotinylated Biotin-AGTCAGACCTTGGCTCTCCA to amplify a 248 bp long region encompassing IVS1+1505. The total yield of biotin labelled PCR product was immobilized on 3µl Steptavidin labelled Sepharose beads (GE Healthcare) at room temperature. Single stranded DNA was prepared at a Vacuum Work Station (Biotage AB) and transferred into a PSQ reaction plate (Biotage AB) where the sequencing primer GCCTGAATAAGTGTTTTCT was annealed. Pyrosequencing® reactions were performed using the PyroGold™ SNP reaction kit (Biotage AB) following the manufacturer's manual. The sequence to analyse was defined as TAACAC**RC**CTG and the dispensation order for the single nucleotide injection was calculated to be GTACAC**G**AGC (bold: polymorphic site) by the PSQ 98MA software (Version 2.1, Biotage AB). Results were calculated and analysed by the PSQ 98MA software.

### **Animal growth, body mass and composition**

To study the phenotypic consequences of the two alleles of *Ucp3* intron 1 *in vivo*, on a broad genetic background and in all genotypes we crossed heterozygous hamsters. To identify founder animals we genotyped position IVS1+1505 of 90 animals randomly chosen from our colony. The progeny of 14 heterozygous breeding pairs displayed an allele frequency of 0,5 for IVS1+1505G and 0,5 for IVS1+1505A in 171 animals as expected. The alleles were distributed among genotypes in accordance with Hardy-Weinberg equilibrium. The body weight of all animals was continuously monitored on a weekly basis. On day 81±3 after birth 66 hamsters were transferred to an ambient temperature of 4°C for two days and sacrificed.

All determinations of body fat mass and femur length were performed under isoflurane anesthesia with DEXA (PIXImus2 scanner, software version 1.46.007, GE Medical Systems, Madison, Wisconsin, USA). The head of the animals was excluded from the measurement. Bone mass is not included in DEXA-provided values for total body mass (head excluded) and lean mass.

Animal experiments were conducted in accordance with the German animal welfare law.

### **Quantitative PCR**

We extracted total RNA from BAT and skeletal muscle with TRIzol (Invitrogen) and quantified photometrically. RNA was reverse transcribed with the Superscript III First Strand Synthesis Kit (Invitrogen). To quantify transcript levels by qPCR we used ImmoMix (Bioline) supplemented with SYBR Green (Bioline) and 20 nM Fluorescein (Biorad) on an iCycler (Biorad). The efficiency of amplification was calculated based on dilution series standard curves by the Biorad iCycler IQ 3.0 software and used to determine starting quantity levels (PCR base line subtracted) normalized to  $\beta$ -actin levels. Primers:  $\beta$ -actin AGAGGGAAATCGTGCGTGAC, CAATAGTGATGACCTGGCCGT; *Ucp3* AGGAAGGAATCAGGGGCTTA, TCCAGCAGCTTCTCCTTGAT. Results were statistically analysed by t-tests (SigmaStat 3.1, Systat Software).

### **Vector construction**

Using genomic DNA of animals either homozygous for [IVS1+1505G; IVS1+2668A] or [IVS1+1505A; IVS1+2668G], we PCR amplified fragments of 4338 bp spanning position -4234 to +103 of the *Ucp3* genomic locus with primers CCTTGGGAAGTCAATGTCCT / CCAGGGGGAAGGTGAGTAGGTCT and Pfu polymerase (Fermentas). Amplicons were

used in a nested Pfu-PCR to amplify the region between positions -4027 to +14 with primers GGGGGAAGGGAAACGGGGAGAC / GAAGTCCAACCATGGTGCCCCAGCAG, the latter of which is heterologous in one base position (underlined) creating a NcoI recognition site around the endogenous start codon of the Ucp3 gene. Respective amplicons were digested with BglII and NcoI, the resulting fragment spanning the region between -3555 to +3 gel purified and cloned into the respective restriction sites of pGL3-basic (Promega). By sequencing we identified clones without PCR introduced errors representing the two alleles [IVS1+1505G; IVS1+2668A] and [IVS1+1505A; IVS1+2668G] (corresponds to #1 and #2 in Figure 2A).

We next generated constructs representing the two alleles not present in our colony [IVS1+1505A; IVS1+2668A] and [IVS1+1505G; IVS1+2668G] (corresponds to #3 and #4 in Figure 2A). To do so we cut vectors #1 and #2 into two fragments each with KpnI (Fermentas) with both fragments either containing IVS1+1505 or IVS1+2668. These fragments were gel purified and ligated crosswise.

### ***Reporter gene assays***

HIB1B cells were grown in DMEM/F12 (Gibco) containing 10% FCS (Biochrom) until confluence. To differentiate the cells we decreased FCS content to 7% and added 17nM insulin (Sigma) for approx. 10 days. C2C12 cells were grown in DMEM containing 10% FCS until confluence and switched to DMEM with 2% horse serum to induce differentiation.

Both cell lines were transfected by the nucleofection method (Amaxa) according to the manufacturer's recommendations for the respective cell line. After nucleofection cells were incubated for an additional 24 hours with fresh medium. 20µM Rosiglitazone solved in ethanol and 10µM Wy14,643 in DMSO were added during this medium change where stated. In all measurements without stimulant, medium was supplied with a comparable volume of DMSO and ethanol only. Photinus luciferase activity was measured with components of the Dual Luciferase Reporter Assay System (Promega). All measurements were replicated at least three times independently including nucleofection.

### ***Electrophoretic mobility shift assay***

HIB1B cells on a 10cm culture plate were harvested after full differentiation and 24h stimulation with 20µM Rosiglitazone and 10µM Wy14,643 and nuclear protein was isolated; complementary oligonucleotides were annealed and labelled as described before [17]. Sequence of the double stranded oligonucleotide probes (sense strand): wt:

GTGTTTTCTTAACACGCCTGCACTGTTGGTA; mut:  
GTGTTTTCTTAACACACCTGCACTGTTGGTA.

For gel retardation assays we incubated 3 $\mu$ g nuclear extract with ~7.5 fmol probe for 20 min on ice in a final volume of 2 $\mu$ l containing 4% (v/v) glycerol, 1mM MgCl<sub>2</sub>, 0.5mM EDTA, 0.5mM DTT, 50mM NaCl, 10mM Tris/HCl (pH 7.5) and 50 $\mu$ g/ml poly(dIdC)·poly(dIdC). Samples were analyzed by electrophoresis in a 5.2% nondenaturing polyacrylamide gel at 4°C and 200V for 3 hours in 0.5xTBE. The gel was exposed to a phosphoscreen for 18 hours.

### **Western Blot**

Total protein was prepared from skeletal muscle and BAT of control hamsters and protein concentrations determined using the Bradford method. 30  $\mu$ g protein was loaded on a SDS-PAGE and transferred to a nitrocellulose membrane (Hybond-C extra, Amersham Biosciences) in a semi-dry electroblotting chamber. Successful protein transfer was controlled by Ponceau staining of the membrane. Ucp3 protein was detected using a rabbit Ucp3 antibody (kindly provided by R. Porter, Dublin) in turn bound by a goat anti-rabbit-IgG-horseradish peroxidase-conjugated secondary antibody (Dako) and developed by a chemiluminescence reagent (Supersignal, Pierce).

### **Statistical analysis**

We statistically analyzed the body weight development of hamsters with different genotype. Raw body mass data were included into a 2-Way Repeated-Measures ANOVA with “sex” (m, f) and “genotype” (IVS1+1505: AA, GA, GG) as factors for *between*-comparisons and “age” as *within*-comparison factor (33 measurements) (Statistika '99 Edt., StatSoft Inc.). All complete individual data sets were included, collected between week 4 and week 36 of age.

The mRNA expression levels of the *Ucp3* gene as measured by qPCR were tested for group differences with the Mann-Whitney rank sum test (SigmaStat 3.1, Systat Software).

## Results

### ***The hamster Ucp3 gene exhibits two alleles***

To detect possible sequence variations associated with the lack of Ucp3 expression in BAT we sequenced 12,721 bp of the *P. sungorus Ucp3* gene including all seven exons, all introns and 3632 bp of the promoter region. We compared sequences derived from two wildtype with two Ucp3 deficient (“mutant”) hamsters. Sequences were identical except for two positions within the first intron (Figure 1A). At position IVS1+1505 both wildtype hamsters were heterozygous G/A, while both mutant animals were homozygous for allele A. At position IVS1+2668 wildtype hamster were heterozygous G/A while mutant animals were homozygous for G (Fig. 1 A).

We developed RFLP assays for both sequence variations IVS1+1505G>A and IVS1+2668A>G and genotyped 43 hamsters of our breeding colony. Genotype distribution indicated the presence of two haplotypes [IVS1+1505G; IVS1+2668A] and [IVS1+1505A; IVS1+2668G].

### ***A single base exchange is responsible for expression phenotype***

To elucidate whether these two polymorphic sites are responsible for the expression phenotype we constructed four different reporter gene vectors all harbouring a minimal *Ucp3* promoter, the first exon, the complete first intron and the untranslated region of the second exon. The endogenous ATG was utilized as start codon for the luciferase open reading frame. The four vectors represent all possible haplotypes of the two intron 1 polymorphic sites as indicated in Figure 2A.

Nucleofection of these vectors into differentiated HIB1B brown adipocytes revealed allele specific reporter gene expression (Figure 2B). Basal activity of vectors #1 and #4 was 10-fold higher than of #2 and #3. Induction by PPAR agonists led to a strong increase of expression in #1 and #4 but not in #2 and #3. In this condition the two vectors exhibiting IVS1+1505G displayed an about 100-fold higher reporter gene activity than vectors with IVS1+1505A. Thus both basal activity and induction by PPAR agonists was dependent on the presence of a G at position IVS1+1505.

In differentiated C2C12 myotubes we did not observe differences in basal expression levels of the four vectors. Upon stimulation with PPAR agonists however the expression of vectors with IVS1+1505G was slightly upregulated, while vectors with IVS1+1505A retained their basal level (Figure 2B).

### ***Ucp3 expression is silenced by allele IVS1+1505A in vivo***

We analyzed *Ucp3* expression of 2 days cold exposed hamsters at the age of  $83 \pm 3$  days with respect to genotypes at positions IVS1+1505 and IVS1+2668. In BAT, *Ucp3* mRNA expression showed marked differences based on genotypes at respective polymorphic sites (Figure 3A). Heterozygous animals had a 30% lower mRNA abundance than homozygous IVS1+1505G animals while homozygous IVS1+1505A hamsters were virtually devoid of *Ucp3* mRNA. In SKM *Ucp3* mRNA expression was lowest in homozygous IVS1+1505A and significantly different from homozygous +IVS1+1505G animals with an intermediary level in heterozygous hamsters.

The *Ucp3* protein level of control animals reflected the mRNA data. There was a clear genotype- and tissue-specific difference in expression (Figure 3B).

### ***Mutant allele is naturally occurring***

To determine allele frequencies we cumulated RFLP results from the 43 animals initially genotyped and of 90 animals genotyped to establish heterozygous breeding pairs. By pyrosequencing we genotyped an additional 97 animals randomly chosen from our breeding colony totalling 230 hamsters. Of these 105 were homozygous IVS1+1505G, 104 heterozygous and 21 homozygous IVS1+1505A resulting in an allele frequency of 0,68 for IVS1+1505G and 0,32 for IVS1+1505A (Figure 4). The observed genotypes were in Hardy-Weinberg equilibrium.

To evaluate the worldwide distribution of IVS1+1505A we collected samples from five different breeding colonies of *P. sungorus* in the US, Canada and Europe (Figure 4), two of which were established independently from the Marburg colony. Most Djungarian hamsters in research laboratories nowadays can be traced back to K. Hoffmann and J. Figalas colony at the Max Planck institute in Andechs, Germany [22]. This is true for our own animals (allele frequency IVS1+1505A = 0,37) as well as for the commercial supplier Wrights of Essex (UK) where J. Mercer (0,97) and A. Loudon (1,00) obtained their founder animals (personal communication and [23]). S. Steinlechner (0,03) and C. Wynne-Edwards (0,23) trapped animals in Siberia in the wild and established independent colonies in their laboratories that have never been interbred with animals of a different origin (personal communication and [24]). In samples of hamsters from both colonies we identified the mutant allele. Since in S. Steinlechner's samples we only found a single heterozygous animal we confirmed our

result by genotyping offspring of this animal and could again identify IVS1+1505A. T. Bartness' hamsters (IVS1+1505A = 0,07) originate from the Hoffmann/Figala line and were interbred with animals from S. Steinlechner and C. Wynne-Edwards (personal communication). Taken together the allele IVS1+1505A was found in every colony analysed including all independently established ones.

### ***Differential complex formation in EMSA***

One potential link between a sequence variation and a defective transcriptional regulation is the loss or impairment of a transcription factor binding site. To investigate this possibility we performed electrophoretic mobility shift assays with probes representing the polymorphic intronic site IVS1+1505 and nuclear extracts isolated from the brown adipocyte cell line HIB1B stimulated with Wy14,643 and Rosiglitazone. This cell culture system had proven to be a suitable environment to visualize the allele specific expression phenotype in our reporter gene assays. On the wildtype probe we observed complex formation that was absent when using the mutant oligonucleotide (Figure 5A).

### ***Identification of a forkhead domain binding element in several vertebrate species***

The sequence element surrounding IVS1+1505 was identified in the first intron of the *Ucp3* gene in all analyzed vertebrates (Figure 5B). Among these, G at position IVS1+1505 is conserved. We derived a consensus sequence from this alignment and analysed it for potential transcription factor binding sites. Considering the pattern of conserved bases, a binding site for forkhead domain transcription factors is predicted.

### ***G allele at position IVS1+1505 led to an altered body weight development***

We kept offspring of heterozygous breeding pairs at room temperature under long day condition (16:8 h L:D) with *ad libitum* access to food and water and monitored body weight. At the age of 81±3 days 66 animals were transferred to 4°C ambient temperature for two days, sacrificed and organ weights determined. We weighed suprasternal BAT, interscapular BAT, inguinal WAT and spleen, none of which displayed a significant difference with respect to genotype at IVS1+1505. The same was true for the difference in body mass before and after cold exposure (supplemental data).



We did, however, find a differential development of body weight (Figure 6). Both male and female animals being homozygous IVS1+1505G displayed a lower body mass than carriers of IVS1+1505A. Heterozygous hamsters tended to behave in a similar way as hamsters homozygous IVS1+1505A. This pattern of genotype specific body weight trajectories was very similar in male and in female hamsters. The development of body weight over time was significantly influenced by the genotype of the animals (Table 1).

To allocate this difference we measured body composition of 108 hamsters aged 259 to 289 days by DEXA, but we did not detect any significant genotype effects on body composition. As a measure for body size we determined the lengths of the femur of all animals from these X-ray pictures and did not find a significant genotype effect on size (supplemental data). The significant difference in body mass trajectories was neither clearly attributable to fat or lean mass nor to an overall increase in body size.

## Discussion

In our breeding colony of the Djungarian hamster *Phodopus sungorus* we identified animals exhibiting a heritable BAT specific lack of *Ucp3* mRNA [15]. We were able to pinpoint the underlying genetic variation by re-sequencing of the *Ucp3* gene in several animals. Surprisingly it was located in the first intron far away from all known regulatory elements known so far, which are located in the proximal promoter region and further upstream [16;17;25]. Differential complex formation in electrophoretic mobility shift assays imply a function as binding site for a transcriptional regulator.

In reporter gene assays as well as *in vivo* allele IVS1+1505A led to complete loss of expression in BAT only, while in skeletal muscle cells only a mild phenotype could be observed. Therefore the affected element very probably is a regulator of tissue specific *Ucp3* expression. So far the molecular basis of this tissue specificity has been unknown and differences in the activity of known transcription factors like PPAR $\alpha$  and  $\delta$  have been implicated [26]. Our findings prove the presence of a distinct intronic regulatory element that is responsible and essential for BAT specific expression of *Ucp3*. Analysis of the conserved consensus sequence based on sequence comparison of several vertebrate species revealed a binding site for a forkhead domain transcription factor.

More than 40 members of this transcription factor family are known to date [27] and for many of these factors a role in adipose tissue metabolism and other *Ucp3* related fields has been described [28-31]. On the one hand this corroborates the view of a forkhead factor being responsible for BAT specific *Ucp3* transcription, on the other hand together with the sheer number of family members it prevents a straight forward candidate approach. Furthermore most of the forkhead factor family members have not even been investigated in detail so far.

The presence of *Ucp3* in both skeletal muscle and brown adipose tissue has been reported for all species analysed in this respect so far including mice [1] and rats [2]. Since hamsters carrying the IVS1+1505G allele display this known distribution of *Ucp3*, we consider IVS1+1505A to be the more recently emerged allele. Our screening for IVS1+1505A and IVS1+1505G in several international breeding colonies of *P. sungorus* identified IVS1+1505A to be present in all colonies including three independently founded ones. This clearly shows that the mutation generating IVS1+1505A did not occur in captivity but in the wild. In fact it indicates a rather high allele frequency in the wild population being incidentally trapped for three times at different times and places. Without any knowledge about the actual allele frequencies in the wild, however, we can merely conclude the lack of any dramatic negative consequences of IVS1+1505A regarding overall fitness.

Beyond this study the knowledge about the existence of IVS1+1505A and its primary expression phenotype may prove valuable to further study the function of Ucp3. So far there are *Ucp3*(-/-) mouse models available and transgenic mice overexpressing the protein [32-35]. With the Djungarian hamster we now have access to an animal model with a tissue specific lack of expression that can be applied to elucidate the tissue specific protein function. Furthermore knowledge about IVS1+1505A will help researchers working with Djungarian hamsters to select animals of the appropriate genotype for their respective study.

The implication of Ucp3 in the regulation of body mass has long been disputed. There are several studies that describe an interrelation of polymorphisms within the human *UCP3* gene and markers of obesity, especially -55(T/C) located in the promoter region [12-14]. The proximity of the *UCP2* gene has always raised the question whether these effects can doubtlessly be ascribed to *UCP3* or possibly to additional polymorphisms within linkage disequilibrium [14]. In this study we demonstrate that a change in *Ucp3* expression can be responsible for an altered body weight development. In this respect heterozygous hamsters seemed to resemble homozygous IVS1+1505A rather than homozygous IVS1+1505G hamsters. This dominant body weight phenotype would imply that small changes of *Ucp3* expression levels could already lead to a full scale impact on body weight development.

The involvement of Ucp3 in energy balance is substantiated by its transcription being correlated to serum fatty acid levels and its presence in tissues with exceptional  $\beta$ -oxidative capacities [7]. The absence of a body weight phenotype in *Ucp3*(-/-) mice [34;35], however, questioned the relevance of Ucp3 in this context. Our demonstration of a differential body weight development in response to an altered *Ucp3* expression reopens this discussion. In fact it cannot be ruled out that comparable effects were merely overlooked in *Ucp3*(-/-) mice. All published analyses of body weight development in these animal models utilized far less animals and shorter study periods than in this study and would probably not have revealed an effect of this size. In contrast to *Ucp3*(-/-) mice, however, our hamster model lacks Ucp3 specifically in BAT, whereas skeletal muscle expression is only mildly impaired. Nevertheless we cannot decide on the tissue that fundamentally accounts for the body weight divergence. While a complete lack of Ucp3 in BAT seems tempting to be held responsible, even a small change in skeletal muscle may significantly contribute to this phenotype given the huge fraction of body mass and metabolism it represents. In any case it is surely worthwhile to comparatively resequence the human *UCP3* intron 1 to identify possible SNPs in this novel regulatory region.

Taken together we have identified an intronic element within the *Ucp3* gene that is essential for BAT expression of this gene and constitutes a forkhead domain transcription factor binding site. A naturally occurring mutation disrupting this element in the homozygous state leads to complete loss of BAT *Ucp3* and an altered body weight development.

## **Acknowledgements**

This work was supported by the Deutsche Forschungsgemeinschaft (DFG), grant KL973/7-3 and NGFN2 [01GR0504, 01GS0483(TP23)]. T. Fromme was recipient of a fellowship of the Friedrich-Naumann-Foundation. We thank S. Steinlechner, C. Wynne-Edwards, J. Mercer, A. Loudon and T. Bartness for kindly supplying samples of their respective hamster colonies, R. Porter for providing the Ucp3 antibody and J. Kämper for the generous provision of access to an iCycler.

## Reference List

- 1 Vidalpuig, A., Solanes, G., Grujic, D., Flier, J. S., and Lowell, B. B. (1997) *Biochem Biophys Res Commun* **235**, 79-82
- 2 Boss, O., Samec, S., Paolonigiacobino, A., Rossier, C., Dulloo, A. G., Seydoux, J., Muzzin, P., and Giacobino, J. P. (1997) *FEBS Lett* **408**, 39-42
- 3 Millet, L., Vidal, H., Andreelli, F., Larrouy, D., Riou, J. P., Ricquier, D., Laville, M., and Langin, D. (1997) *J Clin Invest* **100**, 2665-2670
- 4 von Praun, C., Burkert, M., Gessner, M., and Klingenspor, M. (2001) *Physiol Biochem Zool* **74**, 203-211
- 5 Giacobino, J. P. (1999) *Int J Obes Relat Metab Disord.* **23 Suppl 6**, S60-S63
- 6 Stavinocha, M. A., RaySpellicy, J. W., Essop, M. F., Graveleau, C., Abel, E. D., Hart-Sailors, M. L., Mersmann, H. J., Bray, M. S., and Young, M. E. (2004) *Am J Physiol* **287**, E888-E895
- 7 Weigle, D. S., Selfridge, L. E., Schwartz, M. W., Seeley, R. J., Cummings, D. E., Havel, P. J., Kuijper, J. L., and Beltrandelrio, H. (1998) *Diabetes* **47**, 298-302
- 8 Schrauwen, P., Hoeks, J., Schaart, G., Kornips, E., Binas, B., Van De Vusse, G. J., Van Bilsen, M., Luiken, J. J., Coort, S. L., Glatz, J. F., Saris, W. H., and Hesselink, M. K. (2003) *FASEB J* **17**, 2272-2274
- 9 Nedergaard, J. and Cannon, B. (2003) *Exp Physiol* **88**, 65-84
- 10 Talbot, D. A., Lambert, A. J., and Brand, M. D. (2004) *FEBS Lett* **556**, 111-115
- 11 Trenker, M., Malli, R., Fertschai, I., Levak-Frank, S., and Graier, W. F. (2007) *Nature Cell Biology* **9**, 445-U156
- 12 Otabe, S., Clement, K., Dina, C., Pelloux, V., Guy-Grand, B., Froguel, P., and Vasseur, F. (2000) *Diabetologia* **43**, 245-249
- 13 Cassell, P. G., Saker, P. J., Huxtable, S. J., Kousta, E., Jackson, A. E., Hattersley, A. T., Frayling, T. M., Walker, M., Kopelman, P. G., Ramachandran, A., Snehelatha, C., Hitman, G. A., and McCarthy, M. I. (2000) *Diabetologia* **43**, 1558-1564
- 14 Walder, K., Norman, R. A., Hanson, R. L., Schrauwen, P., Neverova, M., Jenkinson, C. P., Easlick, J., Warden, C. H., Pecqueur, C., Raimbault, S., Ricquier, D., Silver, M. H., Shuldiner, A. R., Solanes, G., Lowell, B. B., Chung, W. K., Leibel, R. L., Pratley, R., and Ravussin, E. (1998) *Hum.Mol.Genet.* **7**, 1431-1435
- 15 Liebig, M., von Praun, C., Heldmaier, G., and Klingenspor, M. (2004) *Physiol Biochem Zool* **77**, 116-126
- 16 Solanes, G., Pedraza, N., Iglesias, R., Giralt, M., and Villarroya, F. (2003) *Mol Endocrinol* **17**, 1944-1958

- 17 Fromme, T., Reichwald, K., Platzer, M., Li, X. S., and Klingenspor, M. (2007) *BMC Mol.Biol.* **8**, 1
- 18 Rozen, S. and Skaletsky, H. J. Primer3. Code available at [http://www-genome.wi.mit.edu/genome\\_software/other/primer3.html](http://www-genome.wi.mit.edu/genome_software/other/primer3.html). 1996.
- 19 Staden, R. (1996) *Mol.Biotechnol.* **5**, 233-241
- 20 den Dunnen, J. T. and Antonarakis, S. E. (2001) *Hum.Genet.* **109**, 121-124
- 21 Biobase Biological Databases. 2006.  
Ref Type: Computer Program
- 22 Steinlechner, S. (1998) *Eur Pin Soc NEWS* **38**, 7-11
- 23 Ebling, F. J. P. (1994) *Gen Comp Endocrinol* **95**, 475-482
- 24 Wynne-Edwards, K. E. (2003) *Advances in the Study of Behavior, Vol 32* **32**, 207-261
- 25 Solanes, G., Pedraza, N., Calvo, V., Vidal-Puig, A. J., Lowell, B. B., and Villarroya, F. (2005) *Biochem J* **386**, 505-513
- 26 Pedraza, N., Rosell, M., Villarroya, J., Iglesias, R., Gonzalez, F. J., Solanes, G., and Villarroya, F. (2006) *Endocrinology* **147**, 4695-4704
- 27 Wijchers, P. J. E. C., Burbach, J. P. H., and Smidt, M. P. (2006) *Biochemical Journal* **397**, 233-246
- 28 Wolfrum, C., Shih, D. Q., Kuwajima, S., Norris, A. W., Kahn, C. R., and Stoffel, M. (2003) *J Clin.Invest.* **112**, 345-356
- 29 Wang, F., Nguyen, M., Qin, F. X., and Tong, Q. (2007) *Aging Cell*
- 30 Subauste, A. R. and Burant, C. F. (2007) *Am.J Physiol Endocrinol.Metab.*
- 31 Cederberg, A., Gronning, L. M., Ahren, B., Tasken, K., Carlsson, P., and Enerback, S. (2001) *Cell* **106**, 563-573
- 32 Clapham, J. C., Arch, J. R., Chapman, H., Haynes, A., Lister, C., Moore, G. B., Piercy, V., Carter, S. A., Lehner, I., Smith, S. A., Beeley, L. J., Godden, R. J., Herrity, N., Skehel, M., Changani, K. K., Hockings, P. D., Reid, D. G., Squires, S. M., Hatcher, J., Trail, B., Latcham, J., Rastan, S., Harper, A. J., Cadenas, S., Buckingham, J. A., Brand, M. D., and Abuin, A. (2000) *Nature* **406**, 415-418
- 33 Echtay, K. S., Roussel, D., St Pierre, J., Jekabsons, M. B., Cadenas, S., Stuart, J. A., Harper, J. A., Roebuck, S. J., Morrison, A., Pickering, S., Clapham, J. C., and Brand, M. D. (2002) *Nature* **415**, 96-99
- 34 Vidal-Puig, A. J., Grujic, D., Zhang, C. Y., Hagen, T., Boss, O., Ido, Y., Szczepanik, A., Wade, J., Mootha, V., Cortright, R., Muoio, D. M., and Lowell, B. B. (2000) *J.Biol.Chem.* **275**, 16258-16266

- 35 Gong, D. W., Monemdjou, S., Gavrilova, O., Leon, L. R., Marcus-Samuels, B., Chou, C. J., Everett, C., Kozak, L. P., Li, C., Deng, C., Harper, M. E., and Reitman, M. L. (2000) *J.Biol.Chem.*2000.May.26;275(21):16251-7. **275**, 16251-16257



## Figure legends

**Figure 1** – The *Ucp3* gene of *Phodopus sungorus* exhibits two sequence variations. **(A)** The genomic organisation of the seven *Ucp3* exons. There are two polymorphic sites at IVS1+1505 and IVS1+2668 in the first intron. *TSS* – *transcriptional start site*, *ATG* – *start codon*, *Stop* – *stop codon*. **(B)** Gel images of the restriction fragment length polymorphism genotyping method.

**Figure 2** – Reporter gene assays revealed the point mutation responsible for the lack of *Ucp3* expression to be at position IVS1+1505. **(A)** Schematic representation of the four reporter gene vector constructs utilized. All four possible haplotypic combinations were tested. **(B)** Luciferase activity is shown relative to the activity of unstimulated construct #1 representing the wildtype allele, errors are standard deviation. In HIB1B cells both constructs containing IVS1+1505G showed a 10-fold higher basal activity than constructs harbouring IVS1+1505A while position IVS1+2668 did not seem to play a role. Stimulated with PPAR agonists this difference increased to 100-fold. In C2C12 cells basal activity of all constructs is comparable. When stimulated IVS1+1505G constructs increased activity by ~50%, while IVS1+1505A constructs did not change expression.

**Figure 3** – *Ucp3* expression *in vivo* was silenced by IVS1+1505A. **(A)** *Ucp3* mRNA abundance in tissues from cold exposed animals as measured by qPCR relative to homozygous IVS1+1505G, errors are standard deviation. In brown adipose tissue (BAT) *Ucp3* mRNA abundance was significantly different from each other in all three genotypes with homozygous IVS1+1505A hamsters being virtually devoid of expression. In skeletal muscle (SKM) only homozygous animals differed significantly from each other with an intermediate *Ucp3* mRNA level in heterozygotes. \*\*\* =  $p < 0.001$ , \* =  $p < 0,05$ , n(BAT) = 53 (17/26/20), n(SKM) = 46 (15/15/16). **(B)** Western Blots of protein isolated from tissues of animals under control conditions. The above difference in mRNA amounts is reflected on the protein level. Homozygous IVS1+1505A hamsters did not show any detectable *Ucp3* protein in BAT. In skeletal muscle the *Ucp3* protein level of these animals is slightly decreased.

**Figure 4** – The allele frequencies of IVS1+1505G (white) and IVS1+1505A (black) in six international colonies proved the occurrence of both alleles in the natural habitat. The colonies Klingenspor, Steinlechner and Wynne-Edwards are completely independent and

have never been interbred. Hamsters from Mercer and Loudon can be traced back to the same source as our (Klingenspor) hamsters. The Bartness animals are a product of interbreeding hamsters from all these lines.

**Figure 5** – Differential DNA-protein complex formation occurs on a sequence element conserved in vertebrates. **(A)** Electrophoretic mobility shift assay with a probe harbouring IVS1+1505 surrounded by 15bp on both sides incubated with HIB1B nuclear extracts. With probe IVS1+1505G (WT) we observed a clear complex formation that was absent with probe IVS1+1505A (Mut). **(B)** Alignment of the responsible intronic element of several vertebrate species. The consensus sequence of conserved bases constitutes a forkhead domain transcription factor binding site. \* = fully conserved position, **bold** = IVS1+1505, underlined = EMSA probe. Hs=*Homo sapiens*, Pt=*Pan troglodytes*, Cf=*Canis familiaris*, Bt=*Bos taurus*, Rn=*Rattus norvegicus*, Mm=*Mus musculus*, Md=*Monodelphis domestica*, Ps=*Phodopus sungorus*.

**Figure 6** – Body weight development was dependent on the genotype of hamsters. The body weight of hamsters was monitored on a weekly basis beginning with weaning. Shown is the mean absolute body weight with standard errors. Wt = homozygous IVS1+1505G, het = heterozygous, mut = homozygous IVS1+1505A.

**Table 1** – We statistically analysed body weight data by 2-Way Repeated-Measures ANOVA. The genotype of an animal significantly influenced the development of body weight with age in both sexes.

**Table 1**

Parameter	p-value
Sex	< 0.001
Genotype	0.010
Age	< 0.001
Sex x Genotype	0.920
Sex x Age	< 0.001
Genotype x Age	0.041

## Supplemental data

### Supplemental table 1

On day  $81 \pm 3$  after birth 66 hamsters were transferred to an ambient temperature of  $4^\circ\text{C}$  for two days and sacrificed.  $\Delta$  Body mass indicates the change in body mass over these two days. The column genotype

Sex	Genotype IVS1+1505	Body mass		$\Delta$ Body mass		sBAT		iBAT		iWAT		Spleen	
		g	SD	g	SD	mg	SD	mg	SD	mg	SD	mg	SD
F	GG	27,3	2,9	-0,2	4,7	119,2	41,0	126,7	43,7	614,1	152,9	75,8	52,9
F	AG	28,1	2,2	0,1	2,5	107,5	20,8	106,5	24,8	591,9	107,7	94,3	43,5
F	AA	28,2	3,5	-1,3	1,9	113,2	39,8	123,0	42,1	635,7	97,5	98,8	75,9
M	GG	32,3	2,7	-2,9	2,4	118,6	24,9	121,1	20,6	626,8	83,7	69,7	19,3
M	AG	33,3	4,5	-1,2	1,4	136,1	46,8	130,7	43,3	645,6	130,1	79,0	36,0
M	AA	33,5	3,6	-3,4	2,0	126,0	33,5	125,6	28,9	646,7	130,3	82,8	46,7

### Supplemental table 2

We measured body composition of 108 hamsters aged 259 to 289 days by DEXA, but we did not detect any significant genotype effects on body composition. As a measure for body size we determined the lengths of the femur of all animals from these X-ray pictures (a.u.=arbitrary units) and did not find a significant genotype effect on size.

Sex	Genotype IVS1+1505	Body mass		Lean mass		Fat mass		Femur length	
		g	SD	g	SD	g	SD	a.u.	SD
F	GG	31,04	4,82	19,48	2,41	7,79	2,43	98,71	4,63
F	AG	31,69	3,94	19,22	1,98	8,50	2,11	97,00	4,50
F	AA	30,32	5,26	19,51	3,32	6,96	2,02	99,25	3,42
M	GG	38,02	4,73	24,59	3,03	9,26	2,23	100,60	2,63
M	AG	37,16	5,13	24,76	3,20	8,37	1,98	103,15	4,76
M	AA	35,35	5,01	23,35	3,07	8,08	2,15	100,27	3,61

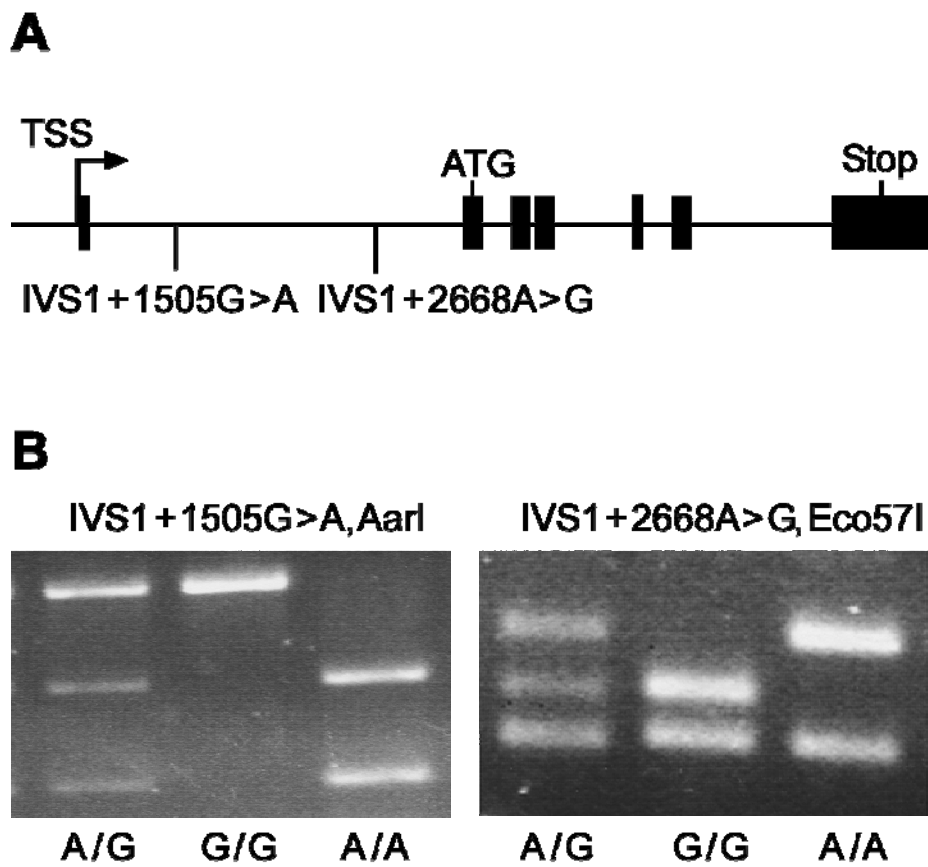


Fig.1

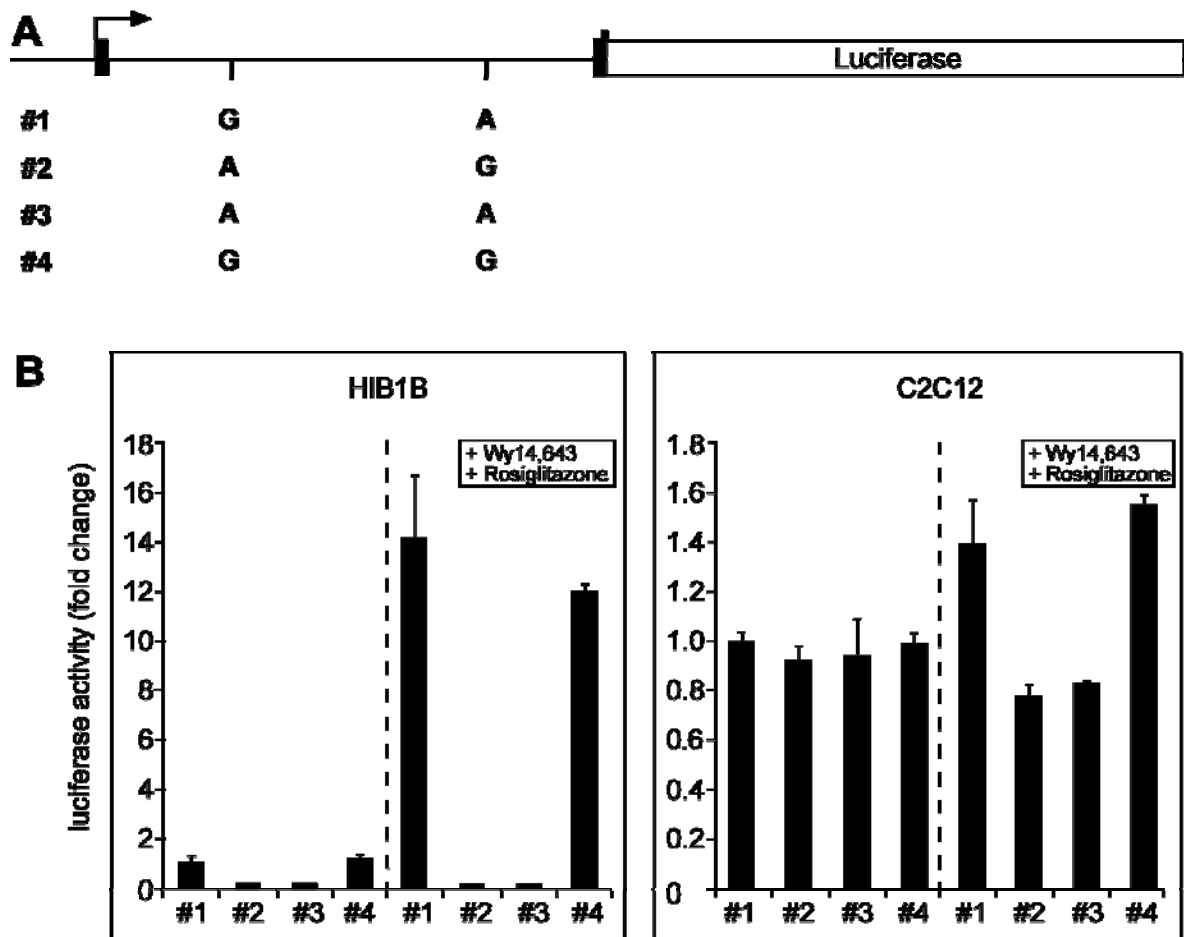


Fig.2

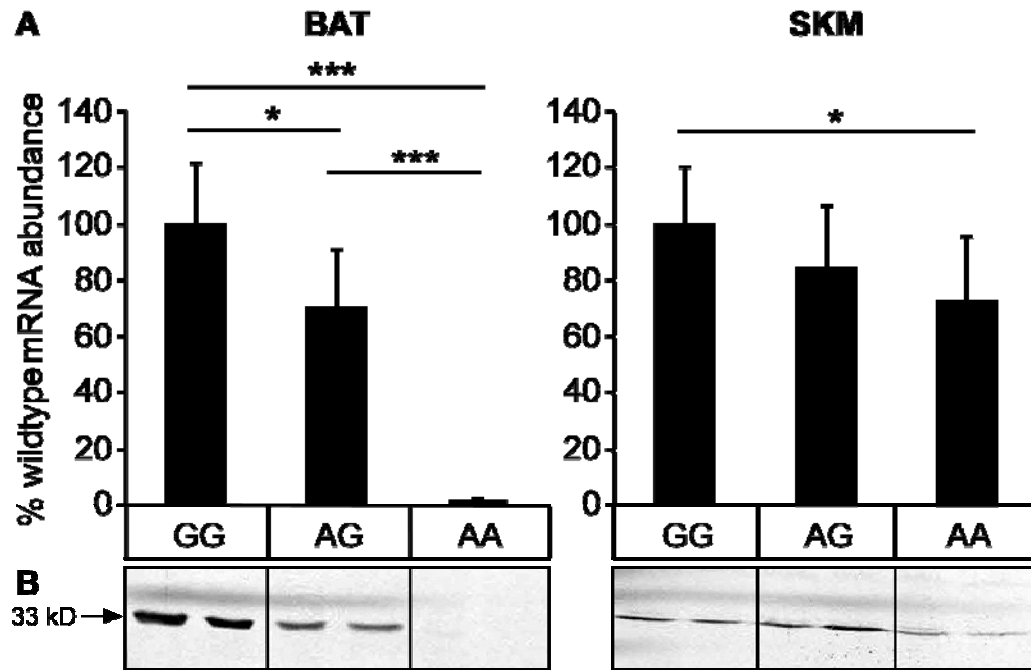


Fig.3

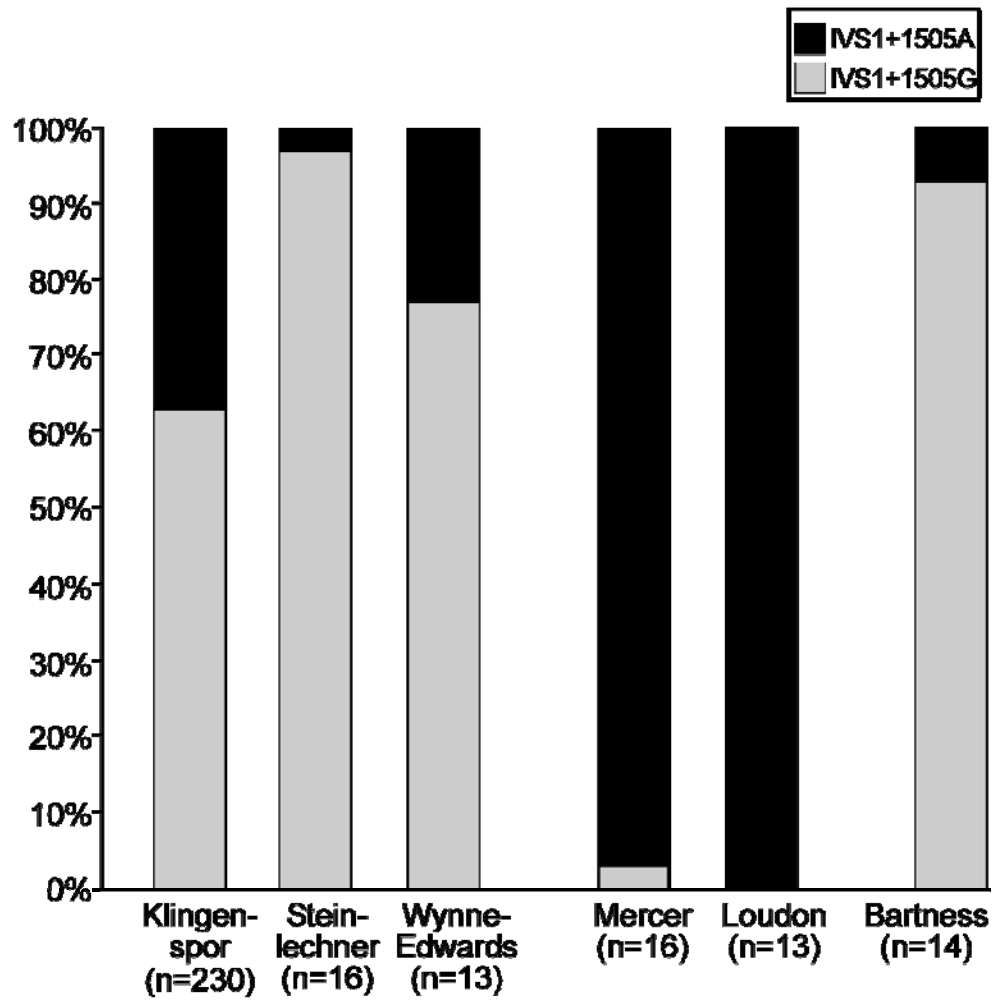


Fig.4

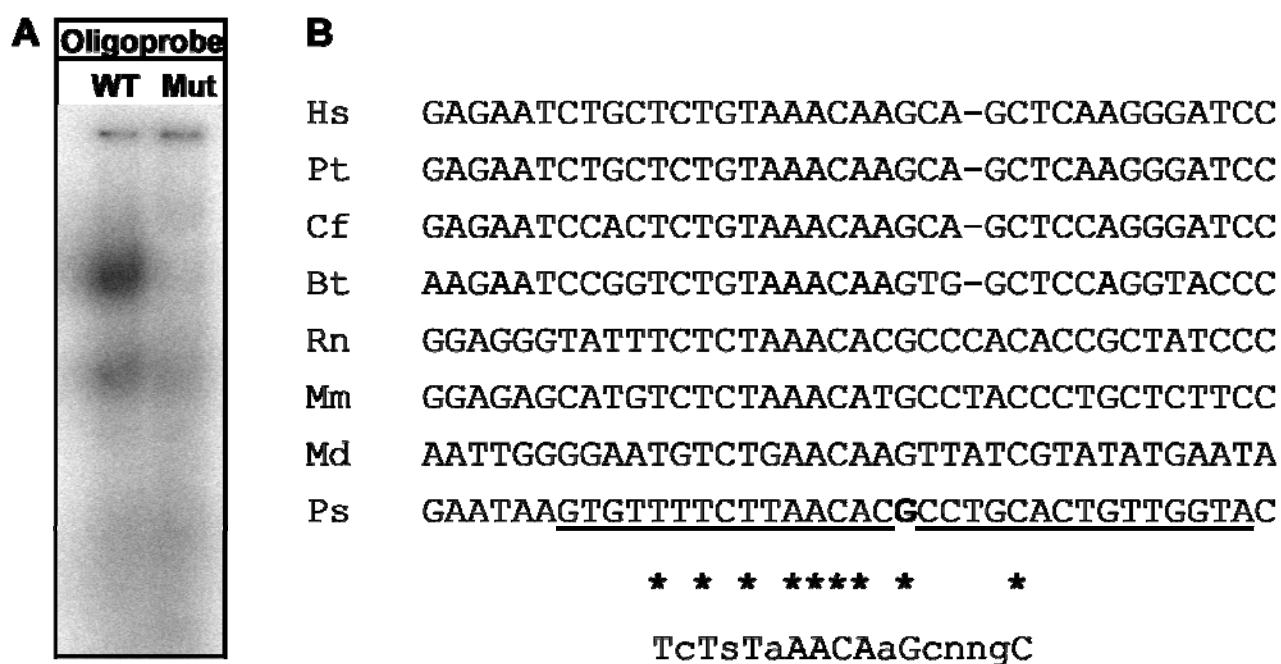


Fig.5



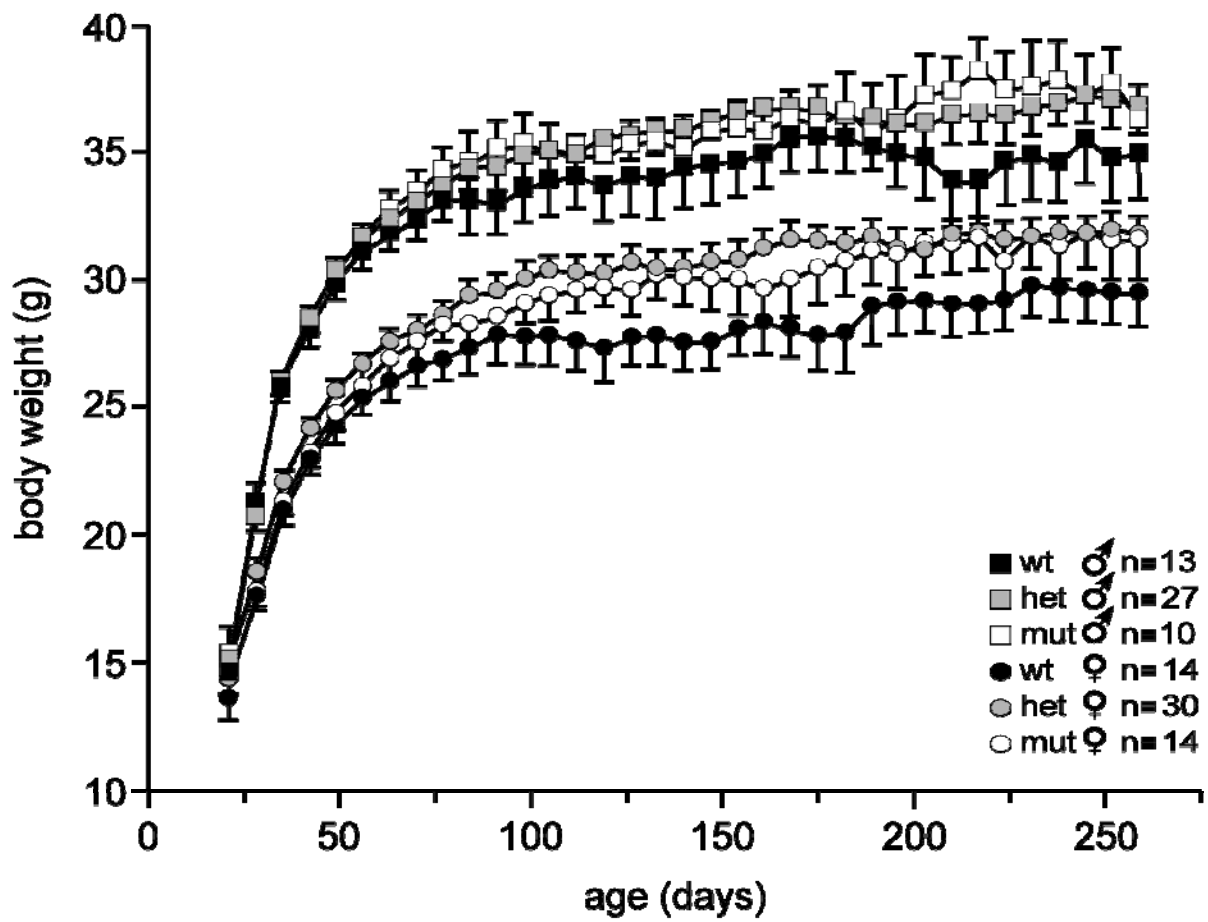


Fig.6



# A single base exchange leads to tissue specific ablation of uncoupling protein 3 (Ucp3) expression

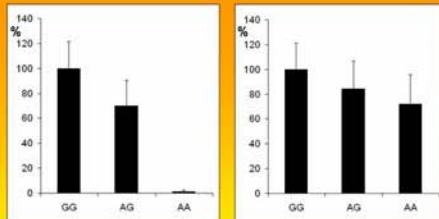
T. Fromme<sup>1#</sup>, K. Weber<sup>1</sup>, C. von Praun<sup>1</sup>, M. Liebig<sup>1</sup>, K. Reichwald<sup>2</sup>, M. Platzer<sup>2</sup>, M. Klingenspor<sup>1</sup>

<sup>1</sup> Philipps-Universität Marburg, Dept. of Animal Physiology, Marburg, Germany

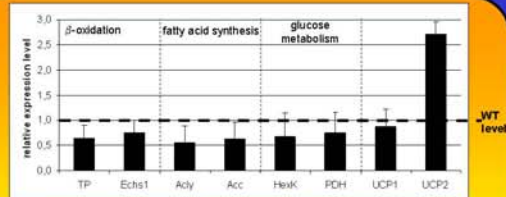
<sup>2</sup> Leibniz Institute for Age Research, Fritz Lipmann Institute (FLI), Jena, Germany

#fromme@staff.uni-marburg.de

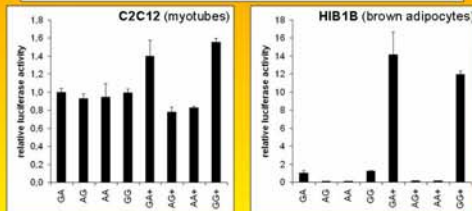
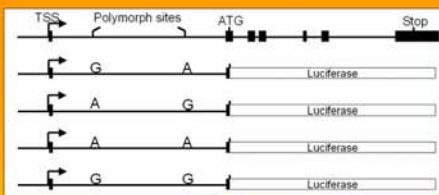
**Introduction** – Uncoupling protein 3 (Ucp3) is an integral protein of the inner mitochondrial membrane with a role in lipid metabolism preventing deleterious effects of fatty acids in states of high lipid oxidation. *Ucp3* is predominantly expressed in brown adipose tissue (BAT) and skeletal muscle. In our breeding colony of the Djungarian dwarf hamster *Phodopus sungorus* we identified animals with a BAT specific lack of Ucp3. We identified two intronic polymorphisms associated with this phenotype, determined the functional base position and analyzed phenotypic consequences.



**Primary phenotype: BAT specific lack of Ucp3 expression**  
We measured Ucp3 expression levels by quantitative PCR in wildtype (GG), heterozygous (AG) and mutant (AA) animals in BAT and skeletal muscle. In BAT expression is semidominantly lost while skeletal muscle is only affected by a slight reduction.

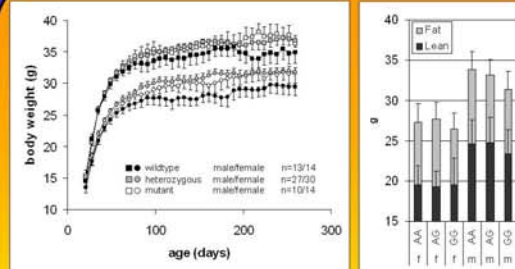


**Mutation leads to global downregulation of metabolic genes**  
Metabolic genes of β-oxidation (TP=trifunctional enzyme, Echs1=enoyl-CoA-hydratase), fatty acid synthesis (Acly=ATP citrate lyase, Acc=Acetyl-CoA-Carboxylase) and glucose metabolism (HexK=hexokinase, PDH=pyruvate dehydrogenase) are downregulated in BAT of Ucp3 deficient hamsters. Ucp2 is compensatory upregulated 2,5-fold, Ucp1 is unchanged.



**A single base position is responsible for loss of expression**  
We constructed reporter gene vectors representing all four possible haplotypes of the polymorphisms observed and measured luciferase activity in HIB1B (brown adipocytes) and C2C12 (myotubes) cell cultures (+ = stimulation with PPAR agonists). The first polymorph site was responsible for loss of expression in a tissue specific manner as observed *in vivo*.

Genotyping of animals caught independently proved natural occurrence of this allele in the wild population.



**BAT specific lack of Ucp3 leads to an increased body weight**  
We genotyped hamsters of our breeding colony and established heterozygous breeding pairs. Body weight development of 108 descendants was monitored over a period of 280 days, afterwards body composition was determined by DXA and animals genotyped by taking ear punches. Wildtype hamsters (GG) displayed a lower body weight as compared to mutant (AA) and heterozygous (AG) hamsters. Body size as measured by femur length does not display a genotype specific difference (not shown), therefore weight changes are caused by body composition. In females it is mainly attributable to lower body fat content, while males show a lower lean mass.

**Oligoprobe**  
WT (G) Mut (A)

**Bandshift assays reveal differential complex formation at polymorph site**  
PPAR-ligand stimulated HIB1B cell nuclear extracts specifically form a protein/DNA-complex with a wildtype 30mer oligonucleotide probe.  
We are currently investigating this complex and analyzing the proteins involved by column chromatography and MALDI-TOF-MS.

## Summary and Conclusion

- We identified an intronic point mutation that leads to
  - brown adipose tissue specific lack of Ucp3 expression
  - a lower body weight
  - a global reduction of expression of metabolic genes

This mutation leads to differential protein complex formation in bandshift assays. Further studies may reveal the unknown mechanism of tissue specific *Ucp3* gene regulation. The Djungarian hamster *Phodopus sungorus* can serve as a model organism to study the physiological function of Ucp3 and to distinguish its specific role in brown adipose tissue from that in skeletal muscle.

## Acknowledgements

This work was supported by the Deutsche Forschungsgemeinschaft (DFG), grant KL973/7-3 and NGFN2 [01GR0504, 01GS0483(TP23)]. T. Fromme was recipient of a fellowship of the Friedrich-Naumann-Foundation. K. Reichwald was supported by DHGP2 grant 01KW0007. We thank J. Kämper for the generous provision of access to an iCycler.

## **Brown adipose tissue specific lack of uncoupling protein 3 is associated with impaired cold tolerance and reduced transcript levels of metabolic genes**

Kerstin Nau<sup>#</sup>, Tobias Fromme<sup>#\*</sup>, Carola W. Meyer, Christa von Praun, Gerhard Heldmaier, Martin Klingenspor

Department of Animal Physiology, Faculty of Biology, Philipps Universität Marburg, Germany

\* Corresponding author: Tel. +49(0)6421-2825372, Fax. +49(0)6421-2828937, E-Mail:

[fromme@staff.uni-marburg.de](mailto:fromme@staff.uni-marburg.de)

# These authors contributed equally to this work.

### Alphabetical list of abbreviations:

Acaca - acetyl-Coenzyme A carboxylase alpha, Acacb - acetyl-Coenzyme A carboxylase beta, Acly - ATP citrate lyase, Atgl - adipose triglyceride lipase, Aktb - beta actin, BAT - brown adipose tissue, BMR - basal metabolic rate, Cs - citrate synthase, Dci - dodecenoyl-coenzyme A delta isomerase, Echs1 - enoyl Coenzyme A hydratase, Err $\alpha$  - estrogen related receptor alpha, Glut1 - glucose transporter 1, Glut4 - glucose transporter 4, Hadh - hydroxyacyl-Coenzyme A dehydrogenase, Hexk2 - hexokinase 2, Hsp90 - heat shock protein 90kDa, Idh3a - isocitrate dehydrogenase 3 (NAD<sup>+</sup>) alpha, NE - norepinephrine, NST - nonshivering thermogenesis, Oxct - 3-oxoacid CoA transferase 1, Pdhb - pyruvate dehydrogenase beta, Ppar $\delta$  - peroxisome proliferator activator receptor delta, Pkm - pyruvate kinase muscle, qPCR - quantitative PCR, RMR - resting metabolic rate, ROS - reactive oxygen species, RQ - respiratory quotient, T<sub>a</sub> - ambient temperature, T<sub>b</sub> - body temperature, Tbp - TATA box binding protein, Tp - trifunctional protein, Ucp - uncoupling protein, VO<sub>2</sub> - oxygen consumption, WT - wildtype

## Abstract

Uncoupling protein 3 is located within the mitochondrial inner membrane of brown adipose tissue and skeletal muscle. It is thought to be implicated in lipid metabolism and defense against reactive oxygen species. We previously reported on a mutation in our breeding colony of Djungarian hamsters (*Phodopus sungorus*), that leads to brown adipose tissue specific lack of uncoupling protein 3 expression. In this study we compared wildtype with mutant hamsters on a broad genetic background. Hamsters lacking uncoupling protein 3 in brown adipose tissue displayed a reduced cold tolerance due to impaired nonshivering thermogenesis. This phenotype is associated with a global decrease in expression of metabolic genes but not of uncoupling protein 1. These data implicate that uncoupling protein 3 is necessary to sustain high metabolic rates in brown adipose tissue.

## Keywords

Uncoupling protein 3, brown adipose tissue, nonshivering thermogenesis, gene expression, cold tolerance

## Introduction

Uncoupling protein 3 (Ucp3) is a transport protein located within the mitochondrial inner membrane. Initially, Ucp3 was discovered and named by its homology (57%) to the well known thermogenic uncoupling protein 1 (Ucp1) (Vidalpuig et al., 1997; Boss et al., 1997). The hypothesis that Ucp3 constituted another thermogenic protein at first seemed plausible (Gong et al., 1997) but it was soon demonstrated that neither Ucp3, nor Ucp2, or any other protein, was able to compensate the loss of thermogenic capacity and cold tolerance caused by disruption of the Ucp1 gene (Enerbäck et al., 1997). Subsequently, increased expression of Ucp3 in response to starvation (Boss et al., 1998) and its transcriptional regulation by circulating fatty acid levels (Weigle et al., 1998) was demonstrated, further denying a role of Ucp3 in thermogenesis. As a consequence, cold endurance or tolerance has not been tested in any of the three lines of Ucp3 knockout mice since they became available (Gong et al., 2000; Vidal-Puig et al., 2000; Brand et al., 2002).

Based upon the regulation of gene expression by serum fatty acid levels and its tissue specificity in skeletal muscle and brown adipose tissue (BAT), a role in lipid metabolism has been proposed, possibly exporting non-esterified fatty acids from the matrix into the cytosol. Proton transport dependent on the presence of Ucp3 may therefore be a secondary effect mediated by passive re-entry of protonated fatty acids into the mitochondrial matrix. This

mechanism has in fact also been proposed to be a molecular basis for Ucp1 function in endothermic vertebrates (Jezek et al., 1998).

An alternative hypothesis assigns Ucp3 a role as functional uncoupling protein acting as an overpressure valve to prevent exceedingly high membrane potentials and thus protecting the cell against reactive oxygen species (ROS) formation. Several studies report enhanced Ucp3 gene expression and activation of Ucp3 function by ROS or downstream metabolites of lipid peroxidation (Echtay et al., 2002; Echtay et al., 2003).

Very recently, it has been shown that Ucp3 and Ucp2 are essential for  $\text{Ca}^{2+}$  uniport into mitochondria (Trenker et al., 2007). Until now, this novel finding has not been widely discussed in the literature and is inadequate to assess whether this provides the fundamental molecular basis for Ucp3 function or represents an accompanying secondary phenomenon.

We previously identified a mutation in the Djungarian hamster, *Phodopus sungorus*, that leads to BAT specific loss of Ucp3 expression (Liebig et al., 2004)(Fromme et al., submitted). Here we demonstrate that lack of Ucp3 expression in BAT of Djungarian hamsters is associated with impaired thermogenic capacity and results in lower cold tolerance in-vivo. The metabolic phenotype of the BAT-Ucp3 deficient hamster is associated with reduced gene expression of key metabolic enzymes in this tissue. These combined results support a role for Ucp3 in sustaining high metabolic flux and, hence, maximal nonshivering thermogenesis in BAT.

## Materials and Methods

### Animals

Mutant Djungarian hamsters (*Phodopus sungorus*) and WT controls were derived from heterozygous breeding pairs in our colony and genotyped by AarI restriction fragment length polymorphism analysis (Fromme et al., submitted). Individuals were housed in single cages at an ambient temperature of 23°C, and a long day photoperiod of 16h light: 8h dark. Hamsters had *ad libitum* access to food and water unless stated otherwise.

### In vivo measurements

In order to monitor core body temperature, hamsters at the age of 12 months were intraperitoneally implanted with minimitters (Mini Mitter Company Inc.). For surgery, hamsters were anesthetized with isoflurane (1-4Vol%) and an intraperitoneal injection of Ketamine (50 mg/kg) and Rompun (2%). Implanted hamsters were allowed to recover for at least two weeks before cold tolerance was measured.

For the metabolic measurements, genotypes of hamsters were blinded to the experimenter. Cold tolerance was determined by combined telemetry and indirect calorimetry. The principal setup of the open respirometric system has been reported previously (Heldmaier and Ruf, 1992). In short, single hamsters were placed in a cuvette (1.8 l) inside a chamber which allowed for control of ambient temperatures ( $T_a$ ) in a range of +30 to -40°C ( $\pm 0.5^\circ\text{C}$ ). A second empty cuvette served as a reference control. Extracted air from the hamster cuvette (flow: 40 l/h) was dried and analyzed every 2 minutes for volumes of  $\text{O}_2$  (S3A, Ametek) and  $\text{CO}_2$  (Unor 6N, Maihak). Oxygen consumption ( $\text{VO}_2$  [ $\text{ml}\cdot\text{h}^{-1}$ ]) was calculated as described (Heldmaier and Ruf, 1992). Respiratory quotient (RQ) was calculated by dividing volumes of  $\text{CO}_2$  produced by volumes of  $\text{O}_2$  consumed.

At 8:00 CET a hamster was placed in the respirometry system at 26°C (thermoneutral, (Heldmaier and Steinlechner, 1981)) for 2 to 3 hours. Ambient temperature was then decreased stepwise (20°C, 10°C, 0°C, -10°C, -20°C, -30°C). Each ambient temperature was sustained for about 45 minutes and corresponding resting metabolic rates (RMRs) were determined by calculating the mean of four consecutive resting  $\text{VO}_2$  readings with the lowest variance (equivalent to 8 min). Measurements took on average 8 hours during which a hamster had no access to food or water. Throughout the entire experiment, body temperature was monitored. For each RMR, conductance could be calculated from heat production ( $\text{HP}=(4.44+1.43\cdot\text{RQ})\cdot\text{VO}_2$ ) (Heldmaier, 1974) divided by heat loss ( $T_b-T_a$ ). A hamster was rescued from the chamber if its body temperature dropped below 34°C despite an increase or plateau in metabolic rate. For calculation of individual cold limit, metabolic rates at each temperature level were plotted against ambient temperature, and the cold limit was determined by calculating the point of intersection of highest  $\text{VO}_2$  measured  $\text{VO}_{2\text{max}}$  and the regression of  $\text{VO}_2$  with ambient temperature (Heldmaier et al., 1982).

In small mammals such as hamsters, injection of norepinephrine (NE, Hoechst) can induce the maximal nonshivering thermogenic response normally induced by cold and can therefore be used to determine NST capacity (Böckler et al., 1982). 1-2 weeks after the cold limit test the individual thermogenic response to a subcutaneous injection of NE (0.7mg/kg) was measured, using the technical setup described above. Measurements were performed at an ambient temperature of 18°C to prevent the hamsters from developing hyperthermia (Böckler et al., 1982). Maximal NE-induced thermogenesis was determined from the highest mean of three consecutive  $\text{VO}_2$  readings following injection. Because body mass of hamsters had not changed between the two sets of metabolic experiments, individual NST capacity could be

calculated from subtracting RMR measured at 26°C (= basal metabolic rate, BMR) in the cold limit test and VO<sub>2</sub>max induced by NE injection.

2-way repeated measurement ANOVA (genotype x ambient temperature) was used to detect differences in VO<sub>2</sub>, RQ, conductance and T<sub>b</sub>.

All experimental procedures were approved by the German Animal Welfare authorities.

## **Gene expression analysis**

In a separate experiment eight wildtype and eight mutant hamsters were exposed to cold (5°C) for two days at the age of 81 days. They were anesthetized and killed with CO<sub>2</sub> and suprasternal brown adipose tissue was dissected and frozen in liquid nitrogen. RNA was isolated with TRIzol (Invitrogen) and quantified photometrically. RNA was reverse transcribed with a poly-dT-primer and the Superscript III First Strand Synthesis Kit (Invitrogen). We used Platinum SYBR Green qPCR SuperMix UDG (Invitrogen) supplemented with 20nM Fluorescein (Biorad) to quantify transcript levels by qPCR on an iCycler (Biorad). The efficiency of amplification was calculated based on dilution series standard curves by the Biorad iCycler IQ3.0 software and used to determine starting quantity levels (PCR base line subtracted). Normalization was performed according to Vandesompele et al. (2002) using β-Actin, TATA-box binding protein (TBP) and heat shock protein 90 (HSP90) as housekeeping genes (Vandesompele et al., 2002). Briefly, the reliability (i.e. stability of expression levels) of these transcripts was verified by variance analyses. The geometric mean of all three housekeeping genes was then used for normalization of starting quantities in each individual sample. All primers are listed in Table 1.

We performed two-sided t-tests to investigate differences statistically.

## ***Immunological detection of Ucp1 and Ucp3***

Crude protein homogenates were prepared from suprasternal BAT of hamsters of both genotypes and protein concentrations were determined using the Bradford method. 15µg of protein were loaded to each lane of an SDS-PAGE and transferred to a nitrocellulose membrane (Hybond-C extra, Amersham Biosciences) by semi-dry electroblotting. Protein transfer was controlled by Ponceau staining of the membrane. Ucp3 was detected using a polyclonal rabbit antibody (1:7,000) raised against a synthetic peptide as described previously (Liebig et al., 2004), whereas a rabbit anti-hamster- Ucp1 serum (1:10,000) served for the detection of Ucp1. Both antibodies were in turn detected by chemoluminescence (Supersignal,

Pierce) using a horseradish peroxidase-conjugated goat-anti rabbit secondary antibody (Dako).

## Results

### ***Mutants exhibit a lower cold tolerance***

Homozygous wildtype and mutant hamsters ( $n = 6$  each) of comparable average body weight (mean WT:  $31.9 \pm 5.3$ g (standard deviation, SD), mean mutant:  $32.9 \pm 2.1$ g) were implanted with temperature sensitive transmitters. Core body temperature was registered for 8 successive days and neither the average body temperature ( $T_b$  WT:  $36.0^\circ\text{C} \pm 0.19$  (SD),  $T_b$  mutant:  $36.1 \pm 0.24$ ) nor the daily body temperature pattern (not shown) were different between genotypes.

We then subjected these hamsters to a defined series of decreasing ambient temperatures ( $T_a$ ) in a climate chamber while simultaneously measuring oxygen consumption ( $\text{VO}_2$ ),  $\text{CO}_2$  production and core body temperature ( $T_b$ ) (Figure 1). With decreasing  $T_a$ ,  $\text{VO}_2$  increased linearly and both groups defended a body temperature in the range of  $35.0^\circ\text{C}$  to  $36.5^\circ\text{C}$ . Numerically, mean RMRs of mutant hamsters were always higher than mean RMRs of WT hamsters but except for  $T_a = -10^\circ\text{C}$  there were no significant differences. The respiratory quotient, and hence substrate usage, was not different between groups at any time point. Conductance displayed a consistent trend towards higher values in mutants, but this difference did not reach significance at any temperature level.

More strikingly, five of the six wildtype animals were able to sustain their body temperature above  $34^\circ\text{C}$  at an ambient temperature of  $-30^\circ\text{C}$  for  $>30$  min, i.e. long enough to measure RMR at this ambient temperature. In contrast, five out of six mutant animals were not able to maintain a stable body temperature at  $-30^\circ\text{C}$  and had to be rescued from the cold. In accordance with this observation we found the calculated cold tolerance limits to be significantly different from each other (Figure 2). Wildtype animals were able to withstand an average temperature of  $-32.8^\circ\text{C}$  while mutants displayed a cold tolerance limit of  $-27.4^\circ\text{C}$  ( $p < 0.05$ ).

### ***Nonshivering thermogenesis is impaired in mutants***

In response to severe cold small mammals employ both shivering and nonshivering thermogenic (NST) mechanisms. To identify whether NST is impaired in mutant hamsters, we injected hamsters with NE and measured the resulting increase in oxygen consumption to calculate NST capacity. When expressed as means, neither  $\text{VO}_2\text{max}$  (data from cold tolerance measurement) nor NST capacity was different between mutant and wildtype hamsters



(VO<sub>2</sub>max WT: 323.4±44.1 ml O<sub>2</sub> h<sup>-1</sup>(SD), mutant: 313.1±10.9 ml O<sub>2</sub> h<sup>-1</sup>; NST capacity WT: 154.5±29.1 ml O<sub>2</sub> h<sup>-1</sup>, mutant: 135.5±12.0 ml O<sub>2</sub> h<sup>-1</sup>). Since metabolic rates are highly dependent on body mass, we also analyzed the regression of metabolic parameters plotted against body mass (Figure 3). Individual datapoints of mutant RMRs at thermoneutrality (BMR) and VO<sub>2</sub>max fell within the wildtype regression. In contrast, NST capacity of mutant hamsters was lower than expected from the wildtype regression, indicative of a brown fat specific thermogenic abnormality.

### ***Overall metabolic gene expression but not Ucp1 expression, is decreased in mutant BAT***

To elucidate the molecular basis of the decreased brown fat thermogenic capacity we analyzed BAT mRNA expression levels of key metabolic genes representing major pathways, including fatty acid oxidation and synthesis, citrate cycle, and glycolysis by qPCR (Figure 5). We exposed the hamsters to cold to compare the *in vivo* cold response to molecular processes during cold adaptation.

Ucp3 served as a control and was absent from BAT as reported previously (Liebig et al., 2004). Notably, Ucp2 displayed a threefold increase in mRNA levels in mutant BAT in a possibly compensatory manner, while mRNA levels of the thermogenic Ucp1 remained unchanged. This observation was confirmed on the protein level by performing western blot experiments (Figure 4).

Five genes involved in lipid mobilization and oxidation were analyzed (Figure 5B). On the mRNA level two of them were significantly downregulated in BAT of mutant animals ( $\beta$ -oxidation enzymes trifunctional protein (Tf) and enoyl-CoA-hydratase (Echs1)) while we observed the same trend for adipose triglyceride lipase (Atgl) and dodecenoyl-CoA-delta-isomerase (Dci). The hydroxyacyl-CoA-dehydrogenase mRNA (Hadh) level was not different between mutant and wildtype BAT.

Analyzing the converse process of fatty acid synthesis, we again found the mRNA levels of two genes to be down regulated in mutants, namely ATP citrate lyase (Acl) and Acetyl-CoA-carboxylase  $\alpha$  (Acaca), with a similar trend for Acetyl-CoA-carboxylase  $\beta$  (Acacb) (Figure 5C).

Apart from lipid metabolism, we found a differential expression pattern of genes involved in glucose metabolism, citrate cycle, and ketone body utilization. All eight genes analyzed displayed the same trend towards reduced mRNA levels in BAT of mutant hamsters with a significant difference in 3-oxoacid-CoA-transferase (Oxct) and glucose transporter 4 (Glut4) mRNA expression (Figure 5D-F).

Taken together, we quantified mRNA levels of 16 genes involved in energy metabolism and found 15 genes to be down regulated significantly or in trend in BAT of hamsters lacking Ucp3 in this tissue. These genes include the central steps of key cellular metabolic pathways. When all wildtype and mutant data sets of these 16 metabolic genes are pooled, there is a highly significant difference in overall BAT expression of metabolic genes ( $p < 0,00001$ ).

To investigate whether the expression of transcription factors known to globally regulate energy metabolism genes may account for the observed expression pattern, we determined mRNA levels of *Errα* and *Pparδ* (data not shown). The mRNA levels of both transcription factors were not differentially expressed in wildtype and mutant BAT.

## Discussion

The exceptional thermogenic capacity of the Djungarian hamster is well characterized. Winter-acclimated Djungarian hamsters can defend normothermia at ambient temperature as low as  $-68^{\circ}\text{C}$ , predominantly by employing nonshivering thermogenesis (NST) in brown adipose tissue (BAT) (Heldmaier et al., 1982; Heldmaier et al., 1983). In order to unravel the full thermogenic *in vivo* capacity of hamsters specifically lacking Ucp3 in BAT, we subjected them to stepwise decreasing ambient temperatures to as low as  $-30^{\circ}\text{C}$ . In both mutants and wildtypes,  $\text{VO}_2$  increased linearly during this process, in line with the Scholander model of thermoregulation (Scholander et al., 1950). However, mean  $\text{VO}_2$  values of mutant hamsters tended to be higher at all temperature steps (with a striking difference at  $-10^{\circ}\text{C}$  that we are unable to fully explain) and we observed the same trend for conductance. This suggests that mutant hamsters have an increased heat loss. In order to maintain a stable body temperature they have to display a higher metabolic rate. On the other hand, cold tolerance was significantly lower in mutants compared to wildtype hamsters. The combined results allow the conclusion that lack of Ucp3 leads to lowered or more inefficient thermogenic capacity. In line with a model of impaired BAT function NST capacity was lower in mutant animals. In an earlier study we did not observe a similar trend, but at that timepoint the point mutation causing the mutant phenotype had not yet been identified (Liebig et al., 2004). Therefore, we were not able to distinguish between wildtype and heterozygous animals as both express Ucp3 protein. Furthermore, the previous study was conducted in an inbred mutant line prone to founder effects and not based on a broad genetic background.

If lack of Ucp3 causes an impaired BAT function there are three different principal explanations possible. Firstly, Ucp3 itself may be a thermogenic protein comparable to its relative Ucp1. Secondly, it could be a necessary constituent of the machinery delivering

energy to primary thermogenic mechanisms or, thirdly, lack of Ucp3 may lead to downregulation of Ucp1 expression by unknown mechanisms. To discriminate between these possibilities we analyzed BAT mRNA expression of uncoupling proteins and a set of energy metabolism genes.

Ucp1 expression was not affected in mutant hamsters neither on mRNA nor on protein level. Ucp2 displayed a threefold increase in mRNA abundance in the absence of Ucp3. Owing to the lack of an antibody against Ucp2 that reliably works in our hands, we were not able to verify increased Ucp2 protein levels. An increased mRNA abundance does not necessarily reflect changes in protein levels since Ucp2 is decisively regulated on the level of translation (Hurtaud et al., 2006). Nevertheless, the apparent compensatory response implicates a common function of Ucp2 und Ucp3, e.g. in mitochondrial calcium uniport as recently suggested (Trenker et al., 2007). An increased compensatory Ucp2 expression might contribute to the rather small effect size we observe both in *in vivo* measurements and in gene expression studies.

Strikingly, 15 out of 16 genes involved in energy metabolism displayed at least a trend towards lower mRNA levels in BAT of mutant hamsters. Among the genes most strongly regulated differentially were the central components of fatty acid synthesis (*Acaca*) and  $\beta$ -oxidation (*Tp*) but also pathways of alternative energy sources like ketone bodies (*Oxct*) or glucose (*Glut4*) were affected. These effects in response to lack of Ucp3 can only be accounted for by a remarkable global decrease in BAT energetic capacity.

We also measured mRNA levels of the two transcription factors *Erra* and *Ppar $\delta$* . Both have been described as master regulators of energy metabolism pathways (Mootha et al., 2004; Luquet et al., 2004) and were therefore candidates to play a role in the observed differential gene expression pattern. However, there was no difference in expression, at least on the mRNA level.

Summarizing our gene expression studies, we observed an overall decrease in mRNA expression of energy metabolism genes as a consequence of Ucp3 absence while Ucp1 expression remained unchanged. These data strongly suggest Ucp3 not being itself *a priori* thermogenic but being a constituent of energy metabolism pathways necessary to tolerate situations of high energy flux. Molecular data on gene expression in response to cold and *in vivo* cold tolerance limits and NST capacity both agree with this model. In view of this conclusion, it seems worthwhile to re-evaluate the existing *Ucp3(-/-)* mouse lines in this respect.

Taken together, we compared wildtype hamsters with mutants lacking Ucp3 in BAT. Mutants displayed a reduced cold tolerance limit and a lower NST capacity, indicating defective BAT thermogenesis. This defect could not be attributed to Ucp1 protein levels, but to an overall decrease in expression of genes related to energy metabolism. These data implicate that Ucp3 is necessary to sustain high metabolic rates in BAT.

## **Acknowledgements**

This work was supported by the Deutsche Forschungsgemeinschaft (DFG), grant KL973/7-3. T. Fromme was recipient of a fellowship of the Friedrich-Naumann-Foundation. We thank J. Kämper for the generous provision of access to an iCycler. All experiments comply with current German laws.

**Figure 1** – Djungarian hamsters were subjected to stepwise decreasing ambient temperatures and oxygen consumption ( $VO_2$ ),  $CO_2$  production and body temperature were measured. We calculated the respiratory quotient and conductance for each temperature step. Animals with a lack of Ucp3 in BAT displayed a significantly different  $VO_2$  and  $T_b$  at  $-10^\circ C$  only. We were unable to determine resting metabolic rates at  $-30^\circ$  for 5 out of 6 mutant animals owing to incipient hypothermia, while 5 out of 6 wildtype hamsters were able to sustain at  $-30^\circ$ . Shown are mean values with standard deviations (WT = ■, mutant = □;  $n = 6$  per genotype). \* =  $p < 0.05$ .

**Figure 2** – Djungarian hamsters with a lack of Ucp3 in BAT are less cold tolerant than wildtypes ( $-32.8$  versus  $-27.4^\circ C$ ). Shown are individual cold tolerance limits and mean values with standard deviations ( $n = 6$  per genotype, 3 males (■/□) and 3 females (▲/△) each). \* =  $p < 0.05$ .

**Figure 3** – NST capacity, but not  $VO_{2max}$  or BMR is lower than expected from body mass in Djungarian hamsters lacking Ucp3 in BAT. Shown are individual values for each parameter plotted against body mass. In each plot, the dotted line indicates the WT regression (WT = black symbols, mutant = open symbols,  $n = 6$  per genotype, 3 males (■/□) and 3 females (▲/△) each).

**Figure 4** – Immunological detection of Ucp1 and Ucp3 in BAT of WT and mutant Djungarian hamsters. While Ucp3 is clearly absent in BAT of mutants, UCP1 expression is comparable between genotypes.

**Figure 5** – The mRNA abundance of uncoupling proteins and genes implicated in energy metabolism was determined in brown adipose tissue by qPCR. Shown is mRNA abundance relative to the mean of wildtypes, dots are individual and bars mean values. A – Uncoupling proteins. B – Fatty acid oxidation and mobilization. C – Fatty acid synthesis. D – Glucose utilization. E – Citric acid cycle. F – Ketone body utilization. WT = ■, mutant = □;  $n = 8$  per genotype. Significance levels of two-sided t-tests: \* =  $p < 0.05$ , \*\* =  $p < 0.001$ . A list of p-values is provided in Table 1.

**Table 1** – All primers used for qPCR analyses and reference sequence of the respective product. The given p-value is result of two-sided t-tests comparing expression levels of mutant versus WT hamsters as shown in Figure 5 (**bold** =  $p < 0,05$ ).

Gene	Primer 1	Primer 2	p-value	Genbank
Acac	TTTTCGATGTCCTCCCAAAC	ACATTCTGTTTAGCGTGGGG	<b>0,007</b>	EU107793
Acac	GATGCGCAACTTTGACTTGA	CTGCAGGTAAGGAGG	0,174	EU107794
Acly	GAAGCTGACCTTGCTGAACC	AGGTCTGTTGTTCACTGGGG	<b>0,023</b>	EU107795
Atgl	ACAGTGTCCCATTCTCAGG	CTGTTTGCACATCTCTCGGA	0,157	EU118752
Aktb	AGAGGGAAATCGTGCGTGAC	CAATAGTGATGACCTGGCCG	-	EU107796
Cs	CTGAGGAAGACTGACCCTCG	TTCATCTCCGTCATGCCATA	0,715	EU107797
Dci	GGAGATGTATGGCCGGAAC	AGCAGGCTCTCATTCAATCC	0,222	EU107798
Echs1	GAGAAAGCCCAGTTTGGACA	TTCAAAGGCTGCATTACAG	<b>0,028</b>	EU107799
Erra	GTCCTAGATGAAGAGGGGGC	GCACAGAGTCAGAATTGGCA	0,614	EU107800
Glut1	GACGACACTGAGCAGCAGAG	GCTGTGCTTATGGGCTTCTC	0,076	EU107802
Glut4	TCATTCTTGACGGTTCCTC	GACAGAAGGGCAGCAGAATC	<b>0,040</b>	EU107803
Hadh	CCACCAGACAAGACCGATTT	CGGTTACGATAAATCCAGG	0,661	EU107804
Hexk	GTGGCTGTGGTGAATGACAC	ACATCCCGCTGATCATCTTC	0,054	EU107805
Hsp9	AGGAGGGTCAAGGAAGTGGT	TTTTTCTTGCTTTTGCCGCT	-	EU107806
Idh3a	AGTGCTGTGATGATGCTTCG	GACTGACTGCAGCAAATCCA	0,096	EU107807
Oxct	AAGATTTATGTGCACCGCCT	GTTAGCGTACATGCCGTCCT	<b>0,004</b>	EU107808
Pdhh	GTGTAGCTGCTCAGCACTCG	ACTGGTCTTGAATGGGCAAC	0,054	EU107810
Ppard	TGGAGCTCGATGACAGTGAC	GTAAGGCTGTCAGGGTGGT	0,761	EU107812
Pkm	AGATGCAAACACCATGTCCA	CTGCAGGTGAAGGAGAAAGG	0,253	EU107811
Tbp	ACTTCACATCACAGCTCCCC	CTTCGTGCAAGAAATGCTGA	-	EU107792
Tp	ATGGTCTCCAAGGGCTTCTT	GATCCCTTCTGTAGGCACA	<b>0,003</b>	EU118753
Ucp1	GAAGGGTTGCCGAAACTGTA	TGTAGGTGGCTCTGTGCTTG	0,400	AF271263
Ucp2	TGCAGGTCCAAGGAGAGAGT	GCTCTGAGCCCTTGGTGTAG	<b>&lt;0,001</b>	AF271264
Ucp3	AGGAAGGAATCAGGGGCTTA	TCCAGCAGCTTCTCCTTGAT	<b>&lt;0,001</b>	AF271265

## Reference List

- Böckler,H., Steinlechner,S., and Heldmaier,G. (1982). Complete cold substitution of noradrenaline-induced thermogenesis in the Djungarian hamster, *Phodopus sungorus*. *Experientia* 38, 261-262.
- Boss,O., Samec,S., Kuhne,F., Bijlenga,P., Assimacopoulosjeannet,F., Seydoux,J., Giacobino,J.P., and Muzzin,P. (1998). Uncoupling protein-3 expression in rodent skeletal muscle is modulated by food intake but not by changes in environmental temperature. *J Biol Chem* 273, 5-8.
- Boss,O., Samec,S., Paolonigiacobino,A., Rossier,C., Dulloo,A.G., Seydoux,J., Muzzin,P., and Giacobino,J.P. (1997). Uncoupling protein-3: A new member of the mitochondrial carrier family with tissue-specific expression. *FEBS Lett* 408, 39-42.
- Brand,M.D., Pamplona,R., Portero-Otin,M., Requena,J.R., Roebuck,S.J., Buckingham,J.A., Clapham,J.C., and Cadenas,S. (2002). Oxidative damage and phospholipid fatty acyl composition in skeletal muscle mitochondria from mice underexpressing or overexpressing uncoupling protein 3. *Biochem J* 368, 597-603.
- Echtay,K.S., Esteves,T.C., Pakay,J.L., Jekabsons,M.B., Lambert,A.J., Portero-Otin,M., Pamplona,R., Vidal-Puig,A.J., Wang,S., Roebuck,S.J., and Brand,M.D. (2003). A signalling role for 4-hydroxy-2-nonenal in regulation of mitochondrial uncoupling. *EMBO J* 22, 4103-4110.
- Echtay,K.S., Roussel,D., St Pierre,J., Jekabsons,M.B., Cadenas,S., Stuart,J.A., Harper,J.A., Roebuck,S.J., Morrison,A., Pickering,S., Clapham,J.C., and Brand,M.D. (2002). Superoxide activates mitochondrial uncoupling proteins. *Nature* 415, 96-99.
- Enerbäck,S., Jacobsson,A., Simpson,E.M., Guerra,C., Yamashita,H., Harper,M.E., and Kozak,L.P. (1997). Mice lacking mitochondrial uncoupling protein are cold-sensitive but not obese. *Nature* 387, 90-94.
- Gong,D.W., He,Y.F., Karas,M., and Reitman,M. (1997). Uncoupling protein-3 is a mediator of thermogenesis regulated by thyroid hormone, beta 3-adrenergic agonists, and leptin. *J Biol Chem* 272, 24129-24132.
- Gong,D.W., Monemdjou,S., Gavrilova,O., Leon,L.R., Marcus-Samuels,B., Chou,C.J., Everett,C., Kozak,L.P., Li,C., Deng,C., Harper,M.E., and Reitman,M.L. (2000). Lack of obesity and normal response to fasting and thyroid hormone in mice lacking uncoupling protein-3. *J. Biol. Chem.* 2000. May. 26;275(21):16251-7. 275, 16251-16257.
- Heldmaier,G. (1974). Temperature adaptation and brown adipose tissue in hairless and albino mice. *J Comp Physiol* 98, 161-168.
- Heldmaier,G., Buchberger,A., and Seidl,K. (1983). Contribution of brown adipose tissue to thermoregulatory heat production in the Djungarian hamster. *J therm Biol* 8, 413-415.
- Heldmaier,G. and Ruf,T.P. (1992). Body temperature and metabolic rate during natural hypothermia in endotherms. *J Comp Physiol [B]* 162, 696-706.

- Heldmaier,G. and Steinlechner,S. (1981). Seasonal control of energy requirements for thermoregulation in the Djungarian hamster (*Phodopus sungorus*), living in natural photoperiod. *J Comp Physiol* 142, 429-437.
- Heldmaier,G., Steinlechner,S., and Rafael,J. (1982). Nonshivering thermogenesis and cold resistance during seasonal acclimatization in the Djungarian hamster. *J Comp Physiol* 149, 1-9.
- Hurtaud,C., Gelly,C., Bouillaud,F., and Levi-Meyrueis,C. (2006). Translation control of UCP2 synthesis by the upstream open reading frame. *Cellular and Molecular Life Sciences* 63, 1780-1789.
- Jezek,P., Engstova,H., Zackova,M., Vercesi,A.E., Costa,A.D.T., Arruda,P., and Garlid,K.D. (1998). Fatty acid cycling mechanism and mitochondrial uncoupling proteins. *Biochim Biophys Acta* 1365, 319-327.
- Liebig,M., von Praun,C., Heldmaier,G., and Klingenspor,M. (2004). Absence of UCP3 in brown adipose tissue does not impair nonshivering thermogenesis. *Physiol Biochem Zool* 77, 116-126.
- Luquet,S., Lopez-Soriano,J., Holst,D., Gaudel,C., Jehl-Pietri,C., Fredenrich,A., and Grimaldi,P.A. (2004). Roles of peroxisome proliferator-activated receptor delta (PPARdelta) in the control of fatty acid catabolism. A new target for the treatment of metabolic syndrome. *Biochimie*. 86, 833-837.
- Mootha,V.K., Handschin,C., Arlow,D., Xie,X.H., St Pierre,J., Sihag,S., Yang,W.L., Altshuler,D., Puigserver,P., Patterson,N., Willy,P.J., Schulman,I.G., Heyman,R.A., Lander,E.S., and Spiegelman,B.M. (2004). *Err alpha* and *Gabpa/b* specify PGC-1 alpha-dependent oxidative phosphorylation gene expression that is altered in diabetic muscle. *Proceedings of the National Academy of Sciences of the United States of America* 101, 6570-6575.
- Scholander,P.F., Walters,V., Hock,R., and Irving,L. (1950). Body insulation of some arctic and tropical mammals and birds. *Biol Bull* 99, 225-236.
- Trenker,M., Malli,R., Fertschai,I., Levak-Frank,S., and Graier,W.F. (2007). Uncoupling proteins 2 and 3 are fundamental for mitochondrial Ca<sup>2+</sup> uniport. *Nature Cell Biology* 9, 445-U156.
- Vandesompele,J., De Preter,K., Pattyn,F., Poppe,B., Van Roy,N., De Paepe,A., and Speleman,F. (2002). Accurate normalization of real-time quantitative RT-PCR data by geometric averaging of multiple internal control genes. *Genome Biol* 3, RESEARCH0034.
- Vidal-Puig,A.J., Grujic,D., Zhang,C.Y., Hagen,T., Boss,O., Ido,Y., Szczepanik,A., Wade,J., Mootha,V., Cortright,R., Muoio,D.M., and Lowell,B.B. (2000). Energy metabolism in uncoupling protein 3 gene knockout mice. *J. Biol. Chem.* 275, 16258-16266.
- Vidalpuig,A., Solanes,G., Grujic,D., Flier,J.S., and Lowell,B.B. (1997). UCP3: An uncoupling protein homologue expressed preferentially and abundantly in skeletal muscle and brown adipose tissue. *Biochem Biophys Res Commun* 235, 79-82.
- Weigle,D.S., Selfridge,L.E., Schwartz,M.W., Seeley,R.J., Cummings,D.E., Havel,P.J., Kuijper,J.L., and Beltrandelrio,H. (1998). Elevated free fatty acids induce uncoupling protein



3 expression in muscle: A potential explanation for the effect of fasting. *Diabetes* 47, 298-302.

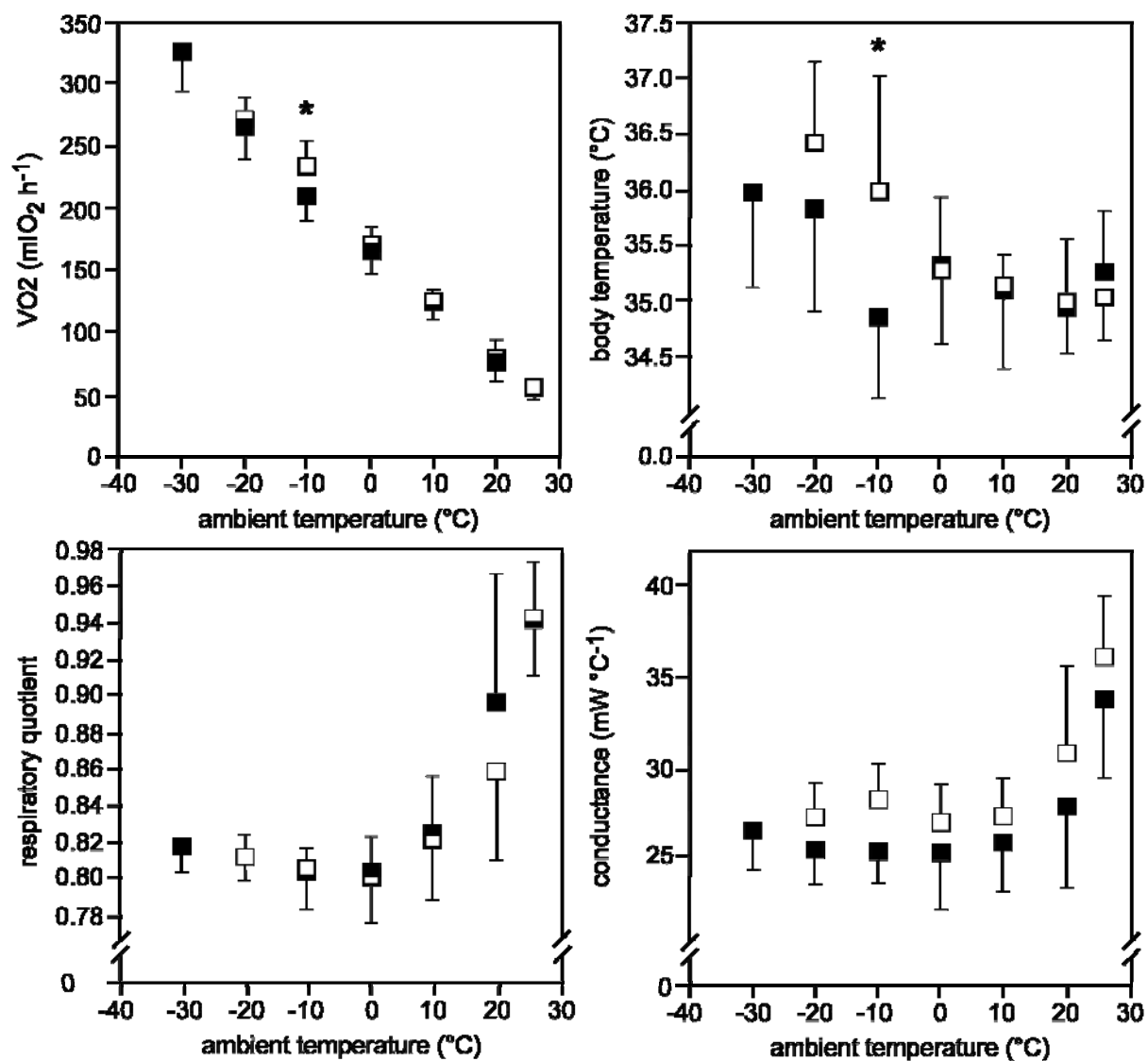


Figure 1

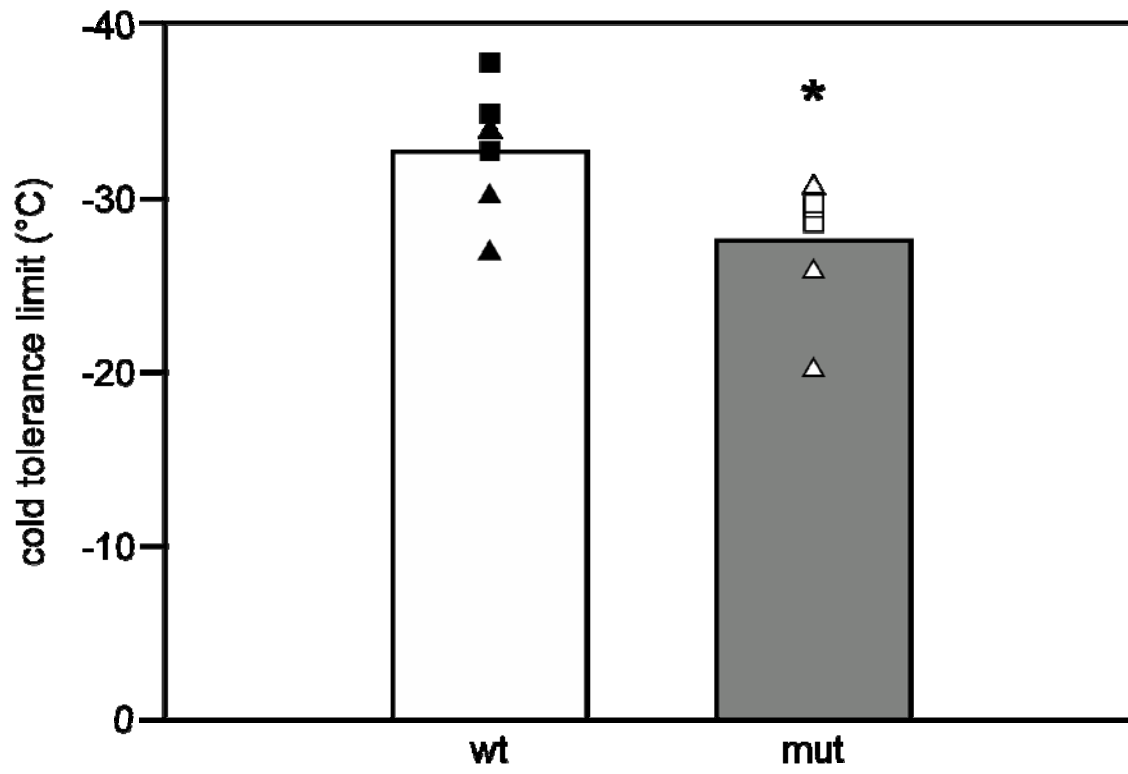


Figure 2

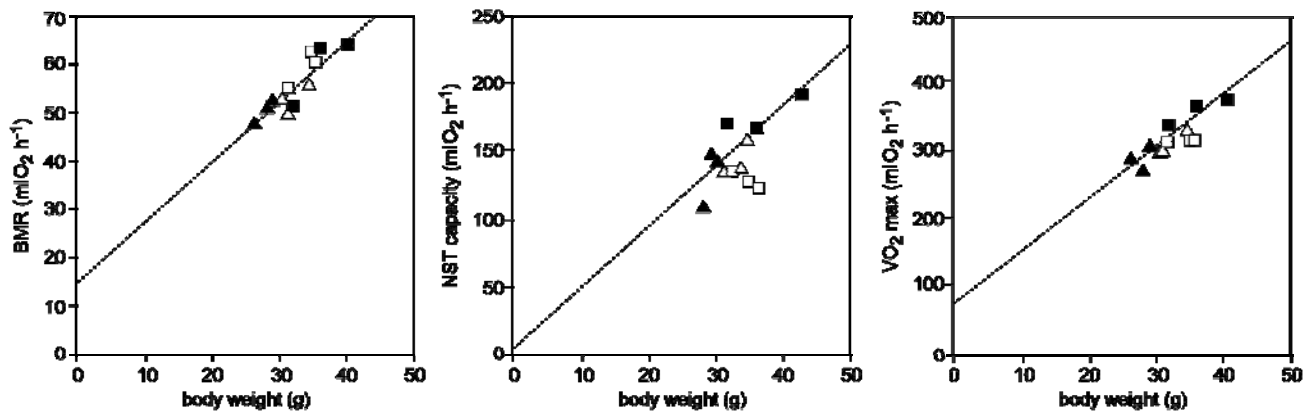


Figure 3

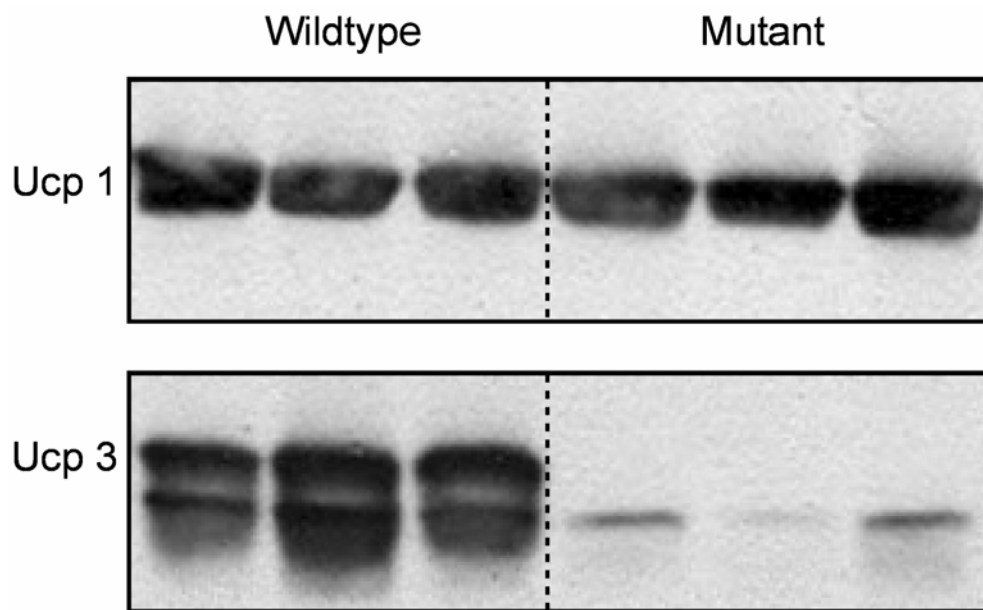


Figure 4

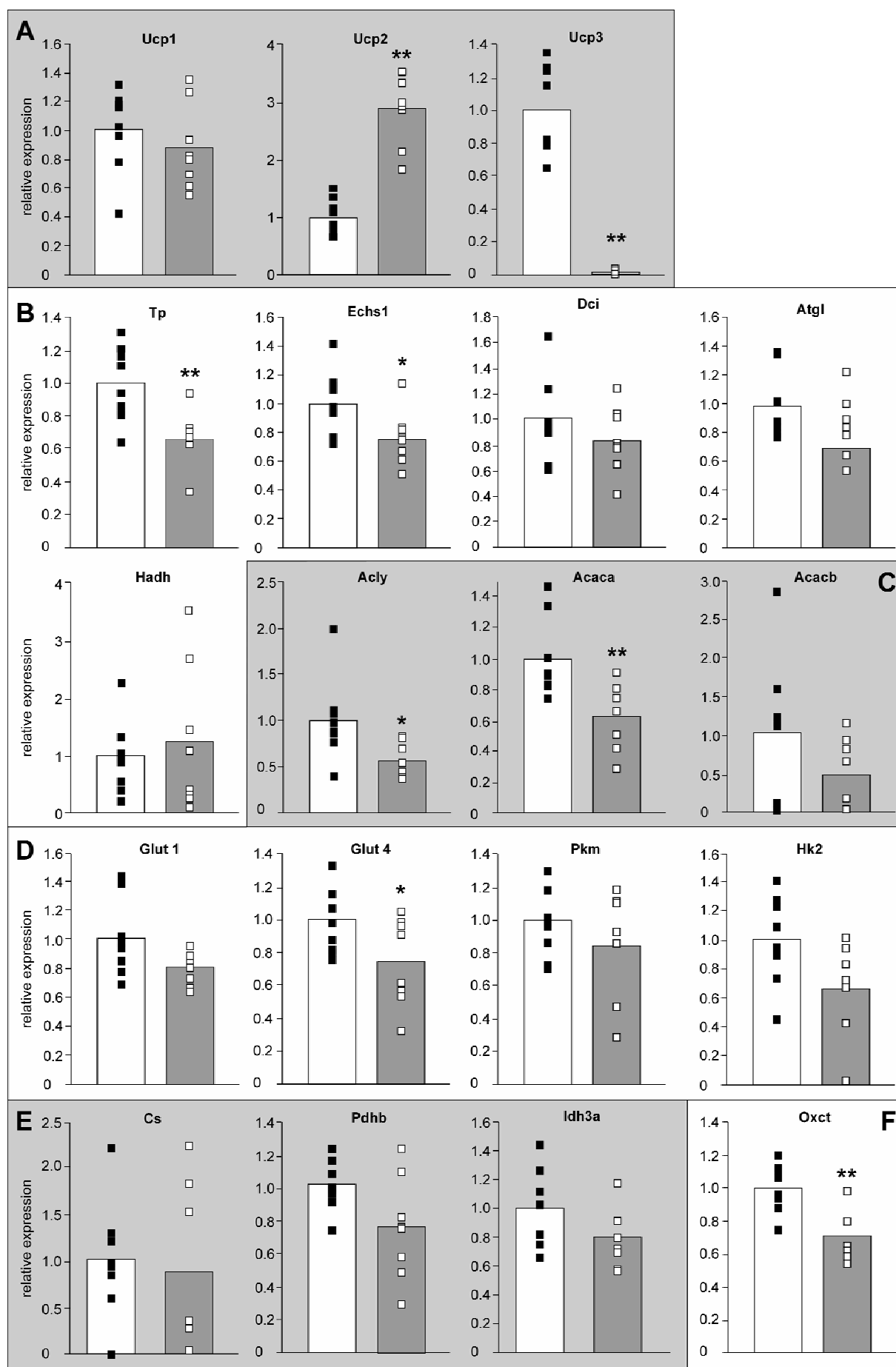


Figure 5



# Tissue-specific lack of UCP3 leads to transcriptional down-regulation of glycolytic, lipogenic and lipolytic pathways in *Phodopus sungorus*

Kerstin Weber<sup>1</sup>, Tobias Fromme<sup>1</sup>, Christa von Praun<sup>1</sup>, Yang Lian-Xing<sup>2</sup>, Martin Klingenspor<sup>1</sup>

<sup>1</sup>Faculty of Biology, Department of Animal Physiology, Philipps-Universität Marburg

<sup>2</sup>The Victor Chang Cardiac Research Institute, Darlinghurst, Australia

## Introduction

Uncoupling protein 3 (UCP3) is a nuclear encoded protein located in the inner mitochondrial membrane and is expressed predominantly in brown adipose tissue (BAT) and skeletal muscle.

In small mammals, BAT is responsible for nonshivering thermogenesis (NST) mediated by UCP1, a paralog of UCP3. In contrast to UCP1, the physiological function of UCP3 is not known to date.

One hypothesis states that UCP3 protects mitochondria from deleterious effects of fatty acids during states of high lipid oxidation (1), whereas an alternative hypothesis suggests a role in the defense against reactive oxygen species(2).

In our colony of Djungarian Hamsters (*Phodopus sungorus*) we identified animals with a BAT-specific lack of UCP3-mRNA and protein, which is caused by a single point mutation in the UCP3 gene. Until now, no phenotypic consequences could be

identified(3).



In gene expression profiling experiments with mouse cDNA macroarrays comparing mRNA from BAT of wildtype and mutant hamsters we found transcripts of several fatty-acid handling enzymes of both lipogenic and lipolytic pathways to be down regulated. The aim of this study was to validate these candidate genes and expand the analysis of gene expression to other metabolic pathways.

## Experimental Design:

cDNA was synthesized from RNA isolated from BAT of wildtype and mutant hamsters (n=8) that had been exposed to cold (5°C) for two days. qRT-PCR was carried out with heterologous primers derived from mouse sequences. For normalization of expression values, the geometric mean of three independent house keeping genes ( $\beta$ -Actin, TBP, HSP90) was calculated according to Vandansompele et al(4). Statistical significance was tested by using two-tailed Student's T-Tests and the level of significance was set at  $p < 0.05$ .

## Results

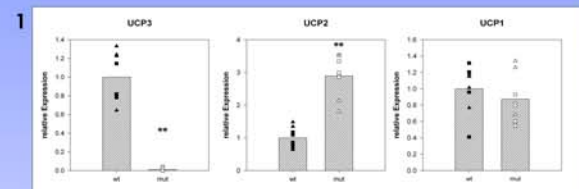


**Figure 1:** Expression of uncoupling proteins as determined by qRT-PCR. As expected, UCP3-mRNA is absent in BAT of mutants. Abundance of UCP2-mRNA is significantly elevated in BAT of mutants, while UCP1-mRNA expression is similar in both genotypes (values are shown relative to wildtype means; n=8; \*\* $p < 0.005$ ;  $\square$  males,  $\Delta$  females).

2	Functional Group	Abbreviation	Name	Regulation	Significance	p-Value
Uncoupling Proteins	UCP3	Uncoupling Protein 3		↓	*	0.000
	UCP2	Uncoupling Protein 2		↑	*	0.000
	UCP1	Uncoupling Protein 1		—	—	0.115
$\beta$ -Oxidation	TF	Tritrionol Protein		↓	*	0.003
	Ech1	Ethyl-CoA Hydratase		↓	*	0.028
	ATGL	Adipose Triglyceride Lipase		↓	—	0.137
	Dci	Dodecanoyl-CoA delta Isomerase		↓	—	0.222
	Hcdh	Hydroxyacyl-CoA Dehydrogenase		—	—	0.661
Fatty Acid Synthesis	Acly	ATP-Citrate Lyase		↓	*	0.023
	Acc	Acetyl-CoA Carboxylase		↓	*	0.007
	Acacab	Acetyl-CoA Carboxylase beta		↓	—	0.174
Glucose Metabolism	GLT 1	Glucose Transporter 1		↓	—	0.076
	GLT 4	Glucose Transporter 4		↓	*	0.040
	Hxk1	Hexokinase		↓	—	0.054
	PK	Pyruvate Kinase		↓	—	0.253
	Pdh	Pyruvate Dehydrogenase		↓	—	0.054
Citric Acid Cycle	PDK 4	PDK-Kinase 4		—	—	0.597
	CS	Citrate Synthase		↓	—	0.715
	IDH	Isocitrate Dehydrogenase		↓	—	0.076
	Oxct	Ketoacyl-CoA Translerase		↓	*	0.004

**Table 1:** Results of gene expression analysis. Tested genes are listed by functional groups, abbreviations and protein names are given. Regulation refers to mutant mean values relative to wildtype mean values. Statistical significance was determined by Student's T-Tests (\*  $p < 0.05$ , —  $p > 0.05$ ).

## Acknowledgements

This work was supported by the Deutsche Forschungsgemeinschaft (DFG) grant KL973/7-3

## References:

- Jezek et al., Fatty acid cycling mechanism and uncoupling proteins. *Biochim Biophys Acta*. 1998; Jun 10;1365(1-2):319-27
- Echtay et al., Superoxide activates mitochondrial uncoupling proteins. *Nature* 2002; Jan;341(5):687-9
- Liebig et al., Absence of UCP3 in brown adipose tissue does not impair nonshivering thermogenesis. *Physiol Biochem Zool* 2004; Jan-Feb;77(1):116-26
- Vandansompele et al., Accurate normalization of real-time quantitative RT-PCR data by geometric averaging of multiple internal control genes. *Genome Biology* 2002;3(7)
- Yu et al., Cold elicits the simultaneous induction of fatty acid synthesis and  $\beta$ -oxidation in murine brown adipose tissue: a prediction from differential gene expression and confirmation in vivo. *FASEB* 2002; Feb;16(2):155-68

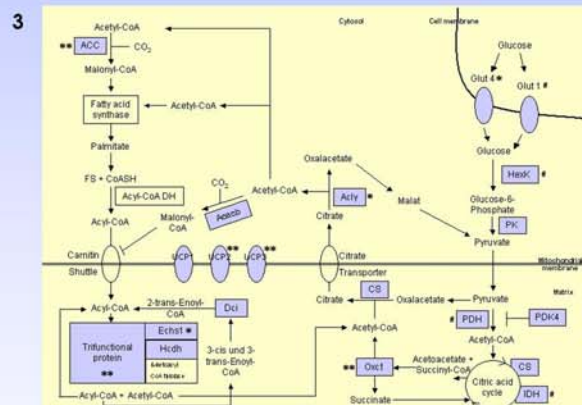


**Figure 2:** Overview gene expression analysis. Schematic representation of metabolic pathways (glycolysis, citric acid cycle, fatty acid synthesis and -oxidation, ketone body utilization) and some of the participating enzymes. Highlighted in blue are those genes selected for expression analysis. Key components of all pathways displayed are negatively regulated in BAT of mutant hamsters (\* $p < 0.05$ , \*\* $p < 0.005$ , #  $p < 0.1$ )

## Conclusions

- as expected, UCP3-mRNA was not detectable in BAT of mutant hamsters
- up-regulation of UCP2-mRNA expression could be part of a compensatory mechanism
- in BAT, glucose is first converted to fatty acids which are then oxidized to provide energy for thermogenesis(5); lack of UCP3 in BAT of hamsters causes down-regulation of key components of these metabolic pathways indicating a global impairment of energy metabolism and therefore possibly NST capacity of mutant hamsters
- these results support the hypothesis that UCP3 is required to maintain high rates of lipid metabolism

## **Marsupial uncoupling protein 1 sheds light on the evolution of mammalian nonshivering thermogenesis**

**Jastroch M. <sup>1#</sup>, Withers K. W. <sup>2</sup>, Taudien S. <sup>3</sup>, Frappell P. B. <sup>4</sup>, Helwig M. <sup>1</sup>, Fromme T. <sup>1</sup>, Hirschberg V. <sup>1</sup>, Heldmaier G. <sup>1</sup>, McAllan B. M. <sup>5</sup>, Firth B.T. <sup>6</sup>, Burmester T. <sup>7</sup>, Platzer M. <sup>3</sup>, and Klingenspor M. <sup>1</sup>**

<sup>1</sup> Department of Animal Physiology, Faculty of Biology, Philipps-Universität Marburg, Karl-von-Frisch-Str. 8, 35043 Marburg, Germany,

<sup>2</sup> Department of Biological and Physical Sciences, University of Southern Queensland, Toowoomba, Qld, Australia,

<sup>3</sup> Genome Analysis, Leibniz-Institute for Age Research – Fritz Lipmann Institute, D-07745 Jena, Germany

<sup>4</sup> Adaptational and Evolutionary Respiratory Physiology Laboratory, Department of Zoology, La Trobe University, Melbourne 3086, Vic., Australia

<sup>5</sup> Physiology, School of Medical Sciences, The University of Sydney, Sydney 2006, NSW Australia

<sup>6</sup> Discipline of Anatomical Sciences, School of Medical Sciences, University of Adelaide, Adelaide, South Australia, Australia

<sup>7</sup> Institute of Zoology, Biozentrum Grindel, University of Hamburg, Martin-Luther-King-Platz 3, D-20146 Hamburg, Germany

Running title: Uncoupling protein 1 in marsupials

# To whom correspondence should be addressed: Martin Jastroch, Department of Animal Physiology, Faculty of Biology, Philipps-Universität Marburg, Karl-von-Frisch-Str. 8, 35043 Marburg, Germany, Email: Jastroch@staff.uni-marburg.de, Phone: +49-6421-2823389, Fax: +49-6421-282893



**Abstract**

Brown adipose tissue expressing uncoupling protein 1 (UCP1) is responsible for adaptive nonshivering thermogenesis giving eutherian mammals crucial advantage to survive the cold. The emergence of this thermogenic organ during mammalian evolution remained unknown as the identification of UCP1 in marsupials failed so far. Here, we unequivocally identify the marsupial *UCP1* orthologue in a genomic library of *Monodelphis domestica*. In South American and Australian marsupials, *UCP1* is exclusively expressed in distinct adipose tissue sites and appears to be recruited by cold exposure in the smallest species under investigation (*Sminthopsis crassicaudata*). Our data suggest that an archetypal brown adipose tissue was present at least 150 million years ago allowing early mammals to produce endogenous heat in the cold, without dependence on shivering and locomotor activity.

## Introduction

The evolution of brown adipose tissue (BAT) and its thermogenic uncoupling protein 1 (UCP1) is of major interest in the understanding of successful mammalian radiation. Adaptive nonshivering thermogenesis generated in BAT enables small eutherian mammals to maintain high body temperature independent of daily and seasonal temperature fluctuations (6). Although brown adipose tissue was first described in 1551 (14), its thermogenic role was not recognized until the 1960s (8; 44) and it is now established that BAT contributes significantly to adaptive nonshivering thermogenesis of rodents, hibernators and newborns (6). During cold exposure, sympathetic noradrenaline release activates BAT by stimulation of lipolysis and futile UCP1-dependent mitochondrial respiration, and recruitment of oxidative capacity. UCP1, a mitochondrial carrier protein, is located in the inner membrane of BAT mitochondria and provides the molecular basis for nonshivering thermogenesis (32). The protein increases proton conductance and uncouples oxidative phosphorylation from ATP synthesis by dissipating proton motive force as heat. All eutherian species investigated so far possess UCP1, with the exception of pigs where a naturally disrupted *UCP1* gene results in poor thermoregulation and sensitivity to cold exposure (3). The observation that UCP1-knockout mice are unable to defend their body temperature when exposed to the cold (15) confirms that UCP1 is crucial for adaptive nonshivering thermogenesis. In contrast to previous expectations, an ancient UCP1 orthologue was identified in the ectothermic teleost fish but it is not expressed in adipose tissue and the physiological function might be other than heat production (25).

Marsupials are proficient thermoregulators and are capable of defending a stable body temperature during cold exposure (9; 13; 42). Evidence for nonshivering thermogenesis is a matter of debate in marsupial mammals, which separated from eutherians about 150 million years ago (4). In macropods the injection of noradrenaline led to an increase in thermogenesis (31; 33), a response attributed to skeletal muscle and not to BAT as found for eutherians (34; 48). It was suggested that adaptive nonshivering thermogenesis may be of major importance in Australian dasyurids as they belong to the smallest marsupials. Indeed, a thermogenic response to noradrenaline has been observed in *Sminthopsis crassicaudata* acclimated at 24°C (7). No thermogenic response to noradrenaline, however, was observed in *Antechinus stuartii* (37), nor in South American marsupials (10; 36). Despite evidence for nonshivering thermogenesis in some marsupials, no study has demonstrated the molecular basis nor the presence of adaptive nonshivering thermogenesis in response to cold.

Nonshivering thermogenesis is usually associated with BAT but the presence of this specialised adipose organ remains controversial. Morphological studies revealed BAT characteristics like

multilocular fat droplets and vascularisation in the interscapular adipose tissue of Bennett's wallaby pouch young (*Macropus rufogriseus rufogriseus*) (31). Another study investigating 38 different marsupial and one monotreme species precluded the presence of BAT in marsupials (16), by pointing out that morphological features for BAT also occurred in white adipose tissue during cold stress (29; 30). Reliance on morphological features only has misled to the erroneous conclusion that birds possess BAT (35).

The discovery of UCP1 (17; 38) and the cloning of the cDNA sequence in rodents (2; 5) has stimulated work to identify UCP1 and its genomic presence in marsupials. Weak UCP1-like immunoreactivity has been seen in the interscapular fat deposit of *S. crassicaudata* (19), however, it is generally accepted that UCP1 antibodies cross-react with other mitochondrial carriers (39) or UCP2/3, both of which have been recently identified in marsupials (24). Previous studies suggested that UCP2/3 do not compensate for the lack of nonshivering thermogenesis mediated by UCP1, suggesting physiological roles other than heat production (15; 24).

Unequivocal detection of marsupial *UCP1* requires genomic or gene transcript sequence data. However, several attempts to identify the *UCP1* sequence have failed so far (24; 27; 28; 41). In this study we searched for the presence of BAT and UCP1 in one South American (*M. domestica*) and two Australian marsupial species (*S. crassicaudata* and *A. flavipes*). Our approach was to search the genomic trace archives for UCP-like sequence fragments of *M. domestica*, and characterise their physiological function.

## Materials and Methods

### Isolation of genomic DNA of *M. domestica* and polymerase chain reactions

DNA was isolated from a tail tip of a female adult *M. domestica* using a standard phenol-chloroform extraction protocol as described previously (24). Following extraction, fifty nanograms of photometrically quantified DNA was used in subsequent PCR.

In order to define specific primers, we initially searched the *M. domestica* whole genome shotgun data provided by the National Centre for Biotechnology Information (<http://www.ncbi.nlm.nih.gov/Traces/trace.fcgi>) for UCP-like sequence fragments using a consensus UCP1 coding sequence deduced from available eutherian sequences. The fragments were assembled according to the intron-exon structure of mouse *Ucp1*. Using the obtained trace alignments for primer definition, primers were generated (MWG Biotech, Ebersberg, Germany) to amplify a *UCP1*-like fragment (“forEx3”: 5'-AGTGGCACAGCCTACAGATGT-3'; “revEx4”: 5'-CTTGGAACGTCATC ATGTTTG-3').

A second primer pair was deduced from *M. domestica* fragments displaying high identity to UCP2 (“forUCP2”: 5'-GCCTACAAGACTATTGCCCGAGAGGAG-3'; “revUCP2”: 5'-AAGCGGAGAAAGGAAGGCATGAACCC-3').

Following 40 cycles of denaturation at 94°C for 1 min, annealing at 54°C (or 58°C for UCP2) for 1 min, and extension at 72°C for 1 min (2 min for UCP2) were performed. A final extension at 72°C was applied for 10 min and followed by rapid cooling to 4°C. The PCR product was gel-purified and ligated into a pGEMT-easy vector (Promega) for sequencing. Nested oligonucleotides were used for the screening of a genomic *M. domestica* BAC library.

### Sequence analysis of opossum BAC clones

High density arrayed grids of the genomic opossum (*Monodelphis domestica*) BAC library VMRC-6 (Virginia Mason Research Center, distributed by BACPAC Resources, Oakland, CA; <http://bacpac.chori.org>) were screened by hybridization with radioactively end-labeled (T4-Polynucleotidekinase, Roche) oligonucleotides (11):

The *M. domestica* UCP1 specific primers were: md1.F 5'-GGGACTTTCCATGCCTACAA-3', md2.R 5'-CAATAGCATTCTTGCCACG-3', md3.F 5'-AATAGCATCCGCAGAAGGAA-3', md4.R 5'-CGTCCCTGGAAAGAGGAAAT-3' and the *M. domestica* UCP2 specific primers were: md5.F 5'-CTCTTGCAGGTGGCATCC-3', md6.R 5'-GACATTGGGCGAAGTTCCT-3' (mdUCP2 specific).

The identified BACs were verified by PCR using the probe oligos as primers. BACs VMRC6-66F14 (GenBank Acc.no. AC171738, containing mdUCP1) and VMRC6-6003 (GenBank

Acc.no. AC171737, containing md1UCP2 and mdUCP3) were sequenced by a combination of shotgun and directed approaches (46). Base calling and assembly were performed by Phred/Phrap. Finishing was performed in accordance to the Human Genome Project standards (<http://genomeold.wustl.edu/Overview/g16stand.php>) with the support of external *Monodelphis domestica* whole genome shotgun data (<http://www.ncbi.nlm.nih.gov/Traces/trace.fcgi>).

### Phylogenetic inference

The coding and amino acid sequences of *M. domestica* UCP1, UCP2 and UCP3 were deduced from the corresponding genes. A comprehensive search for UCP sequences was performed in public databases (Ensembl genome browser, [www.ensembl.org/](http://www.ensembl.org/) NCBI, [www.ncbi.nlm.nih.gov](http://www.ncbi.nlm.nih.gov)) by employing the Blast algorithm (1). An alignment of the UCP amino acid sequences was generated using ClustalX 1.81 (<ftp://ftp-igbmc.u-strasbg.fr/pub/ClustalX>) and adjusted by eye. Bayesian phylogenetic analyses was performed employing MrBayes 3.1.2 (<http://mrbayes.csit.fsu.edu/>) (40). The WAG model of amino acid substitution (47) with gamma distribution of rates was applied. Substitution rates were allowed to change across the tree under the covarion model (20). Prior probabilities for all trees were equal, starting trees were random. Two analyses were run in parallel for 1,000,000 generations. Trees were sampled every 100th generation and posterior probabilities were estimated on the final 3,000 trees (burnin = 7,000). The tree was visualized using Treeview (<http://taxonomy.zoology.gla.ac.uk/rod/treeview>). The branch lengths are mean branch lengths of the consensus tree representing substitution rates.

### Animal Care and Experimental Protocol

The gray short-tailed opossums (*M. domestica*) were kindly donated by P. Giere and U. Zeller (Museum für Naturkunde, Humboldt-Universität zu Berlin, Germany). The opossums were held individually in the animal facility at the Philipps-Universität Marburg on a 12-hour/12-hour light/dark cycle (12:12 L:D) at an ambient temperature ( $T_a$ ) of  $24\text{ }^{\circ}\text{C} \pm 2\text{ }^{\circ}\text{C}$  given water and fed cat food, curd mixed with fruit, and insects *ad libitum*. For cold acclimation experiments, two individuals were transferred into a separate chamber maintained at  $12^{\circ}\text{C}$  for 14 days.

Seven yellow-footed Antechinus (*A. flavipes*) were captured with Elliott traps in several subtropical habitats in Southeast Queensland (Australia) between January and March 2005. Fourteen fat-tailed dunnarts (*S. crassicaudata*) were obtained from a breeding colony at La Trobe University, Melbourne. Both species were housed individually in the animal facility of the University of Southern Queensland (12:12 L:D, lights on at 0700h) at an ambient temperature ( $T_a$ ) of  $24\text{ }^{\circ}\text{C} \pm 2\text{ }^{\circ}\text{C}$ . To investigate the effect of cold acclimation, seven *S. crassicaudata* and four *A. flavipes* were transferred to a climate chamber adjusted to  $10^{\circ}\text{C}$  for 17 – 22 days whereas

the other individuals remained at 24°C. Animals were given water and fed mealworms and cat food mix including calcium carbonate and vitamins *ad libitum*.

For COX activity assays, ten *S. crassicaudata* used were acclimated to 14 and 28°C at the University of Adelaide animal holding facilities in November 1990.

Experimental protocols for the use of Australian marsupials were approved by the Animal Ethics Committee of the University of Southern Queensland, Queensland Environmental Protection Agency (permit number WISP02633304) and Environment Australia (export number WT2005-12380). Animal experiments involving *M. domestica* were performed in accordance with the German Animal Welfare Laws.

### **Tissue dissection**

Two 22 and 25 days old *M. domestica* embryos were euthanased and immediately frozen on dry ice and stored at -70°C prior to cryosectioning. All other individuals of *M. domestica*, *S. crassicaudata* and *A. flavipes* were euthanased (carbon dioxide) and tissues were dissected. The samples were immediately snap frozen in liquid nitrogen. Frozen tissue samples were stored at -70°C until use. Liver, skeletal muscle and adipose tissue of *S. crassicaudata* and *A. flavipes* were shipped from Australia in liquid nitrogen to Marburg, Germany.

### ***In situ* hybridisation of *M. domestica* embryos**

Sagittal body sections (20 µm) were processed using a cryosectioning microtome (Leica CM 3050) and were transferred to precooled object slides. A riboprobe complementary to *M. domestica* UCP1 (225 bp; primers forEx3, revEx4) and UCP2 (350 bp; forUCP2, revUCP2) was generated from a linearised cloned cDNA. Radioactive riboprobes using [<sup>35</sup>S]-UTP (1-2 x 10<sup>7</sup> cpm ml<sup>-1</sup>), pre- and posthybridisation procedures were performed as described previously (Jastroch et al. 2007). Controls were performed by hybridising sections with equal length sense riboprobes of UCP1 and UCP2.

### **RNA isolation and reverse transcriptase - polymerase chain reaction**

Total RNA was isolated with TRIzol (GIBCO-BRL) according to the manufacturer's protocol. As an additional step, the RNA pellet was redissolved in a solution containing 6.3 mol L<sup>-1</sup> guanidinium thiocyanate, 40 mmol L<sup>-1</sup> sodium citrate pH 7, 0.8% sarcosyl, 8 mmol L<sup>-1</sup> 2-mercaptoethanol, precipitated with 1 volume isopropanol, washed in 75% ethanol, and finally dissolved in DEPC-treated water. Total RNA was photometrically quantified at 260 nm and stored at -70°C. The isolated RNA was used for first strand cDNA synthesis (SUPERScript II, GIBCO/BRL) according to the manufacturer's protocol.

*M. domestica* UCP1 primers      5'-AGGTGAAGCCCAGACCATGGAT-3'  
5'-GGCTGACACAAAGTGGCAAGGT-3'

comprising 6.7 kb of the *UCP1* gene and resulting in 550 bp cDNA sequence, were subjected to polymerase chain reaction with cDNAs of selected tissues. 40 cycles of 94°C (1 min), 59°C (1 min) and 72°C (1 min) were performed and terminated by a 10 min extension at 72°C. The PCR products were gel-purified and ligated into a pJET vector (Fermentas). The full coding sequence of *S. crassicaudata* UCP1 including 5'- and 3'-UTR was amplified using the smart RACE cDNA amplification kit (Clontech) combined with gene specific primers deduced from *M. domestica*

UCP1 3'-UTR:      5'-CTACAGATGTGGTGAAAGTCAGAC-3'  
5'-UTR:      5'-GGCTGACACAAAGTGGCAAGGT-3'.

Subsequent sequencing was used to confirm the identity of the PCR products.

### Northern blot analysis

RNA was separated by gel electrophoresis, transferred onto a nylon membrane and hybridised as described previously (24). After hybridization, the blots were washed with 2x SSC/0.1% SDS for 20 min, 1x SSC/0.1% SDS for 10 min, 0.5x SSC/0.1% SDS for 10 min at room temperature, blots were then transferred to 0.1x SSC/0.1% SDS and washed for 10 min at 60°C. Signal intensities were then monitored by exposure to a PhosphorScreen (Molecular Dynamics). The hybridized probes were then detected by phosphor imaging (Storm 860, Molecular Dynamics), and signal intensities were quantified using ArrayVision 7.0 (Imaging Research). Ethidium bromide staining of total RNA served to normalize gel loading.

### Cytochrome c oxidase (COX) activity

COX activity of interscapular fat deposits of *S. crassicaudata* was measured polarographically at 25°C with a Hansa Tech oxygen electrode chamber as described in (Heldmaier and Buchberger 1985) and (Klaus et al 1988).

### Statistical Analysis

Values for COX activity and UCP1 mRNA are expressed as means  $\pm$  S.E.M. The Mann-Whitney U test was applied for two-sample comparisons. Results were considered statistically significant at  $P < 0.05$ .

## Results and Discussion

### *Identification of UCP1 in M. domestica and S. crassicaudata*

Following our trace archive search for UCP-like sequence fragments, a 346 bp fragment was amplified from genomic DNA of *M. domestica* containing a putative 121 bp intron. The 225 bp partial coding sequence displayed highest identity to eutherian *UCP1* (76%) but lower similarity to eutherian *UCP2* and *UCP3* (69%). A second fragment was amplified using *UCP2* primers exhibiting high identity to *UCP2* of *A. flavipes* (92%, summarized in supplement 1). A genomic *M. domestica* BAC library was screened using homologous primers deduced from the cloned *UCP* fragments. The isolated BAC clones were sequenced, analysed and aligned to the human reference sequence (Fig. 1).

The UCP-like gene of BAC VMRC6-66F14 is flanked by highly conserved orthologues of human *ELMOD2* and human *TBCID9* and thereby resembling the region syntenic to the human *UCP1* locus at chromosome 4. The two *UCP* genes on BAC VMRC6-60O3 found in juxtaposition as human *UCP2* and *UCP3* on chromosome 11 and were also enclosed by the orthologues of human *DNAJB13* and *DKFZP586P0123*. The conserved synteny of the loci in vertebrates unequivocally identified the three *M. domestica* genes as *UCP1*, 2 and 3. Therewith, VMRC6-66F14 (GenBank AC171738) contains the *M. domestica UCP1* and VMRC6-60O3 (GenBank AC171737) the *UCP2* and *UCP3* orthologues. Compared to the corresponding human UCP orthologues, the deduced amino acid sequence of *M. domestica UCP2* exhibited highest identity (91%; 95% similarity), followed by *M. domestica UCP3* (82%; 90% similarity) and *M. domestica UCP1* (65%; 77% similarity).

Primers amplifying the *M. domestica* cDNA were also used to amplify a 250 bp *UCP1* cDNA fragment of *S. crassicaudata*. Using 5'- and 3'-RACE-PCR, we identified 1,386 bp of *UCP1* transcript including the full coding sequence (Genbank Acc. No. EF622232). An alignment of the *S. crassicaudata UCP1* coding sequence showed highest identity with *M. domestica UCP1* (92%), and lower identity to eutherian and marsupial *UCP2* and *UCP3* (70–75%) (supplement 2).

Although an ancestral *UCP1* orthologue appears in the vertebrate lineage as early as the divergence of ray-finned and lobe-finned fish 420 million years ago (25), *UCP1* disappears during evolution in the bird lineage (e.g. the chicken genome, unpublished observation) and became inactivated in pigs among eutheria (3). Biochemical studies suggest that fish *UCP1* is an uncoupling protein with broadly the same activatory and inhibitory characteristics as mammalian *UCP1* (23). The physiological role of the ancient fish *UCP1* may be other than heat production and *UCP1* most likely developed its thermogenic function during mammalian evolution. Our



demonstration of marsupial *UCP1* in the present study is important because not only did previous studies fail to demonstrate *UCP1* in marsupials but also marsupial *UCP1* represents a functional intermediate of ectothermic fish *UCP1* and the highly thermogenic eutherian *UCP1*.

#### *Phylogenetic inference*

For classification of the UCP sequences from *M. domestica* and *S. crassicaudata*, we generated a phylogenetic tree using a Bayesian method (21). Our comprehensive search for UCP sequences in public databases revealed 80 UCPS in the animal kingdom. The addition of further sequences, including *UCP1* of *M. domestica* and *S. crassicaudata*, allowed a solid reconstruction of the *UCP1*, *UCP2* and *UCP3* clades (Fig. 2A, supplement 3). In contrast to previous studies (24; 26), this phylogenetic tree clearly resolves a monophyletic clade of all *UCP1* proteins, including the fish *UCP1* orthologues (Fig. 2B). The overall structure of the *UCP1* clade reflects the phylogeny of the major vertebrate groups. A closer inspection of the *UCP1* clade revealed, that the branch length (substitution rate) between marsupials and eutherians is twice the length (0.4 expected mutations per site) than between marsupials and amphibians (0.2 expected mutations per site). This unexpected large distance indicates accelerated evolution of *UCP1* in eutherians in contrast to steady substitution rates found in the *UCP2/3* clades.

#### *Tissue-specific UCP gene expression in the South American marsupial M. domestica*

Based on the identification of the *UCP1* gene in *M. domestica*, we investigated *UCP1* gene expression. We sampled cryosections of pouch embryos (22- and 25-days old), sampled tissues of a juvenile (70 days old, post nest vacation) and young adults (3 month old).

Only in the juvenile we found dispersed adipose tissue deposits (brownish appearance) on the ribcage embedded in between pectoral muscle fibres (pectoral fat). Northern blotting analysis with a *UCP1* cDNA probe was insensitive but using *M. domestica UCP1* primers comprising 6.7 kb of genomic sequence amplified a 550 bp cDNA fragment by PCR only in the pectoral fat (Fig. 3A) and subsequent sequencing clearly identified *UCP1* cDNA.

Hybridisation techniques in all other individuals using a *M. domestica UCP1* cDNA probe demonstrated the lack of significant *UCP1* mRNA expression whereas *UCP2* mRNA was detectable (Fig. 3B, C). In whole-body cryosections of the embryos, *UCP2* mRNA was ubiquitously expressed with highest levels in spleen, heart and liver (Fig. 3B). Non-specific signals, as judged by comparison to the sense-control, occurred in calcified bone tissue. Northern blot analysis of selected tissues from the young adult revealed *UCP2* mRNA in all fat tissues,

spleen and intestine (Fig. 3C). Notably, *UCPI* mRNA expression in the interscapular fat, a typical brown adipose tissue site in eutherians, was undetectable.

Although the observed expression pattern in *M. domestica* is different from rodents, we have to consider that numerous eutherians do not possess significant amounts of BAT during their whole lifespan. In contrast to rodents and hibernators possessing BAT during their entire life, rabbits lose the ability to express *UCPI* one month after birth (Cambon 1998), while in newborn bovine and lambs *UCPI* expression is of significance only two days after physiological birth (Casteilla 1989). BAT, or at least *UCPI*, in marsupials may therefore only be of importance to overcome cold-stress around pouch or nest vacation. Increased responsiveness to noradrenaline coincides with pouch vacation (wallaby (31); Eastern barred bandicoot *Perameles gunnii* (22)). Given the identification of marsupial *UCPI* in this study, these observations can be revisited and the contribution of BAT investigated.

#### *Analysis of the UCPI promoter region in M. domestica*

Our experiments show a high specificity of marsupial *UCPI* expression in distinct adipose tissue sites. In rodents and humans, an enhancer box in the upstream promoter region contains condensed elements targeting *UCPI* expression to BAT and allows responsiveness to the cold (for review see (43)). We searched a 10 kb genomic sequence upstream of the *UCPI* transcriptional start site of *M. domestica* for the presence of the enhancer box. Although we localised the enhancer box in all eutherians, including the ancient Afrotherian species *Echinops telfairii*, *M. domestica* lacks this distinct region suggesting that the enhancer box first evolved in eutherian mammals (supplement 4). Despite the lack of the enhancer box, marsupial *UCPI* shows a remarkably high tissue-specificity targeting gene expression to distinct adipose tissue sites. The respective response elements may be dispersed across the promoter upstream region and their presence cannot be categorically excluded.

#### *Tissue-specific UCP gene expression in the Australian marsupials S. crassicaudata and A. flavipes*

In *S. crassicaudata*, but not *A. flavipes*, we detected *UCPI* mRNA expression exclusively in the interscapular fat deposit whereas no signal was detectable in liver and skeletal muscle (Fig. 4A). Probing with a *UCP2* fragment cloned from *Sminthopsis macroura* (24) detected highest *UCP2* mRNA levels in the interscapular fat region of *S. crassicaudata* and *A. flavipes* whereas mRNA levels in liver and skeletal muscle were rather low (Fig. 4A). Cross-reactivity of the *UCPI* probe

to *UCP2* could be excluded as the *UCP1* probe exhibited only 61% to 69% identity to *Sminthopsis* and *Antechinus* *UCP2*, respectively. Using a *A. flavipes* *UCP3* probe, we detected *UCP3* mRNA in skeletal muscle of both species confirming a previous study (24).

Here, we demonstrate that *UCP1* is constitutively expressed in *S. crassicaudata*, the smallest marsupial under investigation, in contrast to a close dasyurid relative, *A. flavipes*. Previous studies in *Sminthopsis* and *Antechinus* species support the interdependence of nonshivering thermogenesis and marsupial *UCP1*. As would be likely to occur in the presence of brown adipose tissue, *Sminthopsis spec.* elevate metabolic rate by 30% in response to 0.25 mg kg<sup>-1</sup> noradrenaline at 24°C (*S. crassicaudata*) (7), or in response to cold exposure (*S. macroura*) (13). In contrast, *Antechinus ssp.* does not show a thermogenic response to noradrenaline (37). It is likely that the differences seen in *UCP* expression are a functional adaptation to reflect the significant life history differences between these species. *Sminthopsis ssp.* from arid Australia are exposed to pronounced seasonal fluctuations in environmental temperature while the coastal *Antechinus ssp.* experiences less climatic fluctuations (12).

The lack of *UCP1* in adult *A. flavipes* and *M. domestica* is a distinct difference to eutherian species of similar body mass (18). Conventional heating mechanisms like shivering in these marsupials may be adequate to defend body temperature in mild climates.

#### *Effect of cold exposure on the marsupial interscapular fat deposit*

Adaptive nonshivering thermogenesis in rodents requires the recruitment of oxidative capacity and *UCP1* to increase heat production. In a preliminary study on *S. crassicaudata* in 1990, there was a strong trend towards increased cytochrome c oxidase (COX) activity in the interscapular fat deposit of cold-acclimated individuals (Fig. 4B) but we were not able to detect *UCP1* mRNA using a rat *UCP1* cDNA probe. By using a marsupial *UCP1* probe in the present study, we demonstrated a significant up-regulation of *UCP1* gene expression in response to cold. *UCP1* mRNA levels in cold-acclimated *S. crassicaudata* were two-fold higher than in animals exposed to 24°C (n = 7, p = 0.018, Fig. 4C). Furthermore, appearance of the interscapular fat deposit changed from white in animals held at 24°C to brown in cold-acclimated *S. crassicaudata* (Fig. 4D), a transition that was absent in *M. domestica*. Together with the absence of brownish colour, *UCP1* mRNA expression was absent in the interscapular fat deposit in young adult *M. domestica* (3 months old) after cold exposure (supplement 5). Even post-hybridisation procedures under less stringent conditions revealed no signal in the interscapular fat of *M. domestica* but visualised cross-reactivity of the *M. domestica* *UCP1* cDNA probe to mouse *UCP1*. *M. domestica* *UCP2* mRNA levels remained unchanged in interscapular fat after cold exposure (supplement 4).

Despite some evidence for nonshivering thermogenesis in marsupials, no studies so far had investigated adaptiveness to the cold. In this study, cold-exposure elevated oxidative capacity and UCP1 expression in the interscapular fat of *S. crassicaudata* resembling adaptive molecular adjustments of eutherian BAT. Response of *S. crassicaudata* UCP1 gene expression to cold exposure demonstrates different transcriptional control compared to *M. domestica*. Therefore, genomic UCP1 promotor data of an Australian marsupial are required to identify UCP1 response elements that are conserved during mammalian evolution.

### **Conclusive remarks**

The successful radiation of eutherian mammals to cold environments was most likely facilitated by classical adaptive nonshivering thermogenesis depending on BAT and its crucial protein UCP1 (6). However, the origin and evolution of this thermogenic organ is unknown. Textbooks illustrate BAT as monophyletic trait of eutherians (45), and both UCP1 and BAT have been regarded as absent in marsupials (10; 16; 24; 27; 28; 34; 42), however our study represents the first unequivocal demonstration of UCP1 gene expression in adipose tissue of South American and Australian marsupials. In some marsupials like *M. domestica* or *A. flavipes*, UCP1 may be recruited transiently during early stages of development and is lost during adulthood, whereas other marsupials like *S. crassicaudata* retain UCP1 expression during the entire lifespan. These findings provide the molecular basis to investigate adaptive nonshivering thermogenesis and lead to interesting insights into the evolution of UCP1-mediated heat production. Our results suggest the presence of an archetypal BAT before the divergence of marsupials and eutherians more than 150 million years ago allowing early mammals to pursue life in the cold.

### **Acknowledgements**

This research was supported by Deutsche Forschungsgemeinschaft DFG KL973/7 (to M. K.), by the *Centre for rural and environmental biology*, Department of Biological and Physical Sciences, University of Southern Queensland (to K.W. and M.J.) and the NGFN2. We thank Sigrid Stoehr for excellent technical assistance.

## References

1. **Altschul SF, Gish W, Miller W, Myers EW and Lipman DJ.** Basic local alignment search tool. *J Mol Biol* 215: 403-410, 1990.
2. **Aquila H, Link TA and Klingenberg M.** The uncoupling protein from brown fat mitochondria is related to the mitochondrial ADP/ATP carrier. Analysis of sequence homologies and of folding of the protein in the membrane. *EMBO J* 4: 2369-2376, 1985.
3. **Berg F, Gustafson U and Andersson L.** The uncoupling protein 1 gene (UCP1) is disrupted in the pig lineage: a genetic explanation for poor thermoregulation in piglets. *PLoS Genet* 2: e129, 2006.
4. **Bininda-Emonds OR, Cardillo M, Jones KE, MacPhee RD, Beck RM, Grenyer R, Price SA, Vos RA, Gittleman JL and Purvis A.** The delayed rise of present-day mammals. *Nature* 446: 507-512, 2007.
5. **Bouillaud F, Ricquier D, Thibault J and Weissenbach J.** Molecular approach to thermogenesis in brown adipose tissue: cDNA cloning of the mitochondrial uncoupling protein. *Proc Natl Acad Sci U S A* 82: 445-448, 1985.
6. **Cannon B and Nedergaard J.** Brown adipose tissue: function and physiological significance. *Physiol Rev* 84: 277-359, 2004.
7. **Clements F, Hope PJ, Daniels CB, Chapman I and Wittert G.** Thermogenesis in the marsupial *Sminthopsis crassicaudata*: effect of catecholamines and diet. *Aust J Zool* 46: 381-390, 1998.
8. **Dawkins MJR and Hull D.** Brown adipose tissue and the response of new-born rabbits to cold. *J Physiol* 172: 216-238, 1964.

9. **Dawson TJ and Dawson WR.** Metabolic scope and conductance in response to cold of some dasyurid marsupials and Australian rodents. *Comp Biochem Physiol* 71A: 59-64, 1982.
10. **Dawson TJ and Olson JM.** Thermogenic capabilities of the opossum *Monodelphis domestica* when warm and cold acclimated: similarities between American and Australian marsupials. *Comp Biochem Physiol A* 89: 85-91, 1988.
11. **Galgoczy P, Rosenthal A and Platzer M.** Human-mouse comparative sequence analysis of the NEMO gene reveals an alternative promoter within the neighboring G6PD gene. *Gene* 271: 93-98, 2001.
12. **Geiser F.** Daily torpor and thermoregulation in *Antechinus* (Marsupialia). influence of body mass, season, development, reproduction, and sex. *Oecologia* 77: 395-399, 1988.
13. **Geiser F, Drury RL, McAllan BM and Wang DH.** Effects of temperature acclimation on maximum heat production, thermal tolerance, and torpor in a marsupial. *J Comp Physiol [B]* 173: 437-442, 2003.
14. **Gesner C.** *Medici Tigurini Historiae Animalium Liber I de Quadrupedibusuiiiparis* 840-844, 1551.
15. **Golozoubova V, Hohtola E, Matthias A, Jacobsson A, Cannon B and Nedergaard J.** Only UCP1 can mediate adaptive nonshivering thermogenesis in the cold. *FASEB J* 15: 2048-2050, 2001.
16. **Hayward JS and Lisson PA.** Evolution of brown fat: its absence in marsupials and monotremes. *Can J Zool* 70: 171-179, 1992.
17. **Heaton GM, Wagenvoort RJ, Kemp A and Nicholls DG.** Brown-adipose-tissue mitochondria: photoaffinity labelling of the regulatory site of energy dissipation. *Eur J Biochem* 82: 515-521, 1978.

18. **Heldmaier G.** Zitterfreie Wärmebildung und Körpergröße bei Säugetieren. *Z vergl Physiol* 73: 222-248, 1971.
19. **Hope PJ, Pyle D, Daniels CB, Chapman I, Horowitz M, Morley JE, Trayhurn P, Kumaratilake J and Wittert G.** Identification of brown fat and mechanisms for energy balance in the marsupial, *Sminthopsis crassicaudata*. *Am J Physiol* 42: R161-R167, 1997.
20. **Huelsenbeck JP.** Testing a covariotide model of DNA substitution. *Molecular Biology and Evolution* 19: 698-707, 2002.
21. **Huelsenbeck JP and Ronquist F.** MRBAYES: Bayesian inference of phylogenetic trees. *Bioinformatics* 17: 754-755, 2001.
22. **Ikonomopoulou MP and Rose RW.** The development of endothermy during pouch life in the eastern barred bandicoot (*Perameles gunnii*), a marsupial. *Physiol Biochem Zool* 79: 468-473, 2006.
23. **Jastroch M, Buckingham JA, Helwig M, Klingenspor M and Brand MD.** Functional characterisation of UCP1 in the common carp: uncoupling activity in liver mitochondria and cold-induced expression in the brain. *J Comp Physiol [B]* DOI 10.1007/s00360-007-0171-6: 2007.
24. **Jastroch M, Withers K and Klingenspor M.** Uncoupling protein 2 and 3 in marsupials: identification, phylogeny, and gene expression in response to cold and fasting in *Antechinus flavipes*. *Physiol Genomics* 17: 130-139, 2004.
25. **Jastroch M, Wuertz S, Kloas W and Klingenspor M.** Uncoupling protein 1 in fish uncovers an ancient evolutionary history of mammalian nonshivering thermogenesis. *Physiol Genomics* 22: 150-156, 2005.
26. **Jimenez-Jimenez J, Zardoya R, Ledesma A, Garcia dL, Zaragoza P, Mar Gonzalez-Barroso M and Rial E.** Evolutionarily distinct residues in the uncoupling protein UCP1 are essential for its characteristic basal proton conductance. *J Mol Biol* 359: 1010-1022, 2006.

27. **Kabat AP, Rose RW, Harris J and West AK.** Molecular identification of uncoupling proteins (UCP2 and UCP3) and absence of UCP1 in the marsupial Tasmanian bettong, *Bettongia gaimardi*. *Comp Biochem Physiol B Biochem Mol Biol* 134: 71-77, 2003.
28. **Kabat AP, Rose RW and West AK.** Non-shivering thermogenesis in a carnivorous marsupial *Sarcophilus harrisii*, in the absence of UCP1. *Journal of Thermal Biology* 28: 413-420, 2003.
29. **Loncar D, Afzelius BA and Cannon B.** Epididymal white adipose tissue after cold stress in rats. I. Nonmitochondrial changes. *J Ultrastruct Mol Struct Res* 101: 109-122, 1988.
30. **Loncar D, Afzelius BA and Cannon B.** Epididymal white adipose tissue after cold stress in rats. II. Mitochondrial changes. *J Ultrastruct Mol Struct Res* 101: 199-209, 1988.
31. **Loudon ASI, Rothwell NJ and Stock MJ.** Brown fat, thermogenesis and physiological birth in a marsupial. *Comp Biochem Physiol* 81A: 815-819, 1985.
32. **Nicholls DG and Locke RM.** Thermogenic mechanisms in brown fat. *Physiol Rev* 64: 1-64, 1984.
33. **Nicol SC.** Non-shivering thermogenesis in the potoroo, *Potorous tridactylus* (Kerr). *Comp Biochem Physiol* 59: 33-37, 1978.
34. **Nicol SC, Pavlides D and Andersen NA.** Nonshivering thermogenesis in marsupials: Absence of thermogenic response to beta 3-adrenergic agonists. *Comp Biochem Physiol A* 117: 399-405, 1997.
35. **Oliphant LW.** First observations of brown fat in birds. *Condor* 85: 350-354, 1983.
36. **Opazo JC, Nespolo RF and Bozinovic F.** Arousal from torpor in the chilean mouse-opposum (*Thylamys elegans*): does non-shivering thermogenesis play a role? *Comp Biochem Physiol A Mol Integr Physiol* 123: 393-397, 1999.



37. **Reynolds W and Hulbert AJ.** Cold acclimation in a small dasyurid marsupial: *Antechinus stuartii*. edited by Archer M. Mosman, N.S.W.: Royal Zoological Society of NSW, 1982, p. 278-283.
38. **Ricquier D and Kader JC.** Mitochondrial protein alteration in active brown fat: a sodium dodecyl sulfate-polyacrylamide gel electrophoretic study. *Biochem Biophys Res Commun* 73: 577-583, 1976.
39. **Ricquier D, Raimbault S, Champigny O, Miroux B and Bouillaud F.** Comment to Shinohara et al. (1991) FEBS Letters 293, 173-174. The uncoupling protein is not expressed in rat liver. *FEBS Lett* 303: 103-106, 1992.
40. **Ronquist F and Huelsenbeck JP.** MrBayes 3: Bayesian phylogenetic inference under mixed models. *Bioinformatics* 19: 1572-1574, 2003.
41. **Rose RW, West AK, Ye JM, McCormick GH and Colquhoun EQ.** Nonshivering thermogenesis in a marsupial (the tasmanian bettong *Bettongia gaimardi*) is not attributable to brown adipose tissue. *Physiol Biochem Zool* 72: 699-704, 1999.
42. **Schaeffer PJ, Villarín JJ and Lindstedt SL.** Chronic cold exposure increases skeletal muscle oxidative structure and function in *Monodelphis domestica*, a marsupial lacking brown adipose tissue. *Physiol Biochem Zool* 76: 877-887, 2003.
43. **Silva JE and Rabelo R.** Regulation of the uncoupling protein gene expression. *Eur J Endocrinol* 136: 251-264, 1997.
44. **Smith RE.** Thermoregulation by brown adipose tissue in cold. *Fed Proc* 21: 221, 1962.
45. **Vaughan TA, Ryan JM and Czaplewski NJ.** *Mammalogy*. Saunders College Publishing, 2000.
46. **Wen G, Ramser J, Taudien S, Gausmann U, Blechschmidt K, Frankish A, Ashurst J, Meindl A and Platzer M.** Validation of mRNA/EST-based gene predictions in human

---

Xp11.4 revealed differences to the organization of the orthologous mouse locus. *Mamm Genome* 16: 934-941, 2005.

47. **Whelan S and Goldman N.** A general empirical model of protein evolution derived from multiple protein families using a maximum-likelihood approach. *Mol Biol Evol* 18: 691-699, 2001.
  
48. **Ye JM, Edwards SJ, Rose RW, Steen JT, Clark MG and Colquhoun EQ.** alpha-adrenergic stimulation of thermogenesis in a rat kangaroo (Marsupialia, *Bettongia gaimardi*). *American Journal of Physiology* 40: R586-R592, 1996.

## Figure legends

**Fig.1:** Conservation of *UCP1*, *UCP2*, *UCP3* and their flanking genes between human and opossum (*M. domestica*). The upper panel illustrates the genomic organisation of the human *UCP1*, 2 and 3 locus, the lower panel the opossum orthologues. Nucleotide and amino acid identities between the orthologues are compared in the middle panel.

**Fig. 2:** Bayesian phylogeny of the core UCP family in vertebrates including marsupial UCP1 (*M. domestica* and *S. crassicaudata*). An alignment of all available UCP sequences was analysed by MrBayes 3.1.2, assuming a Whelan and Goldmann model of evolution. A. Simplified tree resolving the phylogenetic relations of the core UCP family. The oxalacetate-malate carrier (OMCP) represents the outgroup. B. Detailed illustration of the UCP1 subgroup. Bayesian posterior probabilities are given at the branch nodes and the scale bar indicates the substitution rate per aligned amino acid position. The complete phylogenetic tree can be found in supplement 3.

**Fig. 3:** Regulation of *UCP1* and *UCP2* gene expression in multiple tissues of the developing marsupial *M. domestica*. Homologous primers and radioactively-labelled cDNA and riboprobes used. A. Low levels of *UCP1* cDNA detected by PCR in multiple tissues of a 70 days old juvenile. The 550 bp *UCP1* fragment was amplified from adipose tissue embedded in the ribcage (pectoral fat).  $\beta$ -actin mRNA served as a cDNA quality control. B. Representative sagittal section showing whole-body in situ hybridisation of 22 – 25 old embryos. The *UCP2* antisense riboprobe clearly hybridised with *UCP2* mRNA in spleen, heart and liver while no *UCP1* signals could be detected using a *M. domestica* *UCP1* antisense riboprobe (left panel). All riboprobes hybridised artefactually with calcified bone as judged by comparison to sense controls (right panel). A photograph of a sagittal transection served to assign radioactive signals to organs. C. Multiple tissue Northern blot analysis of three months old *M. domestica* incl. interscapular fat of warm-acclimated and cold-acclimated individuals (n = 4); and mouse BAT controls. Total RNA (10  $\mu$ g) isolated from selected tissues was hybridised with a 225 bp *UCP1* and a 350 bp *UCP2* cDNA fragment of *M. domestica*. Total RNA from mouse BAT served as a control. Post-hybridisation for *UCP1* was performed under less stringent conditions, detecting mouse *UCP1*. The *M. domestica* *UCP2* probe detected mRNA in spleen, inguinal and interscapular fat of *M. domestica*. Skm, skeletal muscle; int.fat, interscapular fat deposit; ing. fat, inguinal fat; ax. fat, axillary fat.

**Fig. 4:** A. UCP expression in selected tissues of the marsupials *S. crassicaudata* and *A. flavipes*. Ten micrograms of total RNA were hybridised with a *M. domestica* UCP1, *S. macroura* (S.cr.) UCP2 and a *A. flavipes* (A. fl.) UCP3 cDNA probe. Skm, skeletal muscle; int.fat, interscapular fat deposit. B. COX activity in interscapular adipose tissue homogenates of warm-acclimated and cold-acclimated *S. crassicaudata*. C. The effect of cold exposure (10°C) on UCP1 gene expression in *S. crassicaudata*. Radioactive intensities of specific signals are shown as relative units corrected by ethidium bromide staining of the 18S rRNA. The effects of cold acclimation was evaluated by Mann Whitney U test; \*p < 0.05. D. Appearance of interscapular fat due to cold exposure. The photograph shows a dorsal view on the interscapular fat deposits of a warm-acclimated and a cold-acclimated *S. crassicaudata*.

Figure 1

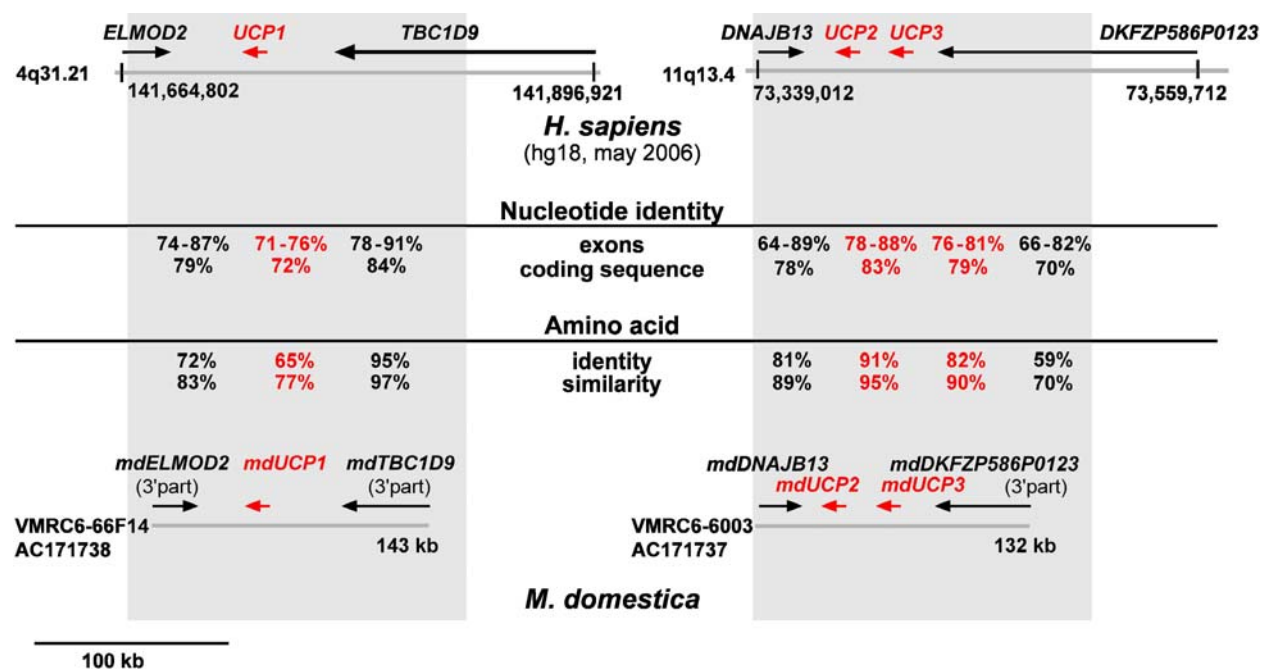


Figure 2

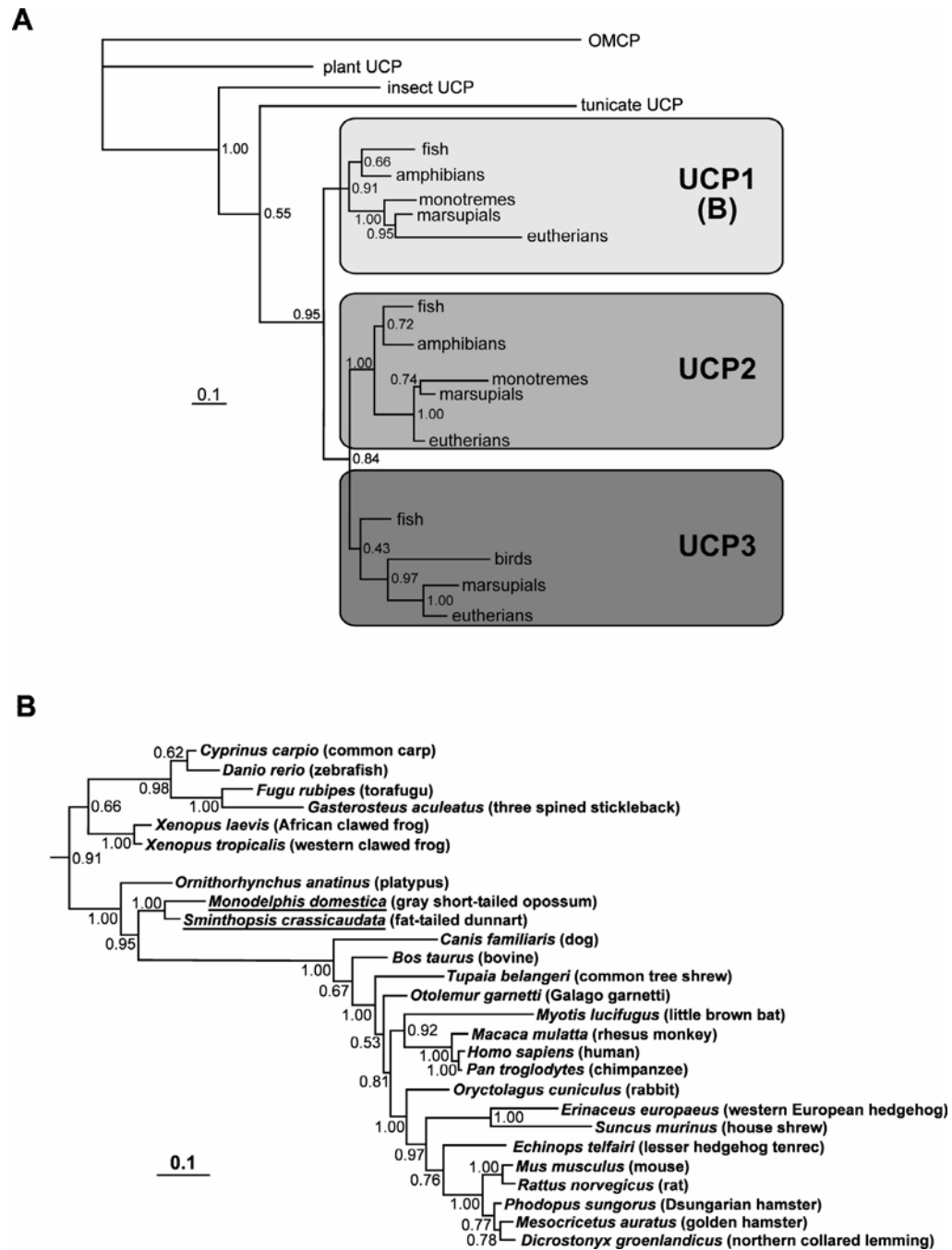


Figure 3

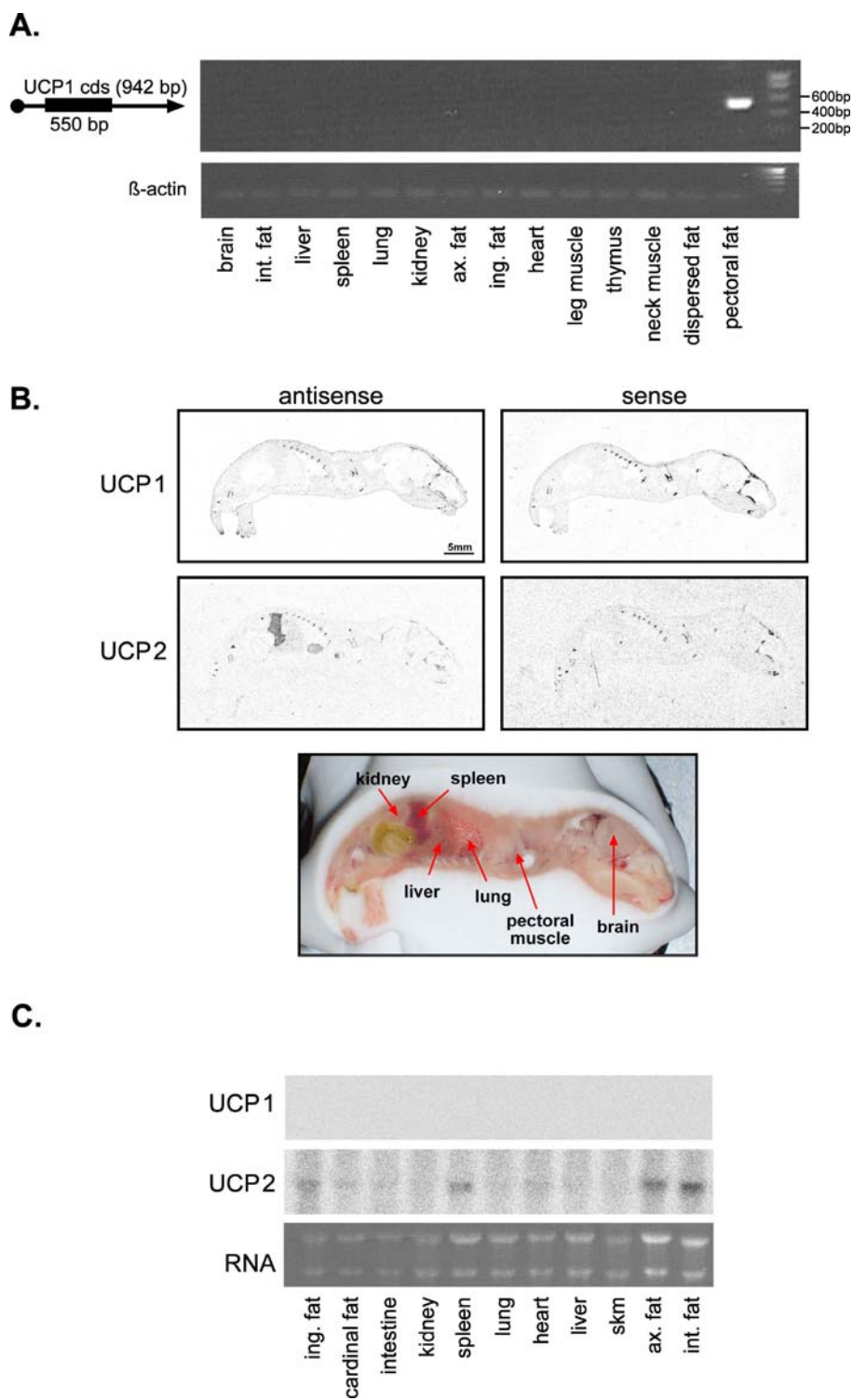
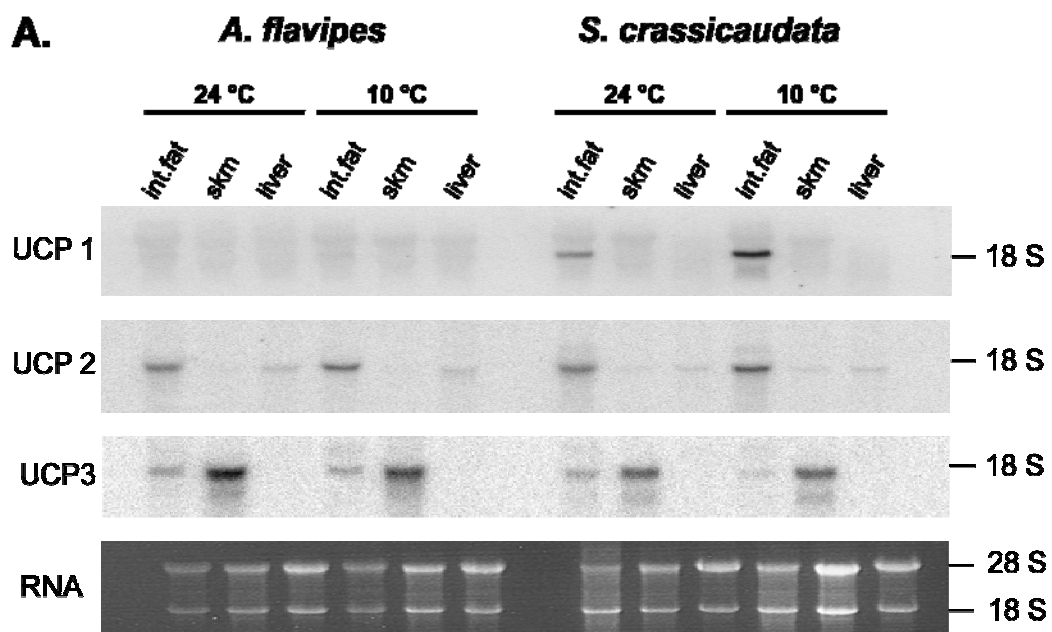
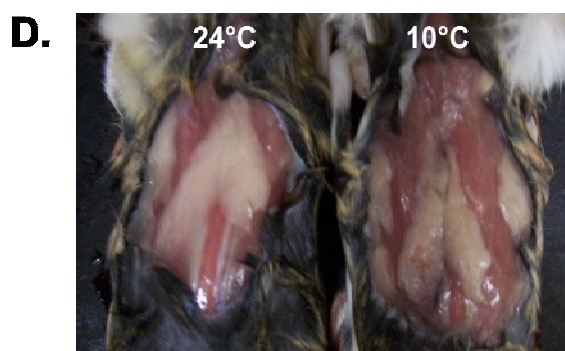
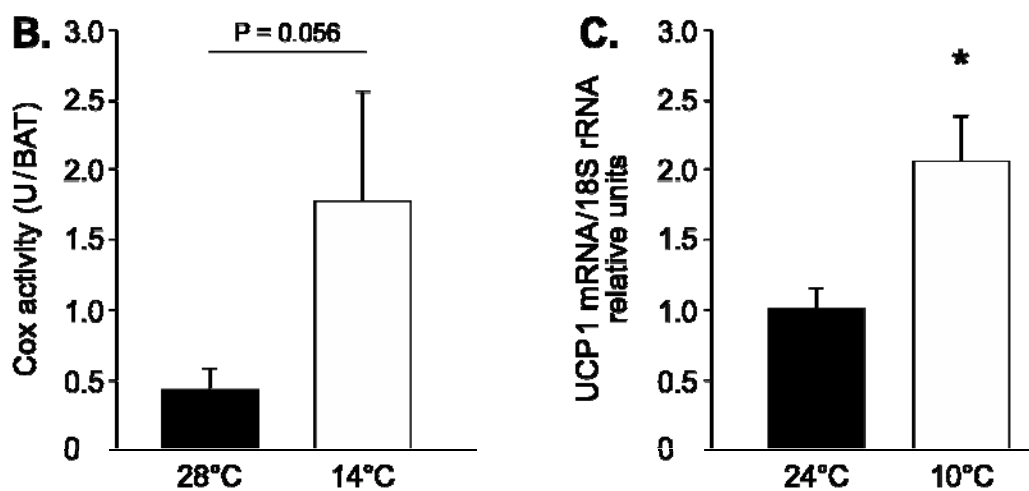


Figure 4



***S. crassicaudata***





**Supporting online material for****Marsupial uncoupling protein 1 sheds light on the evolution of mammalian  
nonshivering thermogenesis**

**Jastroch M. <sup>1#</sup>, Withers K. W. <sup>2</sup>, Taudien S. <sup>3</sup>, Frappell P. B. <sup>4</sup>, Helwig M. <sup>1</sup>, Fromme T. <sup>1</sup>,  
Hirschberg V. <sup>1</sup>, Heldmaier G. <sup>1</sup>, McAllan B. M. <sup>5</sup>, Firth B.T. <sup>6</sup>, Burmester T. <sup>7</sup>, Platzer M. <sup>3</sup>,  
and Klingenspor M. <sup>1</sup>**

# To whom correspondence should be addressed: Martin Jastroch, Department of Animal Physiology,  
Faculty of Biology, Philipps-Universität Marburg, Karl-von-Frisch-Str. 8, 35043 Marburg, Germany,  
Email: Jastroch@staff.uni-marburg.de, Phone: +49-6421-2823389, Fax: +49-6421-282893

## Material and Methods of Supplements

### S1 Gene soeing

Northern blot analysis required the excision of intron sequence from the genomic UCP1 fragment of *M. domestica*. Therefore, we excised intron 3/4 using PCR based gene SOEing (Horton RM, Ho SN, Pullen JK, Hunt HD, Cai Z and Pease LR. Gene splicing by overlap extension. *Methods Enzymol* 217: 270-279, 1993). The *M. domestica* exon 3 fragment (amplified by using primers “forEx3” and 5'-CATCGTCCCTTTCCAAAGCC -3') and exon 4 fragment (using primers forward 2: CTTTGGAAAGGGACGATGCC and “revEx4”) were amplified separately (30 cycles of 94° C (20s), 54°C (30s), and 72°C (1 min) with a final extension at 72°C (10 min)). Both fragments were subjected to a single PCR with an annealing temperature of 52°C using primers “forEx3” and “revEx4”. The resulting fragment was cloned and used as a template for radioactively labelled probing.

### S2 Alignment of *S. crassicaudata* and *M. domestica* UCP1 with mouse UCPs

The deduced UCP protein sequences were aligned using clustalX. The alignment file was exported to genedoc for shaded illustration of amino acid conservation.

### S3 Bayesian phylogenetic tree

For methods see material and methods section. *S3 Bayesian phylogenetic tree*

### S4 Syntenic promotor region

4A *The lack of the UCP1-specific enhancer box controlling UCP1 expression in M. domestica.* –10000 bp to 0 bp upstream region of *UCP1* transcriptional start was retrieved from the ensembl genome browser ([www.ensembl.org](http://www.ensembl.org)) and searched for the presence of the UCP1-enhancer box in selected placental mammals and *M. domestica*. The *M. musculus* upstream region (x-axis) was plotted against the upstream region of the other species (y-axis) using the dotplot function of the spin module (Staden Package; <http://staden.sourceforge.net/>). Red dots indicate a score 9 out of 10. A 45° virtual line indicates conserved regions. The predicted enhancer box is marked with a circle and magnified. 4B. The predict regions for the enhancer box were aligned using clustalX.

### S5 UCP gene expression in the interscapular fat deposit of warm- and cold-acclimated opossums, *M. domestica*, and the mouse, *M. musculus*

Total RNA was extracted from interscapular fat deposits of the Ten micrograms of total RNA were subjected to Northern blot analysis (see Materials and Methods) and hybridised with a *M.*

*domestica* UCP1 cDNA probe. Specific signals were detected in mouse BAT under less stringent post-hybridising conditions (2x SSC/0.1% SDS for 20 min, 1x SSC/0.1% SDS for 10 min). Furthermore, UCP2 mRNA in *M. domestica* was detected using a homologous cDNA probe.

## Captions for supplements:

### *S1 Amplification of genomic UCP fragment from M. domestica*

Upper panel: Gel electrophoresis of a 324 bp *UCP1*-like genomic fragment (lane 2) of *M. domestica*. Excision of the intron using geneSOEing resulted in a 225 bp fragment (lane 1). Lower panel: Gel electrophoresis of a 1200 bp *UCP2* fragment from genomic DNA of *M. domestica* (lane 1/2).

### *S2 Alignment of S. crassicaudata and M. domestica UCP1 with mouse UCPs*

The alignment of the deduced amino acid sequences is illustrated in the conservation mode using genedoc.

### *S3 Bayesian phylogenetic tree*

Phylogenetic relations of the UCP family in vertebrates including *UCP1* of marsupials using Bayesian methods. The oxaloacetate-malate carrier served as the outgroup. P-values are given as internal node labels. *UCP* sequences other than marsupials were either found predicted in public databases or found by search genomic sequence. Table 1 contains according to the abbreviations of the species, full species names and sequence accession numbers.

#### *S4.1 Lack of the UCP1-enhancer box in M. domestica*

The *M. musculus* upstream region (y-axis) was plotted against the upstream region of the other species (x-axis). Red dots indicate a score 9 out of 10. A 45° virtual line indicates conserved regions. The predicted enhancer box is marked with a circle and magnified.

#### *S4.2 Conservation of the UCP1-enhancer box in eutherians*

Alignment of the *UCP1*-enhancer box from selected placental species. Dark shading indicates conservation, responsive elements are underscored, published in blue and novel predicted in red.

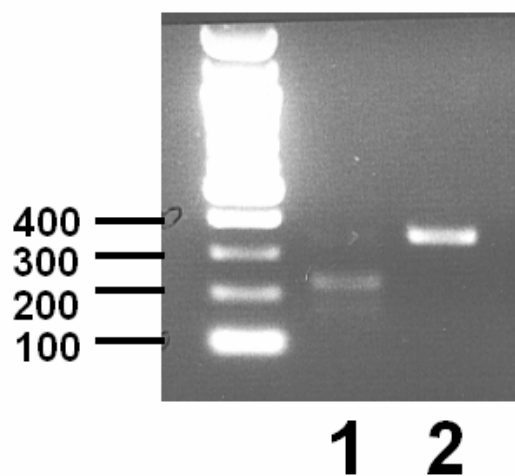
### *S5 UCP gene expression in the interscapular fat deposit of warm- and cold-acclimated opossums, M. domestica, and the mouse, M. musculus*

Neither warm- nor cold-acclimated young adult (3 months old) *M. domestica* express significant amounts of *UCP1* mRNA. *UCP2* mRNA is expressed in the interscapular fat deposit but not upregulated during cold exposure as known for eutherian mammals.

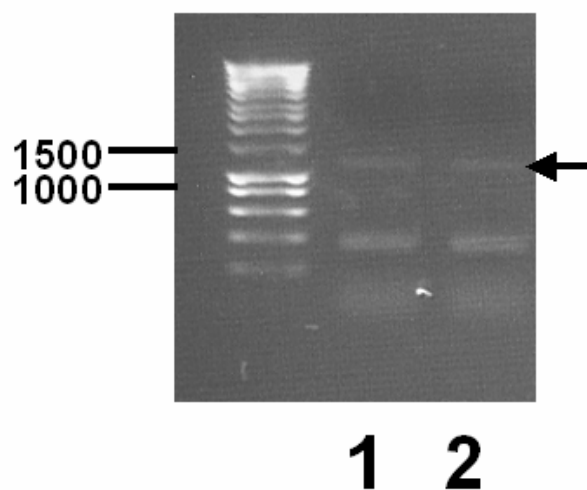
**Supplement 1****UCP1:**

lane 1 225 bp product  
of gene SOEing

lane 2 346 bp fragment

**UCP2:**

lane 1/2 1200 bp fragment



## Supplement 2

```

              *          20      *          40      *          60      *          80      *          100
Smithopsis crassicaudata UCP1 : -----
Monodelphis domestica UCP1 : WGLKQYQPPPCTFLGTANGHADLVTEPLLTARVELOIOQSAGT---MDAVRFSILOTILIVTEPRSLNGHGQQSFASIPIOLTAKL : 1021
Mus musculus UCP1 : WGFKADDPHATHELGTASHALLITTEPLTARVELOIOQSQLVRTAASAQPSVLOTLIVTEPRSLNGHGQQSFASIPIOLTAKL : 1061
Mus musculus UCP2 : WGLQPDPPTVTHELGTASHALLITTEPLTARVELOIOQSNPG---ACSVCPSVLOTLIVTEPRSPSHVAGLDQSFASIPIOLTAKL : 1021
Mus musculus UCP3 : WNPTTELQHGHIFSHALLITTEPLTARVELOIOQSGGA---SSTIRREVLOTILIVTELPKLSHPAGDQQISFASIPIOLTAKL : 1021

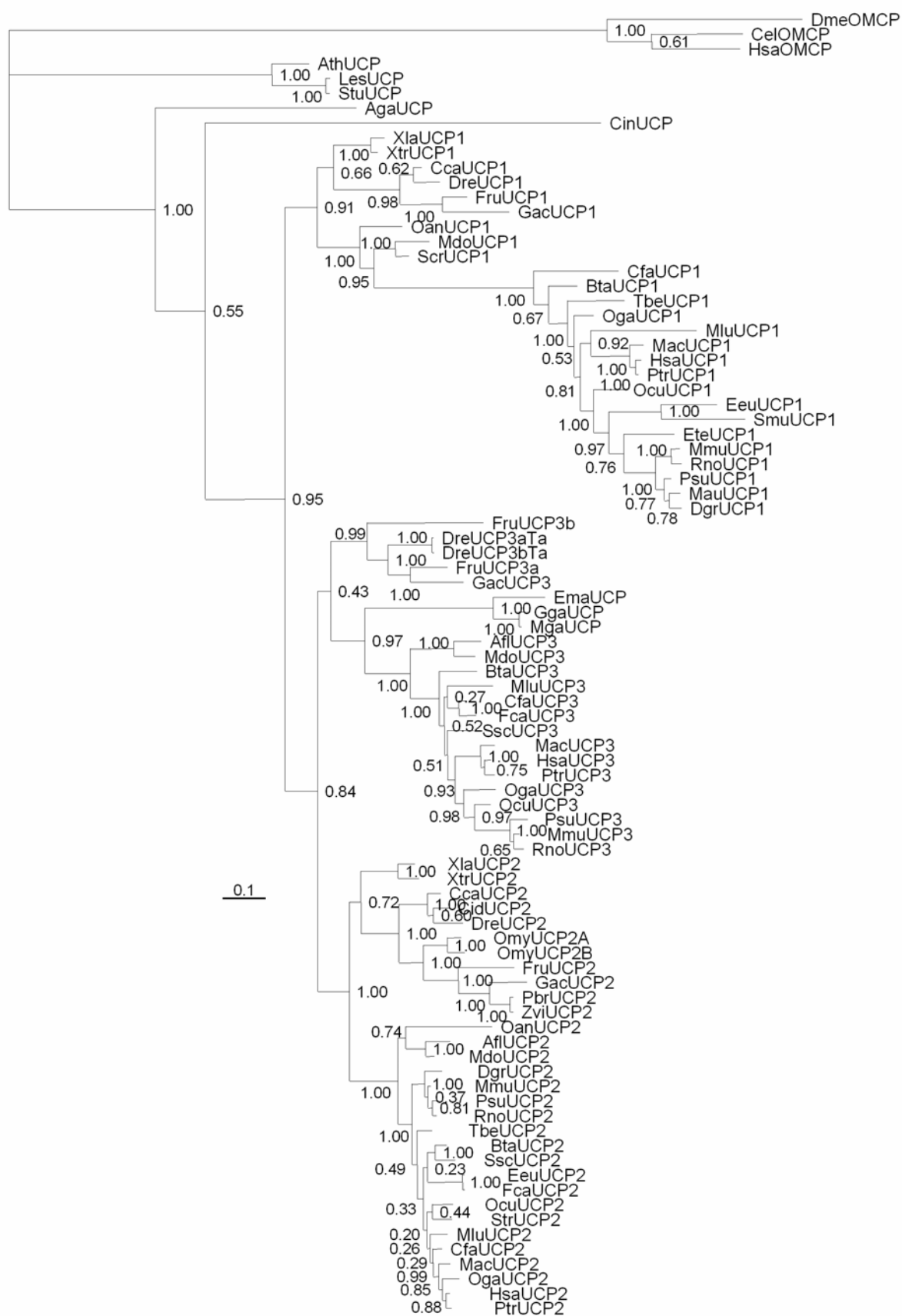
              *          120      *          140      *          160      *          180      *          200
Smithopsis crassicaudata UCP1 : -----
Monodelphis domestica UCP1 : NNGRETAGGSLACTTGAVAIVAPTDVVVFLSSSSAKEDTTAFHATRSSLETPLVRCTPNNNIVNSELVTTDLIRENLRYN : 662
Mus musculus UCP1 : NRGSEHAGGSLACTTGAVAIVAPTDVVVFLSSSSAKEDTTAFHATRSSLETPLVRCTPNNNIVNSELVTTDLIRENLRYN : 2061
Mus musculus UCP2 : NTRGSEHAGGSLACTTGAVAIVAPTDVVVFLSSSSAKEDTTAFHATRSSLETPLVRCTPNNNIVNSELVTTDLIRENLRYN : 2091
Mus musculus UCP3 : NPRGADHSSAISLACTTGAVAIVAPTDVVVFLSSSSAKEDTTAFHATRSSLETPLVRCTPNNNIVNSELVTTDLIRENLRYN : 2091
Mus musculus UCP3 : RSGRETPASGNSALLMDGAFEGPTENVRCSHHEIREDTTAFHATRSSLETPLVRCTPNNNIVNSELVTTDLIRENLRYN : 2071

              220      *          240      *          260      *          280      *          300
Smithopsis crassicaudata UCP1 : DADILPCHFSAFASFCTVVASPVDVVETRHNSPPCHTSARRCDNHITEGHAFFEGFVSFLELGSNVINFVTEQLRLHSGPTDCATSSL : 170
Monodelphis domestica UCP1 : DADILPCHFSAFASFCTVVASPVDVVETRHNSPPCHTSARRCDNHITEGHAFFEGFVSFLELGSNVINFVTEQLRLHSKPTDCATSSL : 310
Mus musculus UCP1 : DADILPCHFSAFASFCTVVASPVDVVETRHNSALGSRSAGESDNHITEGHAFFEGFVSFLELGSNVINFVTEQLRLHS---AYQSRAPF : 309
Mus musculus UCP2 : FADILPCHFSAFASFCTVVASPVDVVETRHNSALGSRSAGESDNHITEGHAFFEGFVSFLELGSNVINFVTEQLRLHS---QVLRSPF : 308
Mus musculus UCP3 : FADILPCHLSALVAGFCTLLASPVDVVETRHNSLFCHREVSCHNGNTHESAFFEGFVSFLELGSNVINFVTEQLRLHSRPTDCAT--- : 307

```

## Supplement 3

## S3 Bayesian tree of the UCP family



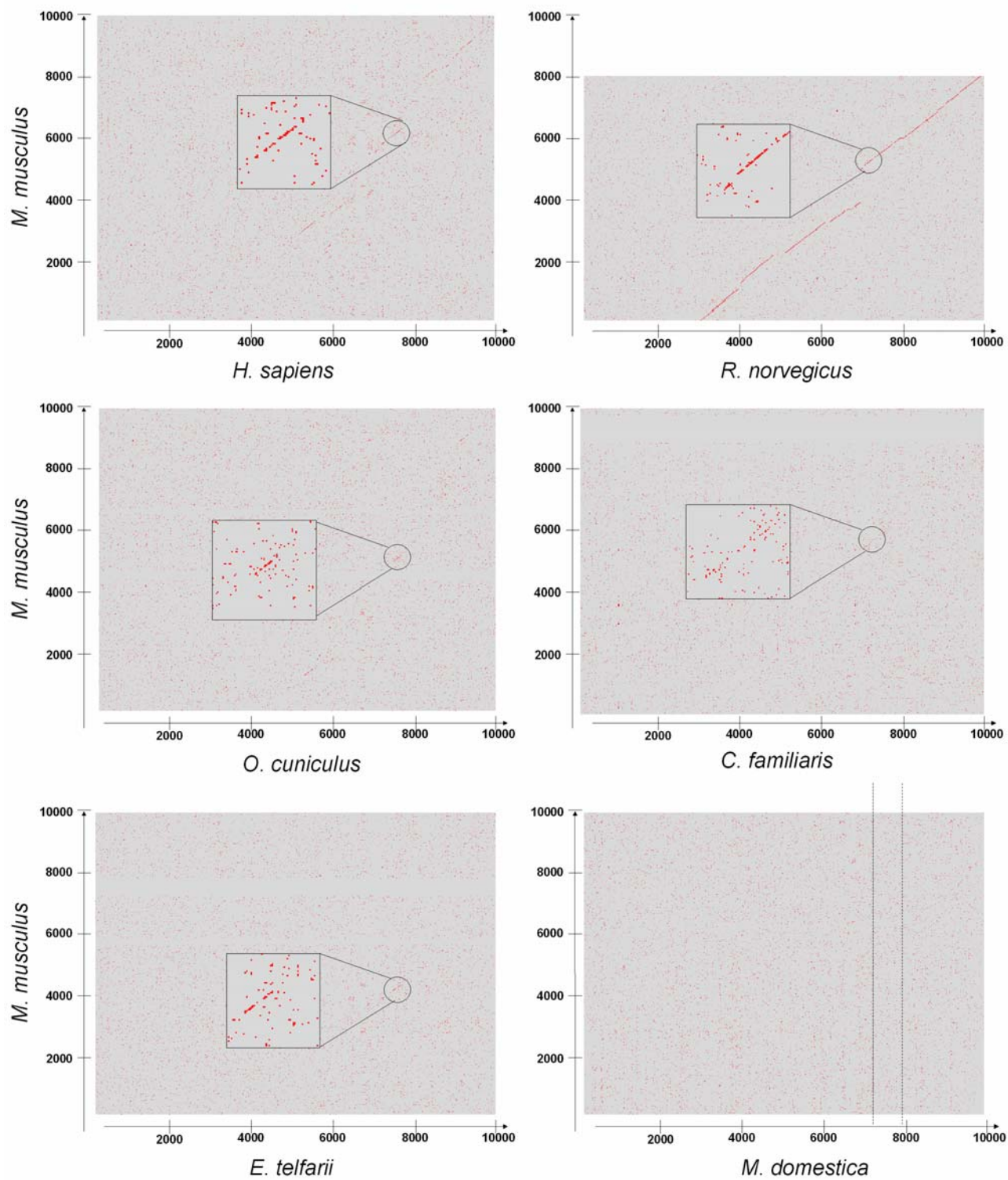
Uncoupling Protein Sequences used for phylogenetic inference

Species	Abbreviation	Common name	UCP1	UCP2	UCP3	UCPX
<i>Anopheles gambiae</i>	Aga	African malaria mosquito				XM_552584
<i>Antechinus flavipes</i>	Afl	yellow-footed Antechinus		AY233003	AY519198.1	
<i>Arabidopsis thaliana</i>	Ath	thale-cress		CAA11757.1		
<i>Bos Taurus</i>	Bta	bovine, domestic Cattle	XP_616977.2	AAI02840.1	AAD33339	
<i>Canis familiaris</i>	Cfa	dog	BAB11684	Q8N2J1	BAA90458	
<i>Ciona intestinalis</i>	Cin	sea squirt				GENSCAN00000088333
<i>Ctenopharyngodon idella</i>	Cid	grass carp		AAX49553.1		
<i>Cyprinus carpio</i>	Cca	common carp	AAS10175.2	Q8W725		
<i>Danio rerio</i>	Dre	zebrafish	ENSDARG00000023151	Q8W720	UCP3a/b identified by Taudien	
<i>Dicrostonyx groenlandicus</i>	Dgr	lemming	AF515781	AY484518		
<i>Echinops telfairi</i>	Ete	lesser hedgehog Tenrec	ENSETEG00000010924			
<i>Erimaceus europaeus</i>	Eeu	hedgehog	ENSEEUG00000005182	ENSEEUT00000007970		
<i>Eupetomena macroura</i>	Ema	swallow-tailed hummingbird			AAK16829	
<i>Felix catus</i>	Fca	cat		Q1LZN3_FELCA	ENSFCAT00000005034	
<i>Fugu rubripes</i>	Fru	pufferfish	Identified by Taudien	SINFRUT000000167188	UCP3a/b identified by Taudien	
<i>Gallus gallus</i>	Gga	chicken			AF287144	
<i>Gasterosteus aculeatus</i>	Gac	stickleback	ENSGACT00000022876	ENSGACT00000026955	ENSGACT00000026952	
<i>Homo sapiens</i>	Has	human	G01858	XP_035029	NP_073714	
<i>Lycopersicon esculentum</i>	Les	tomato				AAL82482
<i>Macaca mulatta</i>	Mac	Rhesus monkey	XP_001090457.1	Q8N1D9_MACMU	Q8N1D8_MACMU	
<i>Meleagris gallopavo</i>	Mga	turkey			AAL28138	
<i>Mesocricetus auratus</i>	Mau	golden hamster	P04575			
<i>Monodelphis domestica</i>	Mdo	oppossum	MS	MS	MS	



Mus musculus	Mmu	Mouse	P12242	AAB17686	P56501	
<i>Myotis lucifugus</i>	Mlu	microbat	ENSMMLUT00000009572	ENSMMLUT00000012109	ENSMMLUT000000012116	
<i>Oncorhynchus mykiss</i>	Omy	rainbow trout		A: ABC00183.1/ B: ABC00185.1		
<i>Ornithorhynchus anatinus</i>	Oan	platypus	ENSOANT000000024079	ENSOANT00000011476		
<i>Oryctolagus cuniculus</i>	Ocu	rabbit	CAA32826	ENSOCUT00000012590	ENSOCUT00000014607	
<i>Otolemur garnettii</i>	Oga	bushbaby	ENSOGAT000000066809	ENSOGAT00000001699	ENSOGAT000000002909	
<i>Pachycara brachycephalum</i>	Pbr	Antarctic eelpout		AAT99593.1		
<i>Pan troglodytes</i>	Ptr	chimpanzee	ENSPTRT000000030801	ENSPTRT000000007559	ENSPTRT000000007561	
<i>Phodopus sungorus</i>	Psu	Djungarian hamster	AAG33983	AAG33984	AAG33985	
<i>Rattus norvegicus</i>	Rno	rat	P04633	AAC98733	P56499	T07783
<i>Solanum tuberosum</i>	Stu	potato				
<i>Spermophilus tridecemlineatus</i>	Str	thirteen-lined ground squirrel		ENNSTOT00000010715		
<i>Suncus murinus</i>	Smu	Asian house shrew	BAE96411.1			
<i>Sus scrofa</i>	Ssc	pig	Extinct	AAD05201	AAD08811	
<i>Tetraodon nigroviridis</i>	Tni	pufferfish	CR640550	Taudien	UCP3a/b identified by Taudien	
<i>Tupaia belangeri</i>	Tbe	treeshrew	ENSTBET000000000042	ENSTBET000000001469		
<i>Xenopus laevis</i>	Xla	African clawed frog	AAH86297.1	AAH44682.1		
<i>Xenopus tropicalis</i>	Xtr	Western clawed frog	ENSXETT000000032640	ENSXETT000000055772	identified by Taudien	
<i>Zoarces viviparus</i>	Zvi	Viviparous blenny		AAT99594.1		

## Supplement 4.1



## Supplement 4.1

```

Ocu : -AAAAGTTTCTTAACTGTT--GGAGGCGAGACGTGGGGTTAGTA-  GTGTGGAACCCATCTTCTTCCCGGTGGTACGTATGAA : 83
Ete : -----TTTAAAGTTTCGGTTCATAAGAAATATAAAGATAAAATA-  SGCTGGAACCTGCTCAACGGCTTGGCAAGTCAAGAA : 81
Hsa : -----GTTTACCTTTT---CAAGAGCGAAGGAGAATTTGTAA-  ATTTCAGAACCTGCTCCACTCCCTTGGCAAGTCAAGAA : 75
Cfa : -AAATGTCGGGTACCTTT---CAAGAGCGAACAAGACTTAAAG-  GAGGCCTA-CCCTGGCCACTCCCTACCTACGTATGGA : 81
Rno : -AAACGCTGATTAACCTCC--AAGGAGAACTAGACACCGGCGG-  GAGTAAACCTGCTCCGCTCCCTTGGCAAGTCAAGAA : 84
Mmu : TAAATGGTGTCTTACCTCT--AAGGAGAACTAGACACCGAGG--  AAGTAAAGCTTCTCTACTCCCTCAAGGTCACAGAA : 82

                                CRE-3
Ocu : *      *      *      *      *
      100      120      140      160
Ocu : A*ACAGCCACCGTTCGCTCAGATGACCTTACCTTACCCG-  CGCCCTGCTCTGAPCCAG---AACAAGAGGTAACTCTGAA : 166
Ete : T*CCAAACACCGTTCGCTCAGCTGACCTTACCTTACCCGCTGGCTTACAGTGCCAPCCA---AGCAAACTTACCTCAAG : 164
Hsa : G*STAGTTCGCGTTCGCTCAGCTTACCTTACCCCTCTGGCTTCT-  CTTTGTGCCAAGAGTAAAGTCTTACCTCTTGG : 161
Cfa : A*GTCTTTACCGCTGCTCCTA-TGACCTCTCTTACCTTG--  GCTTCC---TGGCCCAAGAGCG---TCACTCTCTGG : 157
Rno : G*STACTACCGTTCGCTCAGCTTACCTTACCCCTTCCAGCTT-  CTGCCA---GCATGATCAAGCTTCTGG : 163
Mmu : G*STACTACCGTTCGCTCAGCTTACCTTACCCCTTCCAGCTT-  CTGCCAAGAGCAAACTCAAGCTTCTGG : 164

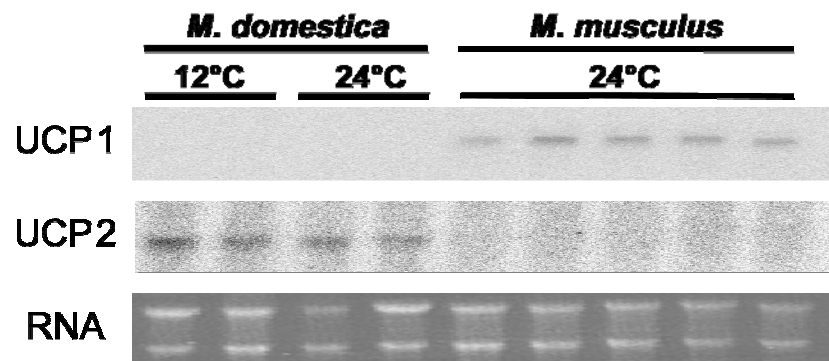
                                PPRE      CRE-2
Ocu : *      *      *      *      *
      180      200      220      240      260
Ocu : -TACGTTCCTCTCCCTACTCTCTCC-  TACTGGAGCAACTTTCTTCCACTTCCAGTCCCTTCCAGAGAGGTGAAAT : 251
Ete : A*TTGCCCTCTCCCTACTCTCTCC-  ACCTGAGCAAACTTTCTTCACTTCTTCCAGCTCTC---GCATGAGAGCA : 248
Hsa : G*ATACCTCTCTCCCTACTCTCTCC-  AACCTGAGCAAACTTTCTTCACTTCCAGAGCTTCCAGAACTGGTGAAGCT : 247
Cfa : G*CCCGCCTCTCTCCCTACTCTCTCC-  GGG-  TACTGGCAAACTTTCTTCACTTCTCCAGCTCCCAAAAGGTGAGCT : 242
Rno : G*ATACGGCTCTCCCTACTCTCTCC-  AGCAAACTTTCTTCACTTCTCCAGAGCTTCCAGAGAGCT : 234
Mmu : G*ATATACCTCTCCCTACTCTCTCC-  TTATGAGCAAACTTTCTTCACTTCTCCAGAGCTTGG-  GCAGCAAGCT : 249

                                TRE      PPRE      NBRE
Ocu : *      *      *
      280      300      320
Ocu : GCTACTCTTGGATCCAGAACCTTTCACAATTTGAA-  T---GAGCC----- : 300
Ete : GCTGCTTCTGCAATCCAGAGCTGTTACAACCTTGT-  CCTATGAC----- : 300
Hsa : GCTGCTCTTGGATCCAGAACCTTTCACAATTTGAA-  TCTGTGACT----- : 300
Cfa : TGGGCTTGGATCCAGAACCTTTCACAATTTGAG-  TCCCGTCCCTCCTC- : 300
Rno : GCTTCTTGGATCCAGAACCTTCTCT-  TTTGCTGACATCAGGGCCCCCTTGAAGT : 300
Mmu : A-  CTTCTTCAATCCAGAACCTTCTCT-  CTTGAGTACATCAGG----- : 300

                                BRE-2

```

## Supplement 5

**Interscapular fat**

**Rapid single step subcloning procedure by combined action of type II and type IIs endonucleases with ligase**

Tobias Fromme\*, Martin Klingenspor

Department of Animal Physiology, Faculty of Biology, Philipps-University, D-35043 Marburg, Germany

\* Corresponding author: Tel. +49(0)6421-2825372, Fax. +49(0)6421-2828937, E-Mail: [fromme@staff.uni-marburg.de](mailto:fromme@staff.uni-marburg.de)

**Abstract**

The subcloning of a DNA fragment from an entry vector into a destination vector is a routinely performed task in molecular biology labs. We here present a novel benchtop procedure to achieve rapid recombination into any destination vector of choice with the sole requirement of an endonuclease recognition site. The method relies on a specifically designed entry vector and the combined action of type II and type IIs endonucleases with ligase. The formulation leads to accumulation of a single stable cloning product representing the desired insert carrying destination vector.

One of the most routinely performed tasks in molecular biology labs around the world undoubtedly is the subcloning of a given DNA fragment from one plasmid vector into a different one. The reasons to do so are as numerous and diverse as are the applied methods. We here describe a further such technique involving the orchestrated action of a type II and a type IIs endonuclease (“outside cutter”) with ligase. This procedure achieves the speed of recombinase based methods without the need for unusual recognition elements in the target vector.

In an example experiment we subcloned a 1167 bp long DNA fragment from an entry vector (modified pGEM-T easy, Promega) into a NheI site of a destination vector (pEGFP-N1, Clontech). The method relies on a specifically engineered entry vector which comprises two key elements flanking the insert to be subcloned (**Figure 1A**). To test our method we accordingly modified the plasmid pGEM-T easy and included a BglII site to be able to insert a DNA fragment between these elements. A blunt end cutting enzyme to Taq-generate T overhangs for TA cloning of PCR products or any other means to insert a fragment of choice are of course feasible as well. Both of the two identical key elements comprise a recognition sequence for a type IIs restriction endonuclease - Esp3I in our case – and a restriction site (**Figure 1B**). The latter one is specifically designed to yield a NheI-compatible single stranded overhang upon digestion with Esp3I. It is essential to design the key element restriction site in a way that the bases directly adjacent to the single stranded overhang are different from those in a NheI recognition site (compare **Figure 1 B** and **C**).

We combined entry vector, destination vector, Esp3I (Fermentas), NheI (Fermentas) and T4 ligase (Promega) in a buffer allowing all three enzyme actions (\*) and incubated at room temperature for 1 hour (**Figure 2**). We transformed 2  $\mu$ l of the resulting solution into DH5 $\alpha$  chemically competent *E. coli* (Invitrogen) and plated on two plates either containing kanamycin or ampicillin. In three independent tests we found between 40 and 73 colonies on the kanamycin plate (indicating pEGFP-N1) and no colonies at all (in two tests) or 10 colonies (in one test) on the ampicillin plate (harbouring pGEM-T easy). Of 10 colonies per kanamycin plate tested for the presence of the subcloned insert in pEGFP-N1 by restriction analysis all proved to be the desired product. Noteworthy the two different resistance markers on entry and destination vector are not necessary for the procedure to function but were used for the sole purpose of easy discrimination between products in our tests. Following this proof of principle the procedure can surely be further optimized.

A limitation of this technique is of course that the entry vector once constructed can only serve to subclone into one selected restriction site. We feel, however, that the speed of this

single-step benchtop procedure makes up for this when routinely cloning PCR products into a variety of destination vectors all containing the same restriction site.

\* Y+/tango-buffer (Fermentas; 33mM Tris acetate, 10mM Mg-acetate, 66mM K-acetate, 0.1 g/L BSA) supplemented with 5 % (w/v) PEG, 10mM DTT and 1mM rATP in a final volume of 10 $\mu$ L. Enzyme amounts: 7.5 units Esp3I, 10 units NheI, 3 weiss units T4 ligase.

### Figure legends

Figure 1 – (A) We cloned this double stranded oligonucleotide into pGEM-T easy to provide two key elements flanking a BglII site. We inserted our PCR amplified fragment into this restriction site. In a future application this step may as well be achieved by TA cloning or other methods. (B) A key element consists of a Esp3I recognition site and a cut site generating a NheI compatible overhang, that is *not* a NheI recognition site. (C) We used NheI as target recognition site in the destination vector.

Figure 2 – The upper box contains the two vectors the reaction starts with, i.e. the entry vector with its two key elements flanking an insert and the destination vector with its NheI recognition site. By the enzymatic action (arrows) of Esp3I and NheI these vectors are linearized to form linear intermediate products as shown in the central box. These intermediates are subject to T4 ligase activity and can be ligated to yield a range of products: the initial vectors (upper box), circular intermediate products (lower box) and the desired product vector. Note that all circular intermediate products are again substrate for Esp3I and thus again linearized. There is a sole stable product in this reaction system, which is the desired product vector.



Figure 1

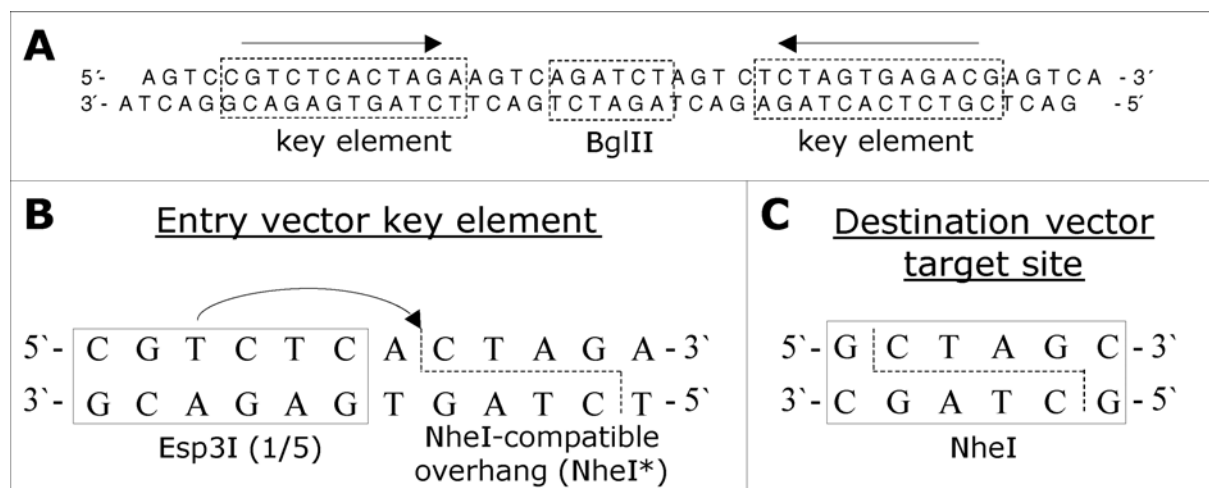
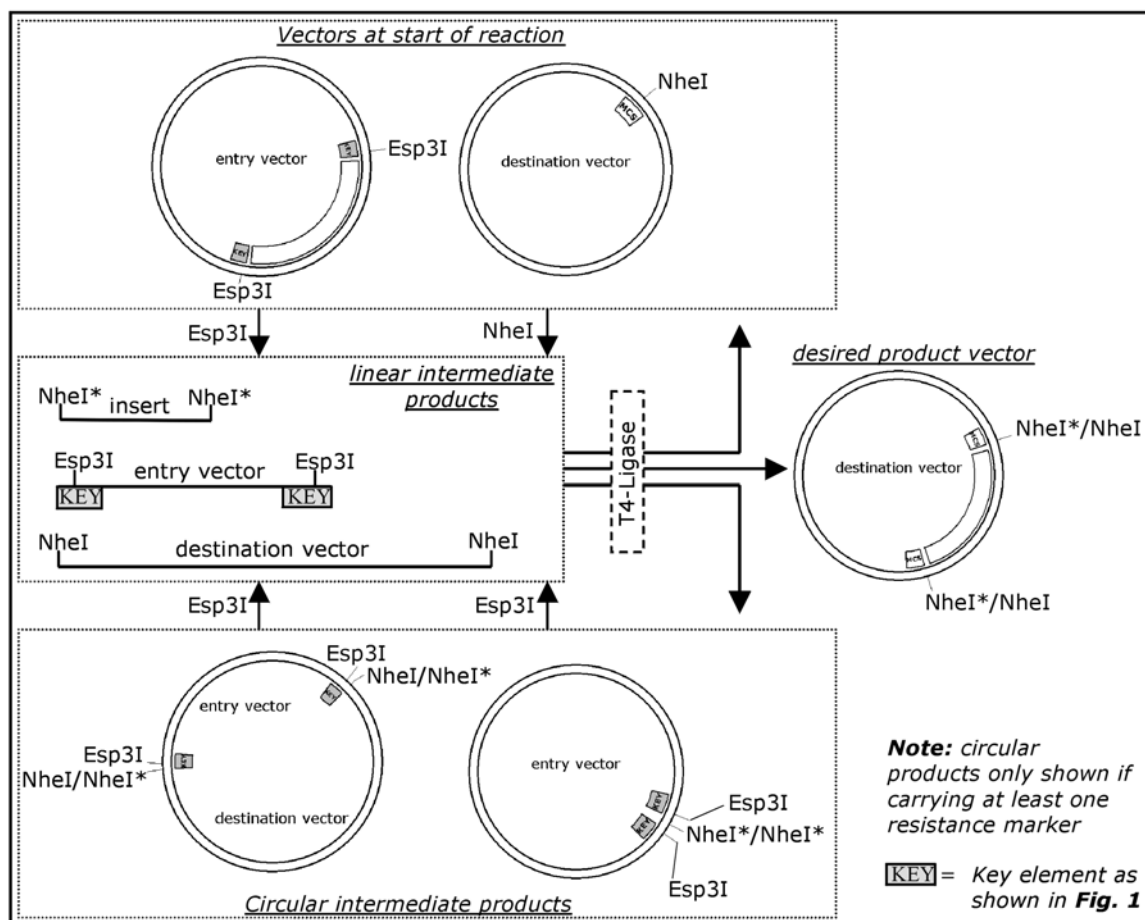


Figure 2





(19)  
Bundesrepublik Deutschland  
Deutsches Patent- und Markenamt

(10) **DE 103 37 407 A1** 2005.03.10

(12)

## Offenlegungsschrift

(21) Aktenzeichen: **103 37 407.8**

(22) Anmeldetag: **13.08.2003**

(43) Offenlegungstag: **10.03.2005**

(51) Int Cl.7: **C12N 15/63**

(71) Anmelder:

**TransMIT Gesellschaft für Technologietransfer  
mbH, 35394 Gießen, DE**

(72) Erfinder:

**Fromme, Tobias, 35039 Marburg, DE; Klingenspor,  
Martin, Dr., 35091 Cölbe, DE**

(56) Für die Beurteilung der Patentfähigkeit in Betracht zu  
ziehende Druckschriften:

**WO 02/0 70 720 A1**

**WO 98/54 336 A1**

**WO 98/33 901 A2**

**WO 92/01 786 A1**

**Szybalski, W., et al.: Class IIS restriction  
enzymes - a review. In: Gene, 1991,  
Vol.100, S.13-26, bes.Fig.5;;**

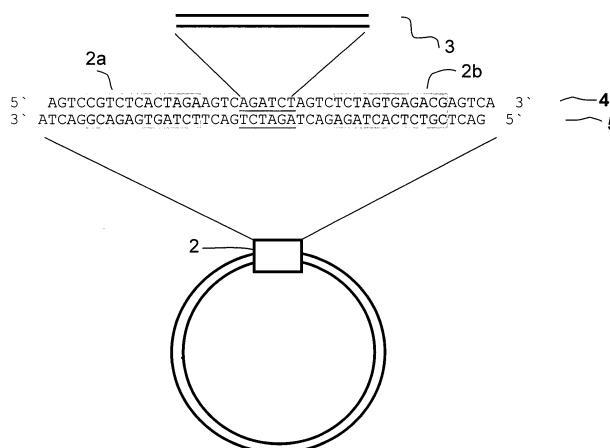
**Die folgenden Angaben sind den vom Anmelder eingereichten Unterlagen entnommen**

Rechercheantrag gemäß § 43 Abs. 1 Satz 1 PatG ist gestellt.

(54) Bezeichnung: **Klonierungssystem**

(57) Zusammenfassung: Die vorliegende Erfindung betrifft ein Verfahren zur Subklonierung eines Nukleinsäure-Fragments von einem Quellvektor in einen beliebigen Zielvektor, wobei die Subklonierung in einem Schritt in Gegenwart von Ligase, Restriktionsenzym und einem outside cutter stattfindet.

Das Verfahren zeichnet sich insgesamt durch kurze Inkubationszeiten aus und wird unabhängig von der Art des Zielvektors, dessen Resistenzmarkern und Zielsequenzen durchgeführt.



### Beschreibung

**[0001]** Die vorliegende Erfindung betrifft ein Verfahren zur effizienten und spezifischen Subklonierung eines Nukleinsäure-Fragmentes von einem Vektor in andere Vektoren.

Stand der Technik

Stand der Forschung

**[0002]** Eine der häufigsten Routinearbeiten in der Molekularbiologie und Gentechnologie ist die Klonierung von Nukleinsäuren (DNA und RNA) und Nukleinsäure-Fragmenten wie z.B. PCR-Produkten in einen geeigneten Vektor bzw. ein Plasmid. Plasmide sind extrachromosomale ringförmige doppelsträngige DNA-Moleküle mit einer Größe von 3 bis 200 kb, die sich unabhängig vom Chromosom der Wirtszelle vermehren können. Sie werden als Vektoren für Klonierung, Vermehrung und Expression beliebiger DNA-Stücke eingesetzt. Man unterscheidet je nach Kopien der Plasmide pro Zelle zwischen low (single)-copy-number Plasmiden mit einer Kopienzahl von 1-2 Kopien pro Zelle, multi-copy-number Plasmiden mit einer Kopienzahl von 10-200 Kopien pro Zelle high-copy-number Plasmiden mit einer Kopienzahl von mehr als 200 Kopien pro Zelle.

**[0003]** Auf dem Weg von der Klonierung eines Nukleinsäure-Fragmentes bis zur Expression von Proteinen im Zielorganismus ist es oft erforderlich, nach der initialen Klonierung des Nukleinsäure-Fragmentes in einen initialen Klonierungsvektor (Quellplasmid) mehrere Subklonierungsschritte durchzuführen und dabei das Nukleinsäure-Fragment in spezialisierte Vektoren (Zielpasmide), je nach Anwendung sogar mehrere verschiedene, zu überführen.

**[0004]** Die prinzipiellen Grundverfahren zum Klonieren sind dem Fachmann seit vielen Jahren bekannt und in Laborstandardwerken, wie Sambrook, Fritsch, Maniatis, 1989, Molecular Cloning, CSH Laboratory Press, Cold Spring Harbour, NY. etc ausführlich beschrieben.

**[0005]** Sie umfassen die Schritte:

- 1) Schneiden der Nukleinsäure mit einem oder mehreren Restriktionsenzymen
- 2) Reinigen der Nukleinsäure-Fragmente z.B. über ein Gelsystem
- 3) Vorbereitung des Vektors durch Linearisieren und Schneiden mit einem oder mehreren Restriktionsenzymen, Behandlung mit alkalischer Phosphatase, Gelaufreinigung
- 4) Ligation des Nukleinsäure-Fragmente in den Vektor
- 5) Transformation in eine Wirtszelle
- 6) Selektion der Zellen
- 7) Isolierung der Nukleinsäure und Restriktionsanalyse

**[0006]** Eine Subklonierung ist erforderlich, wenn z.B. Gen-Experimente in verschiedenen Organismen durchgeführt werden, die Genexpression unterschiedlich reguliert wird oder besondere Antibiotika-Resistenzen, Markierungen oder andere für die Expression vorteilhaften genetischen Zusätze benutzt werden.

**[0007]** Einfache Subklonierungen, bei denen das Nukleinsäure-Fragment klein ist und die Restriktionsstellen mit dem Zielvektor kompatibel sind, können innerhalb von 24 Stunden durchgeführt werden. Andere Subklonierungen erweisen sich als wesentlich aufwändiger und unzuverlässig. Sie können sogar bis zu mehreren Wochen dauern, wenn toxische Gene, lange Nukleinsäure-Fragmente oder nicht kompatible Restriktionsstellen vorliegen.

**[0008]** Für eine erfolgreiche Subklonierung muss das zu klonierende Nukleinsäure-Fragment aus dem Quellplasmid mittels Restriktionsenzymen herausgeschnitten und in einem Gel aufgereinigt werden. Anschließend wird es evtl. mit Enzymen nachbehandelt, um entsprechend kompatible Restriktionsstellen (Zielsequenzen) mit dem Zielvektor herzustellen, falls diese noch nicht vorhanden sind. Das herausgeschnittene Nukleinsäure-Fragment wird in die Zielsequenzen eines linearisierten dephosphorylierten Zielvektors mit DNA-Ligase ligiert. Die DNA-Ligase knüpft dabei zwischen einem Ende des zu klonierenden Nukleinsäure-Fragmentes und einem Ende des Plasmids eine Phosphodiesterbindung.

**[0009]** Dieses Subklonierungssystem mit Restriktionsenzymen und Ligase ist sehr stark beschränkt auf die im Zielvektor vorhandene Art und Anzahl von Restriktionsstellen. So verfügen die derzeit käuflich erwerbenden Plasmide (Bsp. pGem<sup>®</sup>-Plasmide, pSP70-Plasmid, pBR322-Plasmid und pCAT<sup>®</sup>-Plasmide der Firma Promega u.a.) in einer sogenannten multiple cloning site oder in Polylinkern über eine Folge von Restriktionsstellen in

Form von Schnittstellen für verschiedene Restriktionsendonukleasen. Allerdings kommen von den Zielsequenzen für die 150 häufigsten Restriktionsendonukleasen nur etwa 15 Zielsequenzen in den Polylinker-Regionen vor und sind auch dann nicht exklusiv auf diese Region beschränkt, sondern schneiden oft auch an einigen weiteren Stellen im Plasmid. Ebenfalls nachteilig an dieser Art und Weise der Subklonierung ist vor allem der hohe Zeitaufwand.

**[0010]** Eine Verbesserung bei der Klonierung erfolgt durch das Gateway®-Cloning System der Firma Invitrogen (DE 696 23 057 T2), dem das Lambda-Phagen spezifische att-Rekombinationssystem zugrunde liegt. In diesem System ist es erforderlich, die zu klonierende Nukleinsäure mit einer attB-flankierenden Rekombinationsstelle zu versehen, die dann über Rekombination und eine Transferase in attR-Rekombinationsstellen der Zielvektoren kloniert wird.

**[0011]** Nachteil dieser Technik ist die Abhängigkeit vom Vorhandensein entsprechender Rekombinationsstellen in Quell- und Zielplasmid. Oft ist es sogar erforderlich, den gewünschte Zielvektor zuvor dahingehend zu modifizieren, dass er den Ansprüchen genügt.

#### Aufgabenstellung

**[0012]** Aufgabe der vorliegenden Erfindung ist es daher, ein Verfahren zur Subklonierung eines Nukleinsäure-Fragmentes von einem Quellvektor in einen Zielvektor bereitzustellen, dass unabhängig von der Art des Zielvektors, dessen Resistenzmarkern und Zielsequenzen ist und das zeit- und kostensparend durchführbar ist.

#### Lösung der Aufgabe

**[0013]** Diese Aufgabe wird erfindungsgemäß gelöst durch Ansprüche 1-12.

**[0014]** Das erfindungsgemäße Verfahren umfasst die folgenden Schritte:

- a) Bereitstellen eines Quellvektors, der zwei Sequenzabschnitte trägt, die jeweils enthalten, eine Erkennungssequenz für ein outside cutter Restriktionsenzym und angrenzende Nukleotide, die bei Spaltung mit dem outside cutter Restriktionsenzym einen spezifischen Basenüberhang bilden.
- b) Ligation des zu klonierenden Nukleinsäure-Fragmentes in den Quellvektor zwischen die Sequenzabschnitte aus a)
- c) Bereitstellen eines Zielvektors, der mindestens eine Erkennungssequenz für ein spezifisches Restriktionsenzym enthält
- d) Inkubation von Quellvektor und Zielvektor in Gegenwart von outside cutter Restriktionsenzym zur Spaltung der Erkennungssequenzen im Quellvektor, spezifischem Restriktionsenzym zur Spaltung der Erkennungssequenz im Zielvektor und Ligase

**[0015]** Die Vorteile des erfindungsgemäßen Verfahrens liegen darin, dass als einziges Erfordernis zur Subklonierung ein Quellvektor mit zwei Sequenzabschnitten erforderlich ist, die jeweils mindestens eine Erkennungssequenz für ein outside cutter Restriktionsenzym tragen und angrenzende Nukleotide, die bei Spaltung mit dem outside cutter Restriktionsenzym einen spezifischen Basenüberhang bilden. Ein einmal in den Quellvektor ligiertes Nukleinsäure-Fragment kann dann leicht in einem Schritt über die Spaltung mit dem outside cutter Restriktionsenzym aus dem Quellplasmid herausgeschnitten werden und in jeden beliebigen Zielvektor ligiert werden. Das Verfahren zeichnet sich daher insgesamt durch sehr kurze Inkubationszeiten aus und wird unabhängig von der Art des Zielvektors, dessen Resistenzmarkern und Zielsequenzen in einem einzigen Schritt durchgeführt.

**[0016]** Überraschenderweise wurde gefunden, dass Restriktionsendonukleasen, die als sogenannte outside cutter oder TypIIS-Restriktionsenzyme beschrieben sind, sehr gut für ein Subklonierungssystem geeignet sind. Die Erkennungssequenz der outside cutter besteht in der Regel aus 4-8 Basenpaaren, die nicht symmetrisch sind und kein Palindrom darstellen. Charakteristisch ist, dass Schnittstelle und Erkennungsstelle nicht identisch sind, sondern häufig die Schnittstelle in einer definierten Entfernung zur Erkennungssequenz liegt.

**[0017]** Bekannt ist das outside cutter Restriktionsenzym AarL mit der Erkennungssequenz:

5' CACCTGC NNNN NNN 3'

3' GTGGACG NNNNNNNN NNN 5'

wobei die Schnittstelle zwischen der vierten und fünften beliebigen Base (N), die in 5' → 3' Richtung auf die Erkennungssequenz CACCTGC folgt, bzw. der achten und neunten beliebigen Base (N), die in 3' → 5' Richtung

auf die Erkennungssequenz GTGGACG folgt, liegt.

**[0018]** Erfindungsgemäß trägt der Quellvektor im Abstand von 5-20 Basen zum zu klonierenden Insert zwei Sequenzabschnitte mit jeweils einer Erkennungssequenz für ein outside cutter Restriktionsenzym und dazu benachbart Nukleotide, die bei Spaltung mit dem outside cutter Restriktionsenzym einen spezifischen Basenüberhang erzeugen, der kompatibel zu einem spezifischen Basenüberhang im Zielvektor ist. So erzeugt beispielsweise erfindungsgemäß die Spaltung des outside cutter Esp3I durch die Auswahl der Nukleotide einen NheI-kompatiblen Überhang. Alternativ wird die Auswahl der Nukleotide so gestaltet, dass durch Spaltung mit dem outside cutter Restriktionsenzym jeder beliebige Überhang entsteht, der kompatibel zu einer beliebigen Schnittstelle wie beispielsweise EcoRI, BamHI oder ApaI ist. Entscheidend ist: Esp3I schneidet immer einen Überhang von 4 Basen in einem definierten Abstand zu seiner Erkennungs-Stelle. Daher ist Esp3I geeignet, wenn das Restriktionsenzym, das im Zielvektor schneidet auch einen 4-Basen-Überhang schneidet, wie es für die meisten gängigen Enzyme zutrifft.

**[0019]** Andere Beispiele für Restriktionsenzyme, die als outside cutter außerhalb der Erkennungssequenz spalten sind AclII, AclI, BaeI, Bbr7I, BbvI, BbvII, BccI, Bce83I, BceAI, Bcefl, Bcgl, BciVI, Bfil, BinI, BpII, BsaXI, BscAI, BseMII, BseRI, BsgI, Bsml, BsmAI, BsmFI, Bsp24I, BspCNI, BspMI, Bsrl, BsrDI, BstF5I, BtsI, CjeI, CjePI, EciI, Eco31I, Eco57I, Eco57MI, Esp3I, Fall, Faul, FokI, Gsul, HaeIV, Hgal, Hin4I, HphI, HpyAV, Ksp632I, MbolI, MlyI, Mmel, MnlI, PleI, Ppil, PslI, RleAI, SapI, SfaNI, SspD5I, Sth132I, StsI, TaqII, TspDTI, TspGWI, Tth111II deren Erkennungssequenzen aus <http://rebase.neb.com/cgi-bin/outsidelist> bekannt sind.

**[0020]** Alle outside cutter Restriktionsenzyme zeichnen sich durch eine charakteristische Anzahl an Nucleotiden aus, die als Überhang nach der Spaltung entstehen. Die Länge des Überhanges variiert im Durchschnitt zwischen 1-10 Nucleotide. Durch Auswahl eines bestimmten outside cutter Restriktionsenzymes ist das Klonierungssystem für die Nutzung von verschiedenen Erkennungsstellungen für Restriktionsenzymen im Zielvektor, die nach Spaltung einen entsprechend langen oder kurzen Überhang erzeugen, geeignet.

**[0021]** Die Verwendung eines outside cutter Restriktionsenzymes ist besonders vorteilhaft, da beim Schneiden eines Nucleinsäure-Fragmentes mit einem outside cutter die Erkennungsstelle des outside cutter Restriktionsenzymes selbst erhalten bleibt, während die Erkennungssequenzen beim Schneiden mit anderen Restriktionsenzymen zerstört werden und nicht mehr genutzt werden können.

**[0022]** Die nachfolgende Abbildung erläutert den Erfindungsgegenstand:

**[0023]** Fig. 1 zeigt in einer schematischen Darstellung die Modifikation des pGEMTeasy-Vektors zum Quellvektor (1) für die Subklonierung. Dazu werden die Oligonukleotide Oligo 1: AGTCCGTCTCACTAGAAAGT-CAGATCTAGTCTCTAGTGAGACGAGTCA (4) und Oligo 2: GACTCGTCTCACTAGAGACTAGATCT-GACTTCTAGTGAGACGGACTA (5) zu doppelsträngigen DNA-Molekülen zusammengefügt. Diese werden in den TA-Vektor pGEM-Teasy der Firma Promega an Position 60 ligiert über die am 3'-Ende überhängenden Adenosin-Nucleotide. Zentral liegt die Erkennungssequenz für ein Restriktionsenzym, hier beispielsweise die unterstrichen eingezeichnete Bgl II-Schnittstelle, in die ein beliebiges vorzugsweise doppelsträngiges Nucleinsäure-Fragment (3), hier beispielsweise ein 1167 Bp langes DNA-Fragment inkloniert wird. Die grau hinterlegten in fettgeschriebenen Buchstaben markierten Nucleotide zeigen die beiden Erkennungsstellen (2b) rechts und (2a) links für das outside cutter Restriktionsenzym Esp3I der restliche graue Bereich markiert dessen Schnittstelle, die unterstrichenen Nucleotide im zentralen Bereich zeigen die Erkennungsstelle für das Restriktionsenzym Bgl II.

**[0024]** Alternativ zur Schnittstelle für ein Restriktionsenzym liegt der Vektor linearisiert vor, trägt MonoT-Überhänge und wird für TA-Cloning vorbereitet (nicht dargestellt).

**[0025]** Die zu den Erkennungsstellen für das outside-cutter Restriktionsenzym Esp3I benachbarten Sequenzabschnitte sind so gewählt, dass bei Einsatz des outside-cutters Esp3I ein spezifischer Überhang entsteht, der kompatibel ist mit der Zielschnittstelle des Restriktionsenzym NheI im Zielvektor, jedoch in angrenzenden Basen differiert.

**[0026]** Fig. 2 zeigt in einer schematischen Darstellung das erfindungsgemäße Subklonierungsverfahren, wobei das Nucleinsäure-Fragment (3) aus dem Quellvektor (1) in den Zielvektor (6) überführt wird. Der Quellvektor (1), der das zu klonierende Nucleinsäure-Fragment (3) beinhaltet, wird mit dem outside cutter Esp3I gespalten, wobei die Produkte a und b entstehen.

**[0027]** Produkt a stellt den linearisierten Quellvektor mit den beiden Erkennungsstellen (**2b**) rechts und (**2a**) links für das outside cutter Restriktionsenzym Esp3I und den durch die Spaltung entstandenen 5' überhängenden Enden dar.

**[0028]** Produkt b stellt das herausgeschnittene Nukleinsäure-Fragment (**3**) dar. Der Grossbuchstabe T zeigt auf beiden Seiten den Beginn des doppelsträngigen Bereiches. Die kleinen Buchstaben markieren die entstehenden Nukleotide des Überhanges. Sie bilden reguläre NheI-Überhänge. Durch Zugabe des Zielvektors (**6**), spezifischem restriktionsenzym NheI und Ligase wird der Zielvektor linearisiert (Produkt c) und das zu klonierende Nukleinsäure-Fragment wird mittels Ligase zu einem zirkulären Plasmid verbunden. Da sich die Enzyme NheI und outside cutter Esp3I noch immer im Reaktionsgemisch befinden, werden Nebenprodukte, die „falsch“ ligiert wurden wieder geschnitten, nicht aber das Zielplasmid (**6**) mit dem darin enthaltenen Nukleinsäure-Fragment (**3**) (Produkt d).

**[0029]** Erfindungsgemäß enthält der Quellvektor (**1**), in dem sich das zu klonierende Nukleinsäure-Fragment (**3**) befindet, unmittelbar dazu benachbart kurze Sequenzabschnitte (**2a** und **2b**), welche die Zielsequenz für ein outside cutter Restriktionsenzym tragen. Die benachbarten Abschnitte sind in ihrer Nukleotidabfolge derart gewählt, dass bei Einsatz eines bestimmten outside-cutter Restriktionsenzymes ein bestimmter Überhang entsteht, der kompatibel ist mit der durch ein spezifisches Restriktionsenzym entstandenen Zielschnittstelle im Zielvektor (**6**), jedoch in angrenzenden Basen differiert. Gibt man in geeignetem Puffer Quell- und Zielvektor zusammen mit Ligase, outside cutter-Restriktionsenzym und einem spezifischen Restriktionsenzym für die Zielschnittstelle im Zielvektor, entstehen durch Restriktion mehrere Fragmente (**Fig. 2a, b** und **c**). Diese können prinzipiell von der Ligase kombiniert werden, so dass mehrere Produkte entstehen. Alle diese Produkte sind jedoch von den beiden Restriktionsenzymen wieder schneidbar mit einer Ausnahme: das zu klonierende Nukleinsäure-Fragment plus Zielvektor (**d**) ist als einziges stabil.

**[0030]** Beispielhaft zeigt **Fig. 1** die Klonierung eines 1167 bp großen Nukleinsäure-Fragmentes (**3**) in einen Bereich des Quellvektors (**1**), der eine zentrale Schnittstelle für ein Restriktionsenzym, beispielsweise Bgl II, aufweist (unterstrichene Sequenz in **Fig. 1**) mit daran flankierenden Erkennungssequenzen (**2a** und **2b**) für ein outside-cutter Restriktionsenzym, beispielsweise Esp3I, die so zueinander angeordnet sind, dass die Schnittstelle des outside cutter Restriktionsenzymes dem zu klonierenden Nukleinsäure-Fragment zugewandt ist. Die Erkennungssequenzen (**2a** und **2b**) weisen flankierende Bereiche auf, die durch Hybridisierung der Oligonukleotide **4** und **5** und deren Einklonierung erzeugt werden. **Fig. 2** zeigt den Vorgang der Subklonierung des 1167 bp großen Nukleinsäure-Fragmentes (**3**) aus dem Quellvektor (**1**) in einen Zielvektor (**6**), der in der Multiple cloning site eine Erkennungssequenz für ein spezifisches Restriktionsenzym, beispielsweise NheI aufweist. In Puffer führt die Zugabe von Ligase, outside cutter-Restriktionsenzym Esp3I und dem Restriktionsenzym NheI zu mehreren Fragmenten: linearisierter Quellvektor mit NheI\*-Überhängen (**Fig. 2** Fragment a), ausgeschnittenes Nukleinsäure-Fragment (**3**) mit kompatiblen NheI\*-Überhängen (**Fig. 2** Fragment b) und linearisierter Zielvektor (**6**) mit NheI-Überhängen (**Fig. 2** Fragment c). Mit NheI\* werden hierbei die vom outside cutter Restriktionsenzym generierten NheI-kompatiblen Überhänge bezeichnet. Mit NheI ohne Stern werden dagegen die „echten“ von dem Restriktionsenzym NheI erzeugten Überhänge bezeichnet.

**[0031]** Fragment c in **Fig. 2** (linearisierter Zielvektor) besitzt einfache „NheI“-Überhänge, Fragment a (linearisierter Quellvektor) trägt NheI\*-Überhänge, Fragment b (zu klonierendes Nukleinsäure-Fragment) hat ebenfalls NheI\*-Überhänge. Die Sequenzen ergeben sich wie folgt: NheI\* = 3'-Tgatc-5', davon ist mit das großen Buchstaben geschriebene T noch im doppelsträngigen Bereich das mit kleinen Buchstaben geschriebene gatc das überhängende 5'-Ende; NheI = CGATC, davon stellen die mit kleinen Buchstaben geschriebenen Nukleotide gatc das überhängendes 5'-Ende dar.

**[0032]** Falsche Kombinationen mit dem Quellvektor (**1**) NheI/NheI\*, NheI\*/NheI\* werden vom outside cutter-Restriktionsenzym Esp3I wieder geschnitten, jede Kombination aus zwei NheI-Überhängen ergibt eine neue NheI-Stelle und wird entsprechend erneut durch NheI geschnitten.

**[0033]** Das einzig stabile Erzeugnis ist das Produkt d, die Kombination eines NheI-Überhanges aus dem Zielvektor (**6**) mit dem NheI\*-Überhang des zu klonierenden Nukleinsäure-Fragmentes, das aus der Spaltung mit dem outside-cutter Restriktionsenzym Esp3I entstanden ist und eine „falsche“ flankierende Base trägt, ein T anstelle eines C bzw. auf dem Gegenstrang A statt G.

**[0034]** Nach Inkubation bei Raumtemperatur, anschließender Transformation in Zielzellen und Anzucht der Zielzellen erhält man fast ausschließlich Klone, die das zu klonierende Nukleinsäure-Fragment im Zielplasmid tragen.

**[0035]** Das erfindungsgemäße Verfahren ist nicht auf ein procaryotisches Quellplasmid (1) beschränkt, es ist auch auf eucaryotische z.B. Hefepasmide, Cosmide und auf Phagemide anwendbar, auf low- und high-copy-Plasmide.

**[0036]** Dies gilt auch für die Auswahl des Zielvektors (6). Es werden alle gängigen Vektoren, die beispielsweise ein Selektionsgen (z.B. Antibiotikum-Resistenz-Gen), ein Markergen (z.B. lacZ-Gen zur Farbunterscheidung von Vektoren mit und ohne Insert), origin of replication, Promotorregion, multiple cloning site und/oder Elemente für die Expression fremder Proteine enthalten, verwendet.

**[0037]** Der Puffer, in dem die Subklonierungsreaktion abläuft, ist vorteilhafterweise so gewählt, dass sowohl das outside cutter Restriktionsenzym als auch das spezifische Restriktionsenzym darin biologisch wirksam sind. Allerdings ist es zulässig, nach der „double digest“-Empfehlung von z.B. New England Biolabs vorzugehen und bei einer beispielsweise nur 50%igen Aktivität des einen Enzyms im Puffer des anderen mit dem Einsatz der doppelten Enzymunits zu arbeiten.

**[0038]** Als outside-cutter Restriktionsenzyme werden sämtliche bekannten Enzyme verwendet, die außer an den beiden gewünschten Sequenzabschnitten nicht an weiteren Stellen in Quell- oder Zielplasmid und nicht im zu klonierenden Nukleinsäure-Fragment schneiden.

**[0039]** Es werden mit dem erfindungsgemäßen Verfahren Nukleinsäure-Fragmente einer Größe von ca. 20 bp bis zu 20 kb kloniert.

**[0040]** Eine Ausführungsform der Erfindung betrifft einen Kit zur Subklonierung eines Nukleinsäure-Fragmentes in einen beliebigen Zielvektor, mindestens enthaltend

- a) Quellvektor mit wenigstens zwei Sequenzabschnitten, die jeweils enthalten Erkennungssequenzen für ein outside cutter Restriktionsenzym und angrenzende Nukleotide, wobei die Nukleotide bei Spaltung mit dem outside cutter Restriktionsenzym einen Basenüberhang bilden.
- b) Ligase
- c) ein oder mehrere spezifische Restriktionsenzyme
- d) mindestens ein outside cutter Restriktionsenzym
- e) geeignete Reaktionspuffer für die in a) bis d) genannten Vektoren und Enzyme

**[0041]** Auf Grund der Lehre der vorliegenden Erfindung sowie auf Grund des allgemeinen Fachwissens in diesem technischen Gebiet ist dem Hersteller des erfindungsgemäßen Kits bekannt, wie er die einzelnen Komponenten des Kits, z.B. die Puffer herstellt, formuliert und lagert. Der Kit kann, falls es für die Kundenfreundlichkeit gewünscht wird, auch einen bereits linearisierten Quellvektor enthalten. Die Auswahl der im Kit enthaltenen Restriktionsenzyme hängt davon ab, welche Erkennungssequenzen für Restriktionsenzyme im Zielvektor vorhanden sind.

Ausführungsbeispiel

Ausführungsbeispiele

Subklonierung eines Nukleinsäure-Fragmentes mit dem outside cutter Esp3I

**[0042]** Beispielsweise handelt es sich um die Subklonierung einer 1167 bp große Promotorsequenz des UCP3-Gens von *Phodopus sungorus* aus einem modifizierten pGEMTeasy-Vektor (Firma Promega) mit dem outside-cutter Esp3I in die Zielschnittstelle NheI in der Multiple cloning site des Vektors pEGFP-N1 (Firma Clontech).

**[0043]** Als Ausgangsmaterial zur Herstellung des Quellvektors wird beispielsweise der pGEMTeasy-Vektor der Firma Promega verwendet und so verändert, dass er in seinem Polylinker kurze Sequenzabschnitte trägt, welche die Zielsequenz für ein outside cutter Restriktionsenzym enthalten und dazu benachbarte Sequenzabschnitte, die derart gewählt sind, dass bei Einsatz des outside-cutters Esp3I ein Überhang entsteht, der kompatibel ist mit der Zielschnittstelle im Zielvektor, jedoch in angrenzenden Basen differiert.

**[0044]** Dazu werden die komplementären Oligonukleotide verwendet



5' AGTCC**CGTCTC**ACTAGAAAGTCAGATCTAGTCTCTAGT**GAGACG**AGTCA 3'

Bgl II

3' ATCAG**GCAGAGT**GATCTT**CAGTCT**AGATCAGAGATCA**CTCTGC**TCAG 5'

Bgl II

**[0045]** Die grau hinterlegten in fetten Buchstaben markierten Nukleotide zeigen die Erkennungsstelle für das outside cutter Restriktionsenzym Esp3I der restliche graue Bereich markiert dessen Schnittstelle, die unterstrichenen Nukleotide im zentralen Bereich zeigen die Erkennungsstelle für das Restriktionsenzym Bgl II.

**[0046]** Durch Erhitzen und langsames Abkühlen werden die Oligonukleotide Oligo 1 und Oligo 2 zu doppelsträngigen DNA-Molekülen zusammengefügt. An beiden 3'-Enden entsteht ein überhängendes Adenosin-Nukleotid, mit dessen Hilfe das doppelsträngige DNA-Molekül nach Standardvorgaben in den bereits linear mit überhängenden T's vorliegenden pGEMTeasy-Vektor der Firma Promega kloniert wird. Die unterstrichen markierte zentrale Bgl II-Schnittstelle des doppelsträngiges DNA-Moleküls wird genutzt, um ein beliebiges Nucleinsäure-Fragment beispielsweise ein 1167 Basenpaare langes DNA-Fragment, beispielsweise ein UCP3-Promoter-Fragment, nach Standardverfahren einzuklonieren. Dieses Produkt wird im folgenden „Quellvektor“ genannt. Als „Zielvektor“ wird beispielsweise der pEGFP-N1 der Fa. Clontech verwendet. Dieser trägt eine Kanamycinresistenz, während pGEM-T easy das beta-Lactamase-Gen (Amp<sup>r</sup>) als Selektionsmarker trägt. Es ist allerdings nicht unbedingt erforderlich, dass beide Vektoren unterschiedliche Resistenzen haben, es können auch Quell- und Zielvektoren mit jeweils gleichen Resistenzen verwendet werden.

**[0047]** Als outside-cutter Restriktionsenzym wird beispielsweise Esp3I der Fa. MBI Fermentas genutzt, spezifisches Restriktionsenzym für die multiple cloning site des Zielvektors ist beispielsweise NheI (MBI Fermentas). Als Reaktionspuffer wird beispielsweise der Puffer „y+/tango“ (MBI Fermentas) entsprechend den Herstellerangaben verwendet.

**[0048]** Durch die Spaltung mit dem outside cutter entsteht ein für ein spezifisches Restriktionsenzym kompatibler Überhang (mit\* markiert), der zum Klonieren in den Zielvektor, welcher Erkennungssequenzen für NheI aufweist, genutzt wird.

**[0049]** So erzeugt beispielsweise die Spaltung mit Esp3I einen NheI-kompatiblen Überhang (NheI\*).

5' AGTCCGTCTCA | CTAG AAGTCAGATCTAGTCTCTAGTGAGACGAGTCA 3'  
 3' ATCAGGCAGAGT | GATC TTCAGTCTAGATCAGAGATCACTCTGCTCAG 5'

NheI-

kompatibler Überhang (NheI\*)

**[0050]** Die Reaktionszusammensetzung zur Subklonierung ist so gewählt, dass folgende Verhältnisse entstehen:

Komponente	Volumen	Endkonzentration	
Quellvektor 1µg/µl	1,0 µl	100 ng/µl	
Zielvektor 1 µg/µl	1,0 µl	100 ng/µl	
10xPuffer Y+/tango	1,0 µl	33 mM TrisAc, 10 mM MgAc, 66mM Kac, 0,1 mg/ml BSA	
PEG 6000, 40% w/v	1,25 µl	5% w/v	
DTT 100 mM	1,0 µl	10 mM	
rATP, 10 mM	1,0 µl	1 mM	
NheI, 10 U/µl	1,0 µl	1 U/µl	MBI Fermentas
Esp3I, 10 U/µl	0,75 µl	0,75 U/µl	MBI Fermentas
T4-Ligase, 3 WeissU/µl	1,0 µl	0,3 U/µl	Promega
H <sub>2</sub> O	1,0 µl		
<b>Summe</b>	<b>10 µl</b>		

**[0051]** Die Reaktion wird durch die chemischen Additiva wie Dithiotreitol (DTT) und/oder Polyethylenglycol (PEG) optimiert.

**[0052]** Der Reaktionsansatz wird bei Raumtemperatur (23°C–25°C) inkubiert und anschliessend transformiert. Alternativ wird der Reaktionsansatz zur Inaktivierung der Enzyme vor der Transformation für 30 Minuten auf 65°C erhitzt. Die Transformation erfolgt in kompetente E. coli Zellen, beispielsweise DH5alpha (Firma Invitrogen). 50 µl kompetente E. coli DH5alpha (Transformationseffizienz  $2 \cdot 10^6$  cfu/µg) werden mit 2 µl des beschriebenen Ansatzes nach einer Standardmethode transformiert: 20 Minuten auf Eis, 55 Sekunden 42°C, 2 Minuten auf Eis, +950 µl SOC-Medium, 90 Minuten bei 37°C. Jeweils die Hälfte des Transformationsansatzes wird auf LB-Agarplatten mit Ampicillin bzw. Kanamycin plattiert.

**[0053]** Die Klone werden isoliert, und nach Übernachtskultur wird mit Standardmethoden eine Plasmidpräparation und analytische Restriktionen durchgeführt. Bei allen Plasmiden handelt es sich um das pEGFP-N1 Zielplasmid mit dem 1167 bp großen Nukleinsäure-Fragment in der NheI-site der multiple cloning site.

**[0054]** Die Inkubationszeiten sind so gewählt, dass keine Nebenprodukte, sondern nur das einzig stabile Produkt akkumuliert vorliegt.

**[0055]** Der Fachmann kennt viele Entsprechungen oder kann diese mit Hilfe üblicher Experimente zu den spezifischen Anwendungen der hier beschriebenen Erfindung feststellen. Solche Entsprechungen liegen beabsichtigerweise im Rahmen der Ansprüche.

#### Bezugszeichenliste

- 1 Quellvektor
- 2 Erkennungssequenz für Restriktionsenzyme/  
multiple cloning site/Polylinker
- 3 Nukleinsäure-Fragment
- 4 Oligonukleotid 1
- 5 Oligonukleotid 2
- 6 Zielvektor

**Patentansprüche**

1. Verfahren zur Subklonierung eines Nukleinsäure-Fragmentes, umfassend die folgenden Schritte
  - a) Bereitstellen eines Quellvektors, der zwei Sequenzabschnitte trägt, die jeweils enthalten, eine Erkennungssequenz für ein outside cutter Restriktionsenzym und angrenzende Nukleotide, die bei Spaltung mit dem outside cutter Restriktionsenzym einen spezifischen Basenüberhang bilden.
  - b) Ligation des zu klonierenden Nukleinsäure-Fragmentes in den Quellvektor zwischen die Sequenzabschnitte aus a)
  - c) Bereitstellen eines Zielvektors, der mindestens eine Erkennungssequenz für ein spezifisches Restriktionsenzym enthält
  - d) Inkubation von Quellvektor und Zielvektor in Gegenwart von outside cutter Restriktionsenzym zur Spaltung der Erkennungssequenzen im Quellvektor, spezifischem Restriktionsenzym zur Spaltung der Erkennungssequenz im Zielvektor und Ligase
2. Verfahren gemäß Anspruch 1, dadurch gekennzeichnet, dass das Quellplasmid ausgewählt ist aus der Gruppe der procaryotischen oder eucaryotischen Plasmide, ein Hefepiasmid, Cosmid oder Phagemid sowie ein low- oder high-copy-Plasmid ist.
3. Verfahren gemäß Anspruch 1 und 2, dadurch gekennzeichnet, dass der Quellvektor linear oder zirkulär vorliegt.
4. Verfahren gemäß Anspruch 1, dadurch gekennzeichnet, dass das Zielplasmid ausgewählt ist aus der Gruppe der procaryotischen oder eucaryotischen Plasmide, ein Hefepiasmid, Cosmid oder Phagemid sowie ein low- oder high-copy-Plasmid ist.
5. Verfahren gemäß einem der vorangegangenen Ansprüche, dadurch gekennzeichnet, dass das zu klonierende Nukleinsäure-Fragment eine Größe von 20 bp bis 20 kbp besitzt.
6. Verfahren gemäß einem der vorangegangenen Ansprüche, dadurch gekennzeichnet, dass die Subklonierung während der Inkubation von Quellvektor, Zielvektor, outside cutter Restriktionsenzym, spezifischem Restriktionsenzym und Ligase innerhalb von 10 Minuten bis 2 Stunden vorzugsweise 30 bis 60 Minuten erfolgt.
7. Verfahren gemäß einem der vorangegangenen Ansprüche, dadurch gekennzeichnet, dass die Subklonierung bei einer Reaktionstemperatur von 4°C bis 37°C, vorzugsweise bei 25°C erfolgt.
8. Verfahren gemäß einem der vorangegangenen Ansprüche, dadurch gekennzeichnet, dass die Reaktionsbedingung für die Subklonierung durch chemische Additiva optimiert ist.
9. Verfahren gemäß einem der vorangegangenen Ansprüche, dadurch gekennzeichnet, dass die chemischen Additiva Dithiothreitol (DTT) und/oder Polyethylenglycol (PEG) sind.
10. Kit zur Subklonierung eines Nukleinsäure-Fragmentes in einen beliebigen Zielvektor, mindestens enthaltend
  - a) Quellvektor mit wenigstens zwei Sequenzabschnitten die jeweils enthalten Erkennungssequenzen für ein outside cutter Restriktionsenzym und angrenzende Nukleotide, die bei Spaltung mit dem outside cutter Restriktionsenzym einen Basenüberhang bilden
  - b) Ligase
  - c) ein oder mehrere spezifische Restriktionsenzyme
  - d) mindestens ein outside cutter Restriktionsenzym
  - e) geeignete Reaktionspuffer für die in a) bis d) genannten Vektoren und Enzyme
11. Kit gemäß Anspruch 10, dadurch gekennzeichnet, dass der Quellvektor ausgewählt ist aus der Gruppe der procaryotischen oder eucaryotischen Plasmide, ein Hefepiasmid, Cosmid oder Phagemid sowie ein low- oder high-copy-Plasmid ist.
12. Kit gemäß Anspruch 10, dadurch gekennzeichnet, dass der Quellvektor linear oder zirkulär vorliegt.

Es folgen 2 Blatt Zeichnungen

## Anhängende Zeichnungen

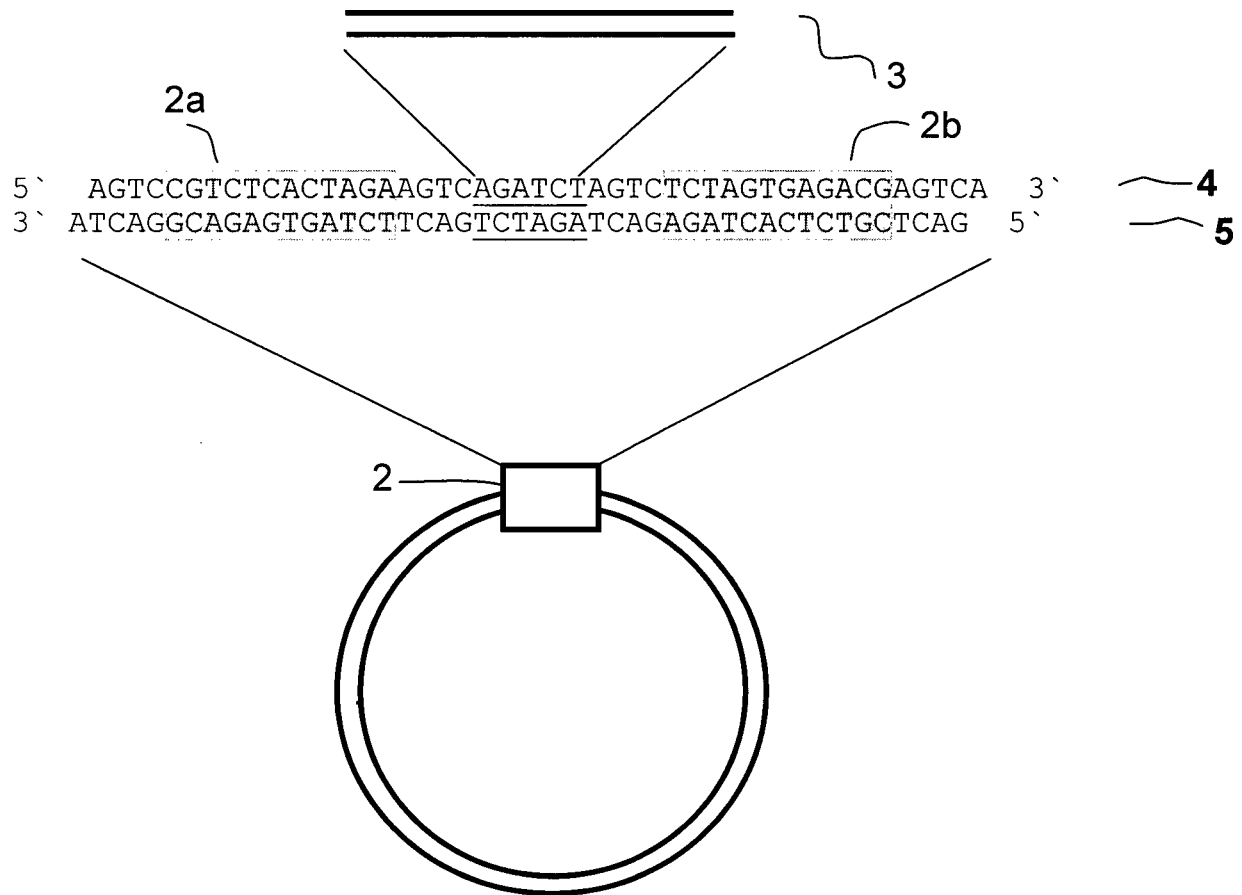


Fig. 1

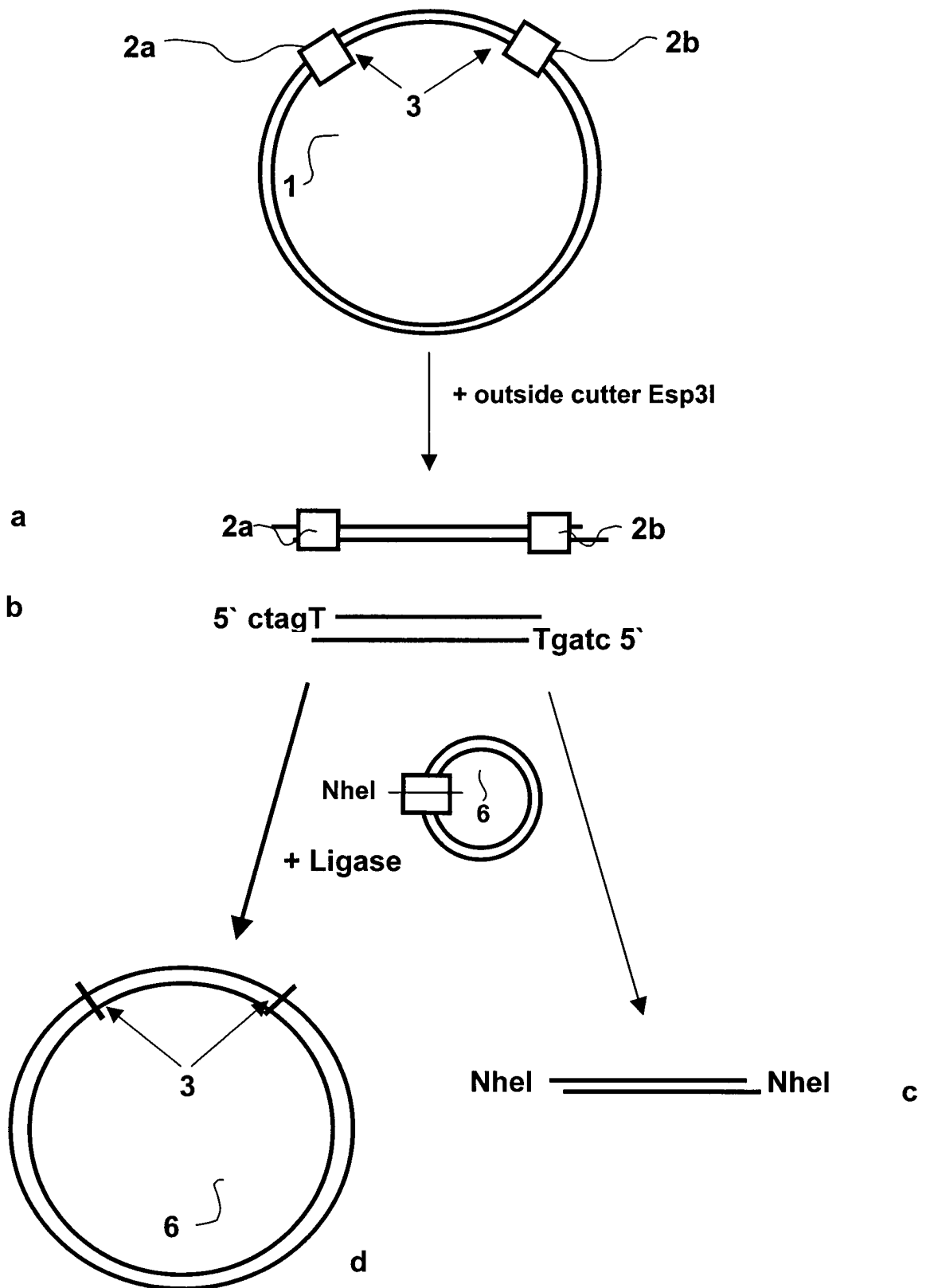


Fig. 2

## Zusammenfassung

Das Entkopplerprotein 3 (*Ucp3*) wird im Braunen Fettgewebe (BAT) und in der Skelettmuskulatur exprimiert und führt dort eine bisher nicht eindeutig belegte Funktion aus. In dieser Arbeit wurde versucht, sich der Funktion des Genprodukts über die Regulation der Transkription des Gens zu nähern.

In einer computergestützten Analyse des *Ucp3* Promotors wurde ein phylogenetisch konserviertes Sequenzelement identifiziert, das den Transkriptionsfaktor Coup-TFII bindet. Dieser Faktor scheint dafür zuständig zu sein, die genaue Transkriptmenge sowohl im BAT, als auch in der Skelettmuskulatur fein einzustellen. Der Mechanismus der Aktivierung durch Coup-TFII scheint die Deaktivierung oder Verdrängung eines noch unbekanntes Repressorproteins einzuschließen. Coup-TFII ist ein Regulator des Wechsels des metabolischen Substrats von Kohlenhydraten zu Fetten. Die Tatsache, dass Coup-TFII das *Ucp3*-Gen positiv reguliert, bestärkt die Hypothese, dass *Ucp3* eine Rolle im Fettstoffwechsel spielt.

Ein Vergleich genomischer Sequenzen von Djungarischen Hamstern (*Phodopus sungorus*) mit und ohne einem erblichen Defekt in der BAT-spezifischen *Ucp3* Expression führte zur Identifizierung einer möglichen Forkhead-Faktor Bindestelle weit im ersten Intron des *Ucp3*-Gens. Ist diese durch eine Punktmutation betroffen, so fällt die *Ucp3* Expression im BAT komplett aus, während sie in der Skelettmuskulatur nur wenig verändert ist. Dies ist der erste und einzige bis heute bekannte, gewebespezifische Regulationsmechanismus des *Ucp3* Gens und könnte zur Entdeckung eines unbekanntes Regulators BAT-spezifischer Genexpression führen. Darüber hinaus ist die intronische Lokalisation des Elements in sich ungewöhnlich und weitere Untersuchung wert.

Phänotypisch zeigen Djungarische Hamster mit einem *Ucp3* Mangel im BAT eine globale Verminderung der mRNA Expression stoffwechselrelevanter Gene. Dies könnte der Grund sein für eine reduzierte Kältetoleranz dieser Tiere, die auf einem Defekt in der zitterfreien Wärmebildung beruht. Die betroffenen Hamster zeichnen sich außerdem durch ein erhöhtes Körpergewicht aus, welches auf einen Defekt in der energieaufwändigen Wärmebildung zurückführbar sein kann.

Zusammengefasst haben diese Studien zwei bisher unbekanntes Mechanismen der transkriptionellen *Ucp3*-Regulation mit einzigartigen Eigenschaften entdeckt und charakterisiert. Diese liefern wertvolle Hinweise auf die Rolle von *Ucp3* im Stoffwechsel und zeigen die Bedeutung von Promotoranalysen für Erkenntnisse über Regulation, Funktion und Herkunft eines Gens.

# Curriculum vitae

## Tobias Fromme

Wilhelmstraße 29  
35037 Marburg  
Phone: 0178-1335039  
E-Mail: fromme@staff.uni-marburg.de

Place of birth: Geseke, Germany  
Date of birth: June 12th, 1978  
Citizenship: German  
Marital status: unmarried

## *Education*

---

08/1984 - 06/1988	Primary School (Grundschule Störmede)
08/1988 - 04/1997	Grammar School (Gymnasium Antonianum Geseke)
07/1997 - 04/1998	Military service, Panzerbataillon 154 in Westerburg
10/1998 - 10/2002	Course of studies 'Biology (Diploma)' at the Philipps-University, Marburg
11/2002 - 07/2003	Diploma thesis at the Philipps-University, Marburg. Title: „Regulation of the <i>Ucp3</i> gene in <i>Phodopus sungorus</i> “
08/2003 - 10/2007	PhD studies at the Philipps-University, Marburg.
04/2004 - 12/2004	Scholar of the Friedrich-Naumann Foundation

## *Practical Training*

---

07/2001 - 10/2001	Practical training at Aventis Pharma Deutschland, Frankfurt. R&D, Department Thrombotic / Degenerative Joint Diseases
02/2002 - 04/2002	Practical training at the Max Planck Institute for experimental Endocrinology, Hannover. Department Signal Transduction
10/2003 - 03/2004	Employment at the Institute for molecular Biotechnology, Jena. Department Genome Analysis

## *Further Engagements*

---

10/2002 - 09/2003	Member of the 38th students' parliament of the Philipps-University, Marburg
01/2003 - 07/2003	Referee for study, practical training and career in the students' self-administration (Allgemeiner Studierendenausschuss, AStA)
11/2004 - 10/2005	Member of the Council of Elders of the student body, Philipps-University Marburg

---

## *Publications*

---

“Chicken ovalbumin upstream promoter transcription factor II regulates uncoupling protein 3 gene transcription in *Phodopus sungorus*”

**Fromme T.**, Reichwald K., Platzer M., Li X.S., Klingenspor M.  
BMC Mol Biol. 2007 Jan 4;8:1.

“Marsupial uncoupling protein 1 sheds light on the evolution of mammalian nonshivering thermogenesis”

Jastroch M., Withers K.W., Taudien S., Frappell P.B., Helwig M., **Fromme T.**, Hirschberg V., Heldmaier G., McAllan B.M., Firth B.T., Burmester T., Platzer M., Klingenspor M.  
Accepted at *Physiol Genomics*

---

## *Manuscripts in preparation*

---

“An intronic single base exchange leads to brown adipose tissue specific lack of Ucp3 and an altered body weight trajectory”

**Fromme T.**, Nau K., Rozman J., Hoffmann C., Reichwald K., Utting M., Platzer M., Klingenspor M.

“Brown adipose tissue specific lack of uncoupling protein 3 is associated with impaired cold tolerance and reduced transcript levels of metabolic genes”

Nau K., **Fromme T.**, Meyer C.W., von Praun C., Heldmaier G., Klingenspor M.

“Rapid single step subcloning procedure by combined action of type II and type IIs endonucleases with ligase”

**Fromme T.**, Klingenspor M.

---

## *Contributions to Meetings*

---

*Keystone Symposium „Nuclear Receptors: Orphan Brothers“, Banff, Canada, 18-23 March 2006.*

Poster: “Chicken ovalbumin upstream promoter transcription factor II (Coup-TFII) regulates the uncoupling protein 3 (Ucp3) gene”

**Fromme T.**, Reichwald K., Platzer M., Li X.S., Klingenspor M.

*14th European Bioenergetics Conference, Moscow, Russian Federation, 22-27 July 2006.*

Poster: “A single base exchange leads to tissue specific ablation of Ucp3 expression”

**Fromme T.**, von Praun C., Liebig M., Reichwald K., Platzer M., Klingenspor M.

*Biochim Biophys Acta*, 366-367 Suppl. S, 2006.

Poster: “Uncoupling protein 1 is expressed in the brain of ectothermic vertebrates”

Klingenspor M., Helwig M., **Fromme T.**, Brand M. D., Kloas W., Taudien S., Platzer M., Jastroch M.

*Biochim Biophys Acta*, 375-376 Suppl. S, 2006

*99. Jahrestagung der Deutschen Zoologischen Gesellschaft, Münster, Germany, 16-20 September 2006.*

Poster: “Tissue specific lack of UCP3 leads to transcriptional down-regulation of glycolytic, lipogenic and lipolytic pathways in *Phodopus sungorus*”

Weber K., **Fromme T.**, von Praun, C., Yang LX., Klingenspor, M.

---

## *Patent*

---

Patent DE000010337407A, filed August 13th, 2003.

“Klonierungssystem - Outside cutter mediated insert transfer“

**Fromme T.**, Klingenspor M.

Deutsches Patent- und Markenamt



## Danksagung

### *Institutionen*

Ich bedanke mich bei der Friedrich-Naumann-Stiftung für die großzügige Finanzierung eines Teils meiner Doktorarbeit. Desweiteren möchte ich den Graduiertenkollegs 767 und 1216 danken für meine Aufnahme als assoziiertes Mitglied und der damit verbundenen Unterstützung meiner Arbeit.

### *Personen*

An allererster Stelle und ganz besonders herzlich bedanke ich mich bei Prof. (!) Dr. Martin Klingenspor, der mich immer und in jeder Hinsicht unterstützt hat. Seine fachliche Inspiration, technische Expertise und moralische Unterstützung waren ebenso unbezahlbar wie das Vertrauen und die Freiheiten, die ich genießen durfte.

Ein großes Danke geht an Matthias Platzer und Kathrin Reichwald, die mich herzlich in Jena aufgenommen haben und für einen hervorragenden Start meiner Promotion gesorgt haben.

Ich bedanke mich bei Kerstin und Christoph für die Hilfe und intensive Mitarbeit am Ucp3-Projekt, ohne die diese Dissertation in vorliegender Form sicherlich nicht möglich gewesen wäre.

Ganz besonders bedanke ich mich bei Siggie und nicht einmal in erster Linie für Westerns und unbezahlbare Abbildungen, sondern für spaßige Rauchpausen, Büro-Leben im Allgemeinen und Speziellen und gemeinsames Timo-huldigen. Eben diesem Timo danke ich ebenso wie Elias für unsere großartige Büro-WG.

Vielen Dank natürlich auch dem ganzen, großen Rest der Arbeitsgruppe für eine wunderbare Arbeitsatmosphäre, tausend kleine Hilfestellungen, erhellende Diskussionen, Klatsch und Tratsch und für das Ertragen meiner Labor-Schimpf-und-Fluch-Mails.

Ich danke Tine dafür, dass sie bei mir ist und ich bei ihr. Diese Zeilen reichen nicht aus, um auch nur entfernt andeuten zu können, wie viel mir das bedeutet.

Ich bedanke mich bei der kombinierten Röpöck und Team Knieps Crew bestehend aus Michael, Achim, Svenja, Matze, Holger und Thomas für die dringend notwendige Kompensation von Arbeitsstress und viele lustige Abende.

Mein Dank gilt Werner Schmidt, der als mein Biologielehrer den Stein überhaupt erst ins Rollen brachte.

Zum Abschluß danke ich meinen Eltern, die mich jeden einzelnen der unzähligen kleinen Schritte bis hierhin voll Vertrauen unterstützt, gefördert und begleitet haben.

## Erklärung

Ich versichere, dass ich meine Dissertation

„Transcriptional Control Mechanisms of the Uncoupling Protein 3 Gene and their Functional Implications“

selbständig, ohne unerlaubte Hilfe angefertigt und mich dabei keiner anderen als der von mir ausdrücklich bezeichneten Quellen und Hilfen bedient habe.

Die Dissertation wurde in der jetzigen oder einer ähnlichen Form noch bei keiner anderen Hochschule eingereicht und hat noch keinen sonstigen Prüfungszwecken gedient.

---

(Ort, Datum)

---

(Unterschrift mit Vor- und Zuname)